

POLITECNICO DI TORINO

Corso di Laurea Magistrale in Ingegneria Energetica e Nucleare

Tesi di Laurea Magistrale

**Simplified transport models
for neutron energy spectra
evaluations**



Relatori

prof. Sandra Dulla
prof. Piero Ravetto

Candidato

Simone Di Pasquale

Ottobre 2019

Contents

List of Figures	IV
Abstract	VIII
1 Introduction	1
2 Neutron transport equation in a homogeneous slab	3
3 Models for the neutron spectra in a homogeneous slab	11
3.1 Fermi continuous slowing down model	11
3.1.1 P_N approximation	13
3.1.2 B_N approximation	15
3.2 Greuling-Goertzel approach	18
3.2.1 P_N approximation	20
3.3 Discrete lethargy approach	22
3.3.1 P_N approximation	23
3.4 Selengut-Goertzel approach	25
3.4.1 P_N approximation	26
4 The numerical procedure to solve the neutron spectra in a homogeneous slab	28
4.1 Discretization	28
4.1.1 Fermi continuous slowing down model, P_N approximation .	30
4.1.2 Fermi continuous slowing down model, B_N approximation .	32
4.1.3 Greuling-Goertzel approach, P_N approximation	34
4.1.4 Discrete lethargy approach, P_N approximation	37
4.1.5 Selengut-Goertzel approach , P_N approximation	39
5 Test cases, results and discussion	43
5.1 Simulation setup	43
5.2 Grid independence	44
5.2.1 Fermi continuous slowing down model, P_N approximation .	45
5.2.2 Fermi continuous slowing down model, B_N approximation .	48

5.2.3	Greuling-Goertzel approach, P_N approximation	49
5.2.4	Discrete lethargy approach, P_N approximation	52
5.2.5	Selengut-Goertzel approach , P_N approximation	55
5.3	Results	57
5.3.1	Geometry dependence	57
5.3.2	Results for a graphite system	59
5.3.3	Results for a light water system	65
5.3.4	Results for a heavy water system	72
5.3.5	Light and heavy water comparison	78
6	Concluding remarks	80
	Bibliography	81

List of Figures

5.1	Grid independence for Fermi continuous slowing down method with P_1 approximation, $B = 0.01$, using graphite as moderator material.	45
5.2	Grid independence for Fermi continuous slowing down method with P_1 approximation, $B = 0.01$, using light water as moderator material.	45
5.3	Grid independence for Fermi continuous slowing down method with P_1 approximation, $B = 0.01$, using heavy water as moderator material.	46
5.4	Grid independence for Fermi continuous slowing down method with P_1 approximation, $B = 0.01$; comparison between graphite, light water and heavy water as moderator material.	46
5.5	Grid independence for Fermi continuous slowing down method with B_1 approximation, $B = 0.01$, using graphite as moderator material.	48
5.6	Grid independence for Greuling-Goertzel approach with P_1 approximation, $B = 0.01$, using graphite as moderator material.	49
5.7	Grid independence for Greuling-Goertzel approach with P_1 approximation, $B = 0.01$, using light water as moderator material.	49
5.8	Grid independence for Greuling-Goertzel approach with P_1 approximation, $B = 0.01$, using heavy water as moderator material.	50
5.9	Grid independence for Greuling-Goertzel approach with P_1 approximation, $B = 0.01$; comparison between graphite, light water and heavy water as moderator material.	50
5.10	Grid independence for discrete lethargy approach with P_1 approximation, $B = 0.01$, using graphite as moderator material.	52
5.11	Grid independence for discrete lethargy approach with P_1 approximation, $B = 0.01$, using light water as moderator material.	52
5.12	Grid independence for discrete lethargy approach with P_1 approximation, $B = 0.01$, using heavy water as moderator material.	53
5.13	Grid independence for discrete lethargy approach with P_1 approximation, $B = 0.01$; comparison between graphite, light water and heavy water as moderator material.	53
5.14	Grid independence for Selengut-Goertzel approach with P_1 approximation, $B = 0.01$, using light water as moderator material.	55

5.15	Grid independence for Selengut-Goertzel approach with P_1 approximation, $B = 0.01$, using heavy water as moderator material.	55
5.16	Grid independence for Selengut-Goertzel approach with P_1 approximation, $B = 0.01$; comparison between light water and heavy water as moderator material.	56
5.17	Neutron spectra, evaluated with Fermi continuous slowing down method in P_{19} approximation, in a homogeneous slab of graphite.	57
5.18	Neutron spectra, evaluated with Fermi continuous slowing down method in P_{19} approximation, in a homogeneous slab of light water.	58
5.19	Neutron spectra, evaluated with Fermi continuous slowing down method in P_{19} approximation, in a homogeneous slab of heavy water.	58
5.20	Neutron spectra, evaluated with Fermi continuous slowing down method, discrete lethargy approach and the Greuling-Goertzel approach in P_{19} approximation, in a homogeneous slab of graphite, with $B = 0.01$	59
5.21	Absolute error with respect to the solution with the P_{19} approximation, using the Fermi continuous slowing down method, in a homogeneous slab of graphite, with $B = 0.01$ in linear scale.	61
5.22	Absolute error with respect to the solution with the P_{19} approximation, using the Fermi continuous slowing down method, in a homogeneous slab of graphite, with $B = 0.01$ in logarithmic scale.	61
5.23	Absolute error with respect to the solution with the P_{19} approximation, using the Greuling-Goertzel approach, in a homogeneous slab of graphite, with $B = 0.01$ in linear scale.	62
5.24	Absolute error with respect to the solution with the P_{19} approximation, using the Greuling-Goertzel approach, in a homogeneous slab of graphite, with $B = 0.01$ in logarithmic scale.	63
5.25	Absolute error with respect to the solution with the P_{19} approximation, using the discrete lethargy approach, in a homogeneous slab of graphite, with $B = 0.01$ in linear scale.	63
5.26	Absolute error with respect to the solution with the P_{19} approximation, using the discrete lethargy approach, in a homogeneous slab of graphite, with $B = 0.01$ in logarithmic scale.	64
5.27	Absolute error with respect to the solution with the B_5 approximation, using the Fermi continuous slowing down method, in a homogeneous slab of graphite, with $B = 0.01$ in logarithmic scale.	65
5.28	Neutron spectra, evaluated with Fermi continuous slowing down method, discrete lethargy approach, Greuling-Goertzel approach and Selengut-Goertzel approach in P_{19} approximation, in a homogeneous slab of light water, with $B = 0.01$	66

5.29	Absolute error with respect to the solution with the P_{19} approximation, using the Fermi continuous slowing down method, in a homogeneous slab of light water, with $B = 0.01$ in linear scale.	67
5.30	Absolute error with respect to the solution with the P_{19} approximation, using the Fermi continuous slowing down method, in a homogeneous slab of light water, with $B = 0.01$ in logarithmic scale. . . .	67
5.31	Absolute error with respect to the solution with the P_{19} approximation, using the Greuling-Goertzel approach, in a homogeneous slab of light water, with $B = 0.01$ in linear scale.	68
5.32	Absolute error with respect to the solution with the P_{19} approximation, using the Greuling-Goertzel approach, in a homogeneous slab of light water, with $B = 0.01$ in logarithmic scale.	69
5.33	Absolute error with respect to the solution with the P_{19} approximation, using the discrete lethargy approach, in a homogeneous slab of light water, with $B = 0.01$ in linear scale.	69
5.34	Absolute error with respect to the solution with the P_{19} approximation, using the discrete lethargy approach, in a homogeneous slab of light water, with $B = 0.01$ in logarithmic scale.	70
5.35	Absolute error with respect to the solution with the P_{19} approximation, using the Selengut-Goertzel approach, in a homogeneous slab of light water, with $B = 0.01$ in linear scale.	71
5.36	Absolute error with respect to the solution with the P_{19} approximation, using the Selengut-Goertzel approach, in a homogeneous slab of light water, with $B = 0.01$ in logarithmic scale.	71
5.37	Neutron spectra, evaluated with Fermi continuous slowing down method, discrete lethargy approach , Greuling-Goertzel approach and Selengut-Goertzel approach in P_{19} approximation, in a homogeneous slab of heavy water with $B = 0.01$	72
5.38	Absolute error with respect to the solution with the P_{19} approximation, using the Fermi continuous slowing down method, in a homogeneous slab of heavy water, with $B = 0.01$ in linear scale.	73
5.39	Absolute error with respect to the solution with the P_{19} approximation, using the Fermi continuous slowing down method, in a homogeneous slab of heavy water, with $B = 0.01$ in logarithmic scale. . .	73
5.40	Absolute error with respect to the solution with the P_{19} approximation, using the Greuling-Goertzel approach, in a homogeneous slab of heavy water, with $B = 0.01$ in linear scale.	74
5.41	Absolute error with respect to the solution with the P_{19} approximation, using the Greuling-Goertzel approach, in a homogeneous slab of heavy water, with $B = 0.01$ in logarithmic scale.	75

5.42	Absolute error with respect to the solution with the P_{19} approximation, using the discrete lethargy approach, in a homogeneous slab of heavy water, with $B = 0.01$ in linear scale.	75
5.43	Absolute error with respect to the solution with the P_{19} approximation, using the discrete lethargy approach, in a homogeneous slab of heavy water, with $B = 0.01$ in logarithmic scale.	76
5.44	Absolute error with respect to the solution with the P_{19} approximation, using the Selengut-Goertzel approach, in a homogeneous slab of heavy water, with $B = 0.01$ in linear scale.	77
5.45	Absolute error with respect to the solution with the P_{19} approximation, using the Selengut-Goertzel approach, in a homogeneous slab of heavy water, with $B = 0.01$ in logarithmic scale.	77
5.46	Neutron spectra, evaluated with Selengut-Goertzel approach in P_{19} approximation, in a homogeneous slab of light water and of heavy water with $B = 0.01$	78
5.47	Absorption cross section for hydrogen and deuterium	79

Abstract

An important issue in the design of nuclear reactor cores is the determination of multigroup cross sections. This task is accomplished by means of a combined procedure involving a space homogenization and an energy averaging to obtain group-collapsed data that can well reproduce the neutronic interactions in the real multiplying system. For this purpose, it is necessary to determine accurate neutron spectra (distribution in the energy domain of the neutron flux) that are used as weights in the collapsing process. In this thesis the energy aspects are analysed. The neutron transport equation is solved through the use of some simplifications: first of all the asymptotic theory is used in order to eliminate the space dependence of the problem and reduce it to a single parameter; then some methods to approximate the collision density and, consequently, the scattering integral are used. In particular, the classic Fermi continuous slowing down approach, the Groeling-Goertzel and the Selengut-Goertzel methods are considered. Adopting these simplifications, the neutron spectra is evaluated for different moderator media, in slab geometry, using the Pn and the Bn methods. The lethargy variable is discretized for the solution of the transport integral equation. In order to reduce the error, a grid independence analysis is performed for each method considered. This thesis is important because it is a first step in order to determine, in a physical consistent way, the energy grid for multigroup models, on which deterministic solvers of the neutron transport equation are based. The results allow also to get a physical insight into the energy collapsing procedure for the generation of multigroup nuclear data.

Chapter 1

Introduction

An interest in spatial homogenization and energy collapsing of nuclear data for reactor neutronic calculations in the field of nuclear reactor physics has been developing in the past years; in fact, since the high geometry complexity of a nuclear reactor, a spatial homogenization is essential in order to reduce the computational cost for its simulation. For the same reason, since the use of a continuous energy approach generates a high computational cost, multigroup theories are used in order to better manage the solution of the neutron transport equation.

In this context, several works have already been published, in order to tackle the problem of spatial homogenization, e.g. [1–6], where methods based on the neutron transport equation are presented. Similarly, in the work presented in ref. [7], a rehomogenization method has been analysed.

The energy collapsing of nuclear data procedure is very important in order to improve the results of deterministic simulations and to reduce the computational cost of deterministic codes based on the multigroup neutron transport equation. Along this line, the present work has as objective to study the basic methods to determine the energy spectrum of the neutron flux and to analyse the performance of each method for different moderating materials. This work constitutes the basis for further developments leading to improve the collapsing procedure.

Moreover the work could also contribute to develop innovative techniques for group collapsing. One example could be the use of the energy spectrum to group neutrons with different energies, but with similar physical characteristics [8]; another example could be the use of these methods for time dependent problems, in order to understand the dynamic evolution of the energy dependent neutron population. At last, the methods could be also applied to other particle transport problems, such as electron slowing down, that is practically a continuous process and can be analysed with the Spencer-Lewis equation [9].

In this work, in order to concentrate the attention on the energy dependence of the neutron flux, the space asymptotic theory is used; in this case the medium is

considered as infinite and the spatial dependence is accounted for through the introduction of the geometrical buckling B [10–12]. This is a historical method used in order to reduce the computational cost due to geometry; even if nowadays the computational power is highly increased with respect to the years of formulation of this method, the asymptotic theory remains an interesting method because it allows to better focus on the energy aspects of the problem; this method could also be used for time dependent problems in order to study pulsed experiments [13]. In the following chapters a short presentation of the nuclear transport equation in a homogeneous slab is reported, using the asymptotic theory and the elastic scattering approximation; then, different models to approximate the scattering integral and to determine the energy spectrum are presented. The numerical procedures used to discretize the problem are presented and discussed. Some test cases and results are analysed and some conclusions are drawn.

Chapter 2

Neutron transport equation in a homogeneous slab

The neutron behaviour in a nuclear reactor is described by the neutron transport equation [14]:

$$\begin{aligned} \frac{1}{v} \frac{\partial \phi(\mathbf{r}, E, \boldsymbol{\Omega}, t)}{\partial t} + \boldsymbol{\Omega} \cdot \nabla (\phi(\mathbf{r}, E, \boldsymbol{\Omega}, t)) + \\ + \Sigma_t(\mathbf{r}, E) \phi(\mathbf{r}, E, \boldsymbol{\Omega}, t) = S(\mathbf{r}, E, \boldsymbol{\Omega}, t) + \\ + \int dE' \oint d\Omega' \Sigma_s(\mathbf{r}, E') \phi(\mathbf{r}, E', \boldsymbol{\Omega}', t) f_s(\mathbf{r}, E' \rightarrow E, \boldsymbol{\Omega}' \rightarrow \boldsymbol{\Omega}), \end{aligned} \quad (2.1)$$

where:

- v is the neutron velocity;
- t is the time variable;
- $\phi(\mathbf{r}, E, \boldsymbol{\Omega}, t)$ is the neutron flux;
- \mathbf{r} is the spatial position vector;
- E is the neutron energy associated to the velocity v ;
- $\boldsymbol{\Omega}$ is the solid angle vector;
- $\Sigma_t(\mathbf{r}, E)$ is the total cross section;
- $S(\mathbf{r}, E, \boldsymbol{\Omega}, t)$ is neutron source;
- $\Sigma_s(\mathbf{r}, E)$ is the scattering cross section;
- $f_s(\mathbf{r}, E' \rightarrow E, \boldsymbol{\Omega}' \rightarrow \boldsymbol{\Omega})$ is the scattering function.

This equation depends on time, position, direction and energy of a neutron. The objective of this work is to focus the attention in the energy aspects comparing different slowing down models. In order to do that it is useful to analyse a simpler case from a geometrical point of view; a uni-dimensional slab is taken as reference geometry. For the same reason, in order to avoid complication due to heterogeneity, a homogeneous case is considered; as a consequence, the cross sections become spatial independent. Considering the uni-dimensional slab hypothesis the equation becomes:

$$\begin{aligned} \mu \frac{\partial \phi(x, E, \mu)}{\partial x} + \Sigma_t(x, E)\phi(x, E, \mu) = S(x, E, \mu) + \\ + \int dE' \oint d\Omega' \Sigma_s(x, E')\phi(x, E', \mu')f_s(x, E' \rightarrow E, \Omega' \rightarrow \Omega), \end{aligned} \quad (2.2)$$

where μ is the cosine of the angle between the neutron direction and x axis. Scattering collisions are assumed to be azimuthally symmetric about Ω' ; with this assumption the final vector Ω has the same probability to lie in any position on a surface of a cone; that cone is generated rotating the vector Ω around the direction of the vector Ω' (see figure 7.5 of [15]). With this assumption the scattering function is dependent only on the cosine between Ω and Ω' and becomes:

$$f_s(x, E' \rightarrow E, \Omega' \rightarrow \Omega) = f_s(x, E' \rightarrow E, \Omega' \cdot \Omega) = \frac{1}{2\pi}q(x, E' \rightarrow E, \mu_0), \quad (2.3)$$

where:

- μ_0 : cosine between Ω and Ω' ;
- $q(x, E' \rightarrow E, \mu_0)$: frequency function.

The solutions are evaluated using the elastic scattering approximation for the scattering function. First of all, it is convenient to transform equation (2.2) from energy variable E to the lethargy variable u . The lethargy variable is defined as:

$$u = \log \left(\frac{E_*}{E} \right), \quad (2.4)$$

where:

- u is the lethargy variable;
- E_* is the upper bound for the energy variable.

The neutrons are generated with a maximum energy value E_* , that correspond to the zero value for the lethargy variable; then they will start the slowing down process, losing part of their energy. In this way the energy variable is decreasing, instead the lethargy variable is increasing. The frequency function is so modified:

$$q(x, E' \rightarrow E, \mu_0)dE'd\mu_0 = q(x, u' \rightarrow u, \mu_0)JdE'd\mu_0, \quad (2.5)$$

where J is the Jacobian, that is defined as:

$$J \equiv \left| \frac{du'}{dE'} \right|.$$

Substituting in equation (2.2), the following formula is obtained:

$$\begin{aligned} \mu \frac{\partial \phi(x, u, \mu)}{\partial x} + \Sigma_t(x, u) \phi(x, u, \mu) &= S(x, u, \mu) + \\ + \int du' \oint d\Omega' \Sigma_s(x, u') \phi(x, u', \mu') &\frac{1}{2\pi} q(x, u' \rightarrow u, \mu_0). \end{aligned} \quad (2.6)$$

Considering the slab as homogeneous media the properties become spatial independent and the neutron transport equation becomes:

$$\begin{aligned} \mu \frac{\partial \phi(x, u, \mu)}{\partial x} + \Sigma_t(u) \phi(x, u, \mu) &= S(x, u, \mu) + \\ + \int du' \oint d\Omega' \Sigma_s(u') \phi(x, u', \mu') &\frac{1}{2\pi} q(u' \rightarrow u, \mu_0). \end{aligned} \quad (2.7)$$

Since the main objective is to evaluate the energy spectrum, the space variable is taken into account through the use of the space asymptotic theory [10–12]; the transport equation is taken in an infinite medium and it is treated by the Fourier transform; the space dependence of the problem is put inside the buckling variable B . The Fourier transform of the neutron flux is:

$$\varphi(B, u, \mu) = \int_{-\infty}^{+\infty} \phi(x, u, \mu) e^{-iBx} dx. \quad (2.8)$$

The Fourier transform of the derivative of the neutron flux is:

$$iB\varphi(B, u, \mu) = \int_{-\infty}^{+\infty} \frac{\partial \phi(x, u, \mu)}{\partial x} e^{-iBx} dx. \quad (2.9)$$

Having done the Fourier transform of formula 2.7, considering the two previous formulas, the following equation is obtained:

$$\begin{aligned} iB\mu\varphi(B, u, \mu) + \Sigma_t(u)\varphi(B, u, \mu) &= S(B, u, \mu) + \\ + \int du' \oint d\Omega' \Sigma_s(u')\varphi(B, u', \mu') &\frac{1}{2\pi} q(u' \rightarrow u, \mu_0), \end{aligned} \quad (2.10)$$

where $S(B, u, \mu)$ is the Fourier transform of $S(x, u, \mu)$. In order to separate the lethargy part from the angular part of the frequency function, the expansion using the Legendre polynomials has been used [15]. The formula (7.117) of [15] for the frequency function is here reported:

$$q(u' \rightarrow u, \mu_0) = \sum_{n=0}^{+\infty} \left(\frac{2n+1}{2} \right) q_n(u' \rightarrow u) P_n(\mu_0), \quad (2.11)$$

where:

- $P_n(\mu_0)$ is the Legendre polynomial of order n ;
- $q_n(u' \rightarrow u)$ is defined as:

$$q_n(u' \rightarrow u) \equiv \int_{-1}^1 q(u' \rightarrow u, \mu_0) P_n(\mu_0) d\mu_0 \quad (2.12)$$

In order to simplify the problem, the Legendre polynomials can be written through the use of spherical harmonics [16]:

$$P_n(\boldsymbol{\Omega} \cdot \boldsymbol{\Omega}') = \frac{4\pi}{2n+1} \sum_{\beta=-n}^{+n} Y_n^\beta(\vartheta, \psi) Y_n^{\beta*}(\vartheta', \psi'), \quad (2.13)$$

where:

- ϑ, ϑ' are the angles with respect to the x axis;
- ψ, ψ' are the angles with respect to the y axis in the $z - y$ plane;
- $\boldsymbol{\Omega}$ is the unit vector with sphere coordinate $(1, \vartheta, \psi)$;
- $\boldsymbol{\Omega}'$ is the unit vector with sphere coordinate $(1, \vartheta', \psi')$.

The spherical harmonics can be written through the use of associated Legendre function as explained in [16]:

$$Y_n^\beta(\vartheta, \psi) = \sqrt{\frac{2n+1}{4\pi} \frac{(n-\beta)!}{(n+\beta)!}} P_n^\beta(\cos \vartheta) e^{i\beta\psi}, \quad (2.14)$$

with:

$$\cos \vartheta = \mu. \quad (2.15)$$

For completeness also the formula for the conjugate is reported:

$$Y_n^{\beta*}(\vartheta, \psi) = (-1)^\beta Y_n^{-\beta}(\vartheta, \psi). \quad (2.16)$$

The formulation for the associated Legendre functions, and their conjugates, are taken from [16] and are here reported:

$$P_n^\beta(\mu) = (-1)^\beta (1 - \mu^2)^{\frac{\beta}{2}} \frac{d^\beta}{dx^\beta} (P_n(\mu)); \quad (2.17)$$

$$P_n^{-\beta}(\mu) = (-1)^\beta \frac{(n-\beta)!}{(n+\beta)!} P_n^\beta(\mu). \quad (2.18)$$

Using those definition, the frequency function can be written as follow:

$$q(u' \rightarrow u, \mu_0) = \sum_{n=0}^{+\infty} \left(\frac{2n+1}{2} \right) q_n(u' \rightarrow u) \frac{4\pi}{2n+1} \cdot \sum_{\beta=-n}^{+n} Y_n^\beta(\vartheta, \psi) Y_n^{\beta*}(\vartheta', \psi'). \quad (2.19)$$

Substituting formulas (2.14, 2.16) the previous equation becomes:

$$q(u' \rightarrow u, \mu_0) = \sum_{n=0}^{+\infty} \left(\frac{2n+1}{2} \right) q_n(u' \rightarrow u) \frac{4\pi}{2n+1} \cdot \sum_{\beta=-n}^{+n} \sqrt{\frac{2n+1}{4\pi} \frac{(n-\beta)!}{(n+\beta)!}} P_n^\beta(\cos \vartheta) e^{i\beta\psi} \cdot \sqrt{\frac{2n+1}{4\pi} \frac{(n-\beta)!}{(n+\beta)!}} P_n^\beta(\cos \vartheta') e^{-i\beta\psi'}. \quad (2.20)$$

Multiplying the square roots and simplifying with the fraction the equation becomes:

$$q(u' \rightarrow u, \mu_0) = \sum_{n=0}^{+\infty} \left(\frac{2n+1}{2} \right) q_n(u' \rightarrow u) \cdot \sum_{\beta=-n}^{+n} \frac{(n-\beta)!}{(n+\beta)!} P_n^\beta(\mu) e^{i\beta\psi} P_n^\beta(\mu') e^{-i\beta\psi'}; \quad (2.21)$$

then the two exponentials are collected:

$$q(u' \rightarrow u, \mu_0) = \sum_{n=0}^{+\infty} \left(\frac{2n+1}{2} \right) q_n(u' \rightarrow u) \cdot \sum_{\beta=-n}^{+n} \frac{(n-\beta)!}{(n+\beta)!} P_n^\beta(\mu) P_n^\beta(\mu') e^{i\beta(\psi-\psi')}. \quad (2.22)$$

Substituting the frequency function in this form, the neutron transport equation becomes:

$$iB\mu\varphi(B, u, \mu) + \Sigma_t(u)\varphi(B, u, \mu) = S(B, u, \mu) + \int du' \oint d\Omega' \Sigma_s(u')\varphi(B, u', \mu') \frac{1}{2\pi} \sum_{n=0}^{+\infty} \left(\frac{2n+1}{2} \right) \cdot q_n(u' \rightarrow u) \sum_{\beta=-n}^{+n} \frac{(n-\beta)!}{(n+\beta)!} P_n^\beta(\mu) P_n^\beta(\mu') e^{i\beta(\psi-\psi')}. \quad (2.23)$$

In order to simplify the problem some manipulations are necessary; first of all, the scattering cross section, that is angular independent, is taken out from the integral in the solid angle and the solid angle integral is divided in two integral as follow:

$$\begin{aligned}
 & iB\mu\varphi(B, u, \mu) + \Sigma_t(u)\varphi(B, u, \mu) = S(B, u, \mu) + \\
 & + \int_u^1 du' \Sigma_s(u') \int_{-1}^1 d\mu' \int_0^{2\pi} d\psi' \varphi(B, u', \mu') \frac{1}{2\pi}. \\
 & \cdot \sum_{n=0}^{+\infty} \left(\frac{2n+1}{2} \right) q_n(u' \rightarrow u) \sum_{\beta=-n}^{+n} \frac{(n-\beta)!}{(n+\beta)!} P_n^\beta(\mu) P_n^\beta(\mu') e^{i\beta(\psi-\psi')};
 \end{aligned} \tag{2.24}$$

then the part independent for ψ' is taken out from the corresponding integral:

$$\begin{aligned}
 & iB\mu\varphi(B, u, \mu) + \Sigma_t(u)\varphi(B, u, \mu) = S(B, u, \mu) + \\
 & + \int_u^1 du' \Sigma_s(u') \int_{-1}^1 d\mu' \varphi(B, u', \mu') \frac{1}{2\pi} \sum_{n=0}^{+\infty} \left(\frac{2n+1}{2} \right) \cdot \\
 & \cdot q_n(u' \rightarrow u) \sum_{\beta=-n}^{+n} \frac{(n-\beta)!}{(n+\beta)!} P_n^\beta(\mu) P_n^\beta(\mu') \int_0^{2\pi} d\psi' e^{i\beta(\psi-\psi')}.
 \end{aligned} \tag{2.25}$$

The solution of this last integral is presented below:

$$\int_0^{2\pi} d\psi' e^{i\beta(\psi-\psi')} = \begin{cases} 0 & \text{if } \beta \neq 0 \\ 2\pi & \text{if } \beta = 0 \end{cases} \tag{2.26}$$

Considering this last information, β has been imposed equal to 0; the neutron transport equation become:

$$\begin{aligned}
 & iB\mu\varphi(B, u, \mu) + \Sigma_t(u)\varphi(B, u, \mu) = S(B, u, \mu) + \int_u^1 du' \Sigma_s(u') \cdot \\
 & \cdot \int_{-1}^1 d\mu' \varphi(B, u', \mu') \sum_{n=0}^{+\infty} \left(\frac{2n+1}{2} \right) q_n(u' \rightarrow u) P_n(\mu) P_n(\mu'),
 \end{aligned} \tag{2.27}$$

that, taking out the terms independent from μ' from the corresponding integral, becomes:

$$\begin{aligned}
 & iB\mu\varphi(B, u, \mu) + \Sigma_t(u)\varphi(B, u, \mu) = S(B, u, \mu) + \int_u^1 du' \Sigma_s(u') \cdot \\
 & \cdot \sum_{n=0}^{+\infty} \left(\frac{2n+1}{2} \right) q_n(u' \rightarrow u) P_n(\mu) \int_{-1}^1 d\mu' \varphi(B, u', \mu') P_n(\mu').
 \end{aligned} \tag{2.28}$$

The flux moment of order n is defined as:

$$\varphi_n(B, u') \equiv \int_{-1}^1 d\mu' \varphi(B, u', \mu') P_n(\mu'); \tag{2.29}$$

considering this last definition the transport equation becomes:

$$iB\mu\varphi(B, u, \mu) + \Sigma_t(u)\varphi(B, u, \mu) = S(B, u, \mu) + \int_u^{+\infty} du' \Sigma_s(u') \sum_{n=0}^{+\infty} \left(\frac{2n+1}{2} \right) q_n(u' \rightarrow u) P_n(\mu) \varphi_n(B, u'); \quad (2.30)$$

the part independent from u' is here taken out from the corresponding integral; the equation becomes:

$$iB\mu\varphi(B, u, \mu) + \Sigma_t(u)\varphi(B, u, \mu) = S(B, u, \mu) + \sum_{n=0}^{+\infty} \left(\frac{2n+1}{2} \right) P_n(\mu) \int_u^{+\infty} du' \Sigma_s(u') q_n(u' \rightarrow u) \varphi_n(B, u'). \quad (2.31)$$

In order to approximate the momenta of order n of the frequency function, the elastic scattering approximation has been used; the elastic scattering approximation is reported in the following formula (for a complete treatment it is possible to refer to chapter 7.3, point e. of [15]):

$$q_n(u' \rightarrow u) = \frac{P_n(\xi(A, u', u)) e^{u'-u}}{1 - \alpha}, \quad (2.32)$$

with:

$$\xi(A, u', u) = \frac{1}{2} \left[(A+1)e^{\frac{1}{2}(u'-u)} - (A-1)e^{-\frac{1}{2}(u'-u)} \right]; \quad (2.33)$$

$$\alpha = \left(\frac{A-1}{A+1} \right); \quad (2.34)$$

$$A = \frac{M}{m}; \quad (2.35)$$

where:

- M is the mass of nucleus where neutron collides;
- m is the mass of neutron.

The neutron transport equation for a slab geometry, with elastic scattering approximation become:

$$iB\mu\varphi(B, u, \mu) + \Sigma_t(u)\varphi(B, u, \mu) = S(B, u, \mu) + \sum_{n=0}^{+\infty} \left(\frac{2n+1}{2} \right) \cdot P_n(\mu) \int_c^u du' \Sigma_s(u') \varphi_n(B, u') \frac{P_n(\xi(A, u', u)) e^{u'-u}}{1 - \alpha}. \quad (2.36)$$

With:

$$c = \max[u + \log(\alpha), 0] \quad (2.37)$$

This final equation is an integral equation in the lethargy variable; in order to solve this equation in the whole lethargy interval, some approximations for the integral are necessary. For this reason, in the following chapter some methods to face up to this integral are presented.

Chapter 3

Models for the neutron spectra in a homogeneous slab

The solution of the neutron transport problem is a complex task because the necessity of the solution in the entire lethargy interval in order to solve the scattering integral and, consequently, to have the value of the flux in a lethargy point. Considering this, the first task is to approximate the scattering integral.

In this chapter some approaches for the approximated solution of the scattering integral are presented.

3.1 Fermi continuous slowing down model

In order to find the energy spectrum, in this section the Fermi continuous slowing down approximation is taken into account; the collision density $\Sigma_s(u')\varphi_n(B, u')$ has been considered as slowly varying functions over the lethargy range of the scattering integral (chapter 7.3, point g of [15]). The main approximation is to consider a linear variation of the collision density for the zero order moment; instead a constant collision density for higher order moment is taken:

$$\begin{aligned}\Sigma_s(u')\varphi_n(B, u') \approx & \Sigma_s(u)\varphi_n(B, u) + \\ & + (u' - u)\frac{\partial}{\partial u}[\Sigma_s(u)\varphi_n(B, u)] \cdot \delta_{n,0}.\end{aligned}\tag{3.1}$$

Substituting this approximation in formula (2.36) the following formula is obtained:

$$\begin{aligned}
 iB\mu\varphi(B, u, \mu) + \Sigma_t(u)\varphi(B, u, \mu) &= S(B, u, \mu) + \\
 &+ \sum_{n=0}^{+\infty} \left(\frac{2n+1}{2} \right) P_n(\mu) \cdot \\
 &\cdot \int_c^u \left[\Sigma_s(u)\varphi_n(B, u) + (u' - u) \frac{\partial}{\partial u} [\Sigma_s(u)\varphi_n(B, u)] \cdot \delta_{n,0} \right] \cdot \\
 &\cdot \frac{P_n(\xi(A, u', u))e^{u'-u}}{1 - \alpha} du';
 \end{aligned} \tag{3.2}$$

then separating the terms of order zero from the other terms and separating the two terms of order zero themselves the equation becomes:

$$\begin{aligned}
 iB\mu\varphi(B, u, \mu) + \Sigma_t(u)\varphi(B, u, \mu) &= S(B, u, \mu) + \frac{1}{2(1 - \alpha)} \cdot \\
 &\cdot P_0(\mu)\Sigma_s(u)\varphi_0(B, u) \int_c^u du' P_0(\xi(A, u', u))e^{u'-u} + \\
 &+ \frac{1}{2(1 - \alpha)} P_0(\mu) \frac{\partial}{\partial u} [\Sigma_s(u)\varphi_0(B, u)] \cdot \\
 &\cdot \int_c^u du' (u' - u) P_0(\xi(A, u', u))e^{u'-u} + \sum_{n=1}^{+\infty} \left(\frac{2n+1}{2} \right) P_n(\mu) \cdot \\
 &\cdot \int_c^u du' [\Sigma_s(u)\varphi_n(B, u)] \frac{P_n(\xi(A, u', u))e^{u'-u}}{1 - \alpha};
 \end{aligned} \tag{3.3}$$

considering that the Legendre polynomial of order zero is equal to one the formula becomes:

$$\begin{aligned}
 iB\mu\varphi(B, u, \mu) + \Sigma_t(u)\varphi(B, u, \mu) &= S(B, u, \mu) + \\
 &+ \frac{1}{2(1 - \alpha)} \Sigma_s(u)\varphi_0(B, u) \int_c^u du' e^{u'-u} + \\
 &+ \frac{1}{2(1 - \alpha)} \frac{\partial}{\partial u} [\Sigma_s(u)\varphi_0(B, u)] \int_c^u du' (u' - u) e^{u'-u} + \\
 &+ \sum_{n=1}^{+\infty} \left(\frac{2n+1}{2} \right) P_n(\mu)\Sigma_s(u)\varphi_n(B, u) \int_c^u du' \frac{P_n(\xi(A, u', u))e^{u'-u}}{1 - \alpha}.
 \end{aligned} \tag{3.4}$$

It can be noticed that the first two integrals are trivial, and the results are given in the following formulas:

$$\int_c^u du' e^{u'-u} = e^{-u} \cdot e^{u'} \Big|_c^u = 1 - e^{c-u}; \tag{3.5}$$

$$\begin{aligned} \int_c^u du' (u' - u) e^{u'-u} &= \left[(u' - u) e^{u'-u} - e^{u'-u} \right] \Big|_c^u \\ &= -1 - (c - u) e^{c-u} + e^{c-u}. \end{aligned} \quad (3.6)$$

The third integral is also trivial because is the integral of the product of a polynomial and an exponential, but the solution is not given analytically because the polynomials depend on the order considered; since the calculation are done also with large order the integral is done numerically in the Matlab program. The formula (3.4) becomes:

$$\begin{aligned} iB\mu\varphi(B, u, \mu) + \Sigma_t(u)\varphi(B, u, \mu) &= S(B, u, \mu) + \\ &+ \frac{1}{2(1-\alpha)} \Sigma_s(u)\varphi_0(B, u)(1 - e^{c-u}) + \\ &+ \frac{1}{2(1-\alpha)} \frac{\partial}{\partial u} [\Sigma_s(u)\varphi_0(B, u)] [-1 - (c - u)e^{c-u} + e^{c-u}] + \\ &+ \sum_{n=1}^{+\infty} \left(\frac{2n+1}{2} \right) \frac{P_n(\mu)}{1-\alpha} \Sigma_s(u)\varphi_n(B, u) \int_c^u du' P_n(\xi(A, u', u)) e^{u'-u}. \end{aligned} \quad (3.7)$$

Before using the P_N method and the B_N method in order to find the solution, some definitions are necessary. First of all, the Fourier transform of the flux is defined as follow:

$$\varphi(B, u, \mu) = \sum_{n=0}^{\infty} \left(\frac{2n+1}{2} \right) \varphi_n(B, u) P_n(\mu); \quad (3.8)$$

the same expansion could be done for the Fourier transform of the source:

$$S(B, u, \mu) = \sum_{n=0}^{\infty} \left(\frac{2n+1}{2} \right) S_n(B, u) P_n(\mu). \quad (3.9)$$

3.1.1 P_N approximation

Before starting with the method, some properties of the Legendre polynomials are necessary [16]. The first property is the orthogonality:

$$\int_{-1}^{+1} P_n(\mu) P_m(\mu) d\mu = \frac{2}{2n+1} \delta_{n,m}. \quad (3.10)$$

The second property that will be used in this section is the recursive formula:

$$\mu P_n(\mu) = \frac{(n+1)P_{n+1}(\mu) + nP_{n-1}(\mu)}{2n+1}. \quad (3.11)$$

First of all the expansion in formulas (3.8,3.9) are substituted in formula (3.7) to obtain:

$$\begin{aligned}
 & iB\mu \sum_{n=0}^{\infty} \left(\frac{2n+1}{2} \right) \varphi_n(B, u) P_n(\mu) + \\
 & + \Sigma_t(u) \sum_{n=0}^{\infty} \left(\frac{2n+1}{2} \right) \varphi_n(B, u) P_n(\mu) = \\
 & = \sum_{n=0}^{\infty} \left(\frac{2n+1}{2} \right) S_n(B, u) P_n(\mu) + \\
 & + \frac{1}{2(1-\alpha)} \Sigma_s(u) \varphi_0(B, u) (1 - e^{c-u}) + \\
 & + \frac{1}{2(1-\alpha)} \frac{\partial}{\partial u} [\Sigma_s(u) \varphi_0(B, u)] [-1 - (c-u)e^{c-u} + e^{c-u}] + \\
 & + \sum_{n=1}^{+\infty} \left(\frac{2n+1}{2} \right) \frac{P_n(\mu)}{1-\alpha} \Sigma_s(u) \varphi_n(B, u) \int_c^u du' P_n(\xi(A, u', u)) e^{u'-u}.
 \end{aligned} \tag{3.12}$$

In order to find an equation for each flux moment the property in formula (3.10) is used; it means to multiply each term of the previous formula per $P_m(\mu)$ and integrate between minus one and plus one in $d\mu$.

$$\begin{aligned}
 & iB \sum_{n=0}^{\infty} \left(\frac{2n+1}{2} \right) \varphi_n(B, u) \int_{-1}^{+1} \mu P_n(\mu) P_m(\mu) d\mu + \\
 & + \Sigma_t(u) \sum_{n=0}^{\infty} \left(\frac{2n+1}{2} \right) \varphi_n(B, u) \int_{-1}^{+1} P_n(\mu) P_m(\mu) d\mu = \\
 & = \sum_{n=0}^{\infty} \left(\frac{2n+1}{2} \right) S_n(B, u) \int_{-1}^{+1} P_n(\mu) P_m(\mu) d\mu + \\
 & + \frac{1}{2(1-\alpha)} \Sigma_s(u) \varphi_0(B, u) (1 - e^{c-u}) \int_{-1}^{+1} P_m(\mu) d\mu + \\
 & + \frac{1}{2(1-\alpha)} \frac{\partial}{\partial u} [\Sigma_s(u) \varphi_0(B, u)] [-1 - (c-u)e^{c-u} + e^{c-u}] \cdot \\
 & \cdot \int_{-1}^{+1} P_m(\mu) d\mu + \sum_{n=1}^{+\infty} \left(\frac{2n+1}{2(1-\alpha)} \right) \int_{-1}^{+1} P_n(\mu) P_m(\mu) d\mu \cdot \\
 & \cdot \Sigma_s(u) \varphi_n(B, u) \int_c^u du' P_n(\xi(A, u', u)) e^{u'-u}.
 \end{aligned} \tag{3.13}$$

Applying the orthogonality property, the results of the integrals are found as follow:

$$\int_{-1}^{+1} P_m(\mu) d\mu = \int_{-1}^{+1} P_0(\mu) P_m(\mu) d\mu = 2\delta_{m,0}; \tag{3.14}$$

$$\int_{-1}^{+1} P_n(\mu)P_m(\mu)d\mu = \frac{2}{2m+1}\delta_{m,n}. \quad (3.15)$$

In order to solve the last integral, the recursive formula is used. The following result is obtained:

$$\begin{aligned} & \int_{-1}^{+1} \mu P_n(\mu)P_m(\mu)d\mu = \\ &= \int_{-1}^{+1} P_n(\mu)\frac{m+1}{2m+1}P_{m+1}(\mu)d\mu + \int_{-1}^{+1} P_n(\mu)\frac{m}{2m+1}P_{m-1}(\mu)d\mu = \\ &= \frac{m+1}{2m+1} \cdot \frac{2}{2(m+1)+1}\delta_{m+1,n} + \frac{m}{2m+1} \cdot \frac{2}{2(m-1)+1}\delta_{m-1,n}. \end{aligned} \quad (3.16)$$

Using these integrals, the formula (3.13) becomes:

$$\begin{aligned} & iB \left[\frac{m+1}{2m+1}\varphi_{m+1}(B, u) + \frac{m}{2m+1}\varphi_{m-1}(B, u) \right] + \Sigma_t(u)\varphi_m(B, u) = \\ &= S_m(B, u) + \frac{1}{1-\alpha}\Sigma_s(u)\varphi_0(B, u)(1 - e^{c-u})\delta_{m,0} + \\ &+ \frac{1}{1-\alpha}\frac{\partial}{\partial u}[\Sigma_s(u)\varphi_0(B, u)] [-1 - (c-u)e^{c-u} + e^{c-u}] \delta_{m,0} + \\ &+ \left(\frac{1}{1-\alpha} \right) \Sigma_s(u)\varphi_{m>0}(B, u) \int_c^u du' P_{m>0}(\xi(A, u', u))e^{u'-u}. \end{aligned} \quad (3.17)$$

From formula (3.8) it is possible to understand that in principle is possible obtain the exact solution, but infinite moments and, consequently, infinite equations with formula (3.17) are necessary. Actually, the value of the flux is approximated truncating the expansion at order N. Doing this procedure is easy to understand from formula (3.17) that N + 1 equation has been obtained with N+2 unknown. A closure equation is necessary in order to have a number of equation equal to the number of unknown and at the end to have an unique solution. The closure equation is set as:

$$\varphi_{N+1}(B, u) = 0. \quad (3.18)$$

3.1.2 B_N approximation

The B_N approximation is a method suitable for the solution of the neutron transport equation with the asymptotic theory assumption. The theory of this section is taken from [17].

In order to introduce the B_n method it is possible to start from formula (3.7). First

of all, the terms with the flux on the left hand side are collected.

$$\begin{aligned}
 \varphi(B, u, \mu) [iB\mu + \Sigma_t(u)] &= S(B, u, \mu) + \\
 &+ \frac{1}{2(1-\alpha)} \Sigma_s(u) \varphi_0(B, u) (1 - e^{c-u}) + \\
 &+ \frac{1}{2(1-\alpha)} \frac{\partial}{\partial u} [\Sigma_s(u) \varphi_0(B, u)] [-1 - (c-u)e^{c-u} + e^{c-u}] + \\
 &+ \sum_{n=1}^{+\infty} \left(\frac{2n+1}{2} \right) \frac{P_n(\mu)}{1-\alpha} \Sigma_s(u) \varphi_n(B, u) \int_c^u du' P_n(\xi(A, u', u)) e^{u'-u}.
 \end{aligned} \tag{3.19}$$

Just for convenience the following change of sign is imposed:

$$B_1 = -B. \tag{3.20}$$

The equation is modified as follow:

$$\begin{aligned}
 \varphi(B, u, \mu) [-iB_1\mu + \Sigma_t(u)] &= S(B, u, \mu) + \\
 &+ \frac{1}{2(1-\alpha)} \Sigma_s(u) \varphi_0(B, u) (1 - e^{c-u}) + \\
 &+ \frac{1}{2(1-\alpha)} \frac{\partial}{\partial u} [\Sigma_s(u) \varphi_0(B, u)] [-1 - (c-u)e^{c-u} + e^{c-u}] + \\
 &+ \sum_{n=1}^{+\infty} \left(\frac{2n+1}{2} \right) \frac{P_n(\mu)}{1-\alpha} \Sigma_s(u) \varphi_n(B, u) \int_c^u du' P_n(\xi(A, u', u)) e^{u'-u}.
 \end{aligned} \tag{3.21}$$

Then the flux term on the right hand side is isolated and the total cross section is collected:

$$\begin{aligned}
 \varphi(B, u, \mu) &= \frac{S(B, u, \mu)}{\Sigma_t(u) \left[1 - \frac{iB_1\mu}{\Sigma_t(u)} \right]} + \\
 &+ \frac{1}{2(1-\alpha)} \frac{\Sigma_s(u) \varphi_0(B, u)}{\Sigma_t(u) \left[1 - \frac{iB_1\mu}{\Sigma_t(u)} \right]} (1 - e^{c-u}) + \\
 &+ \frac{1}{2(1-\alpha)} \frac{\partial}{\partial u} [\Sigma_s(u) \varphi_0(B, u)] \frac{[-1 - (c-u)e^{c-u} + e^{c-u}]}{\Sigma_t(u) \left[1 - \frac{iB_1\mu}{\Sigma_t(u)} \right]} + \\
 &+ \sum_{n=1}^{+\infty} \left(\frac{2n+1}{2} \right) \frac{P_n(\mu)}{1-\alpha} \frac{\Sigma_s(u) \varphi_n(B, u)}{\Sigma_t(u) \left[1 - \frac{iB_1\mu}{\Sigma_t(u)} \right]} \cdot \\
 &\cdot \int_c^u du' P_n(\xi(A, u', u)) e^{u'-u}.
 \end{aligned} \tag{3.22}$$

The expansions presented in formulas (3.8,3.9) are substituted in the previous formula and then, in order to find an equation for each flux moment, the property in

formula (3.10) is used; it means to multiply each term of the previous formula per $P_m(\mu)$ and integrate between -1 and +1 in $d\mu$.

The following equation is obtained:

$$\begin{aligned}
 \varphi(B, u)_m = & \sum_{n=0}^{\infty} \left(\frac{2n+1}{2} \right) \frac{S_n(B, u)}{\Sigma_t(u)} \int_{-1}^{+1} \frac{P_n(\mu)P_m(\mu)}{\left[1 - \frac{iB_1\mu}{\Sigma_t(u)}\right]} d\mu + \\
 & + \frac{\Sigma_s(u)\varphi_0(B, u)(1 - e^{c-u})}{2\Sigma_t(u)(1 - \alpha)} \int_{-1}^{+1} \frac{P_m(\mu)}{\left[1 - \frac{iB_1\mu}{\Sigma_t(u)}\right]} d\mu + \\
 & + \frac{[-1 - (c - u)e^{c-u} + e^{c-u}]}{2\Sigma_t(u)(1 - \alpha)} \frac{\partial}{\partial u} [\Sigma_s(u)\varphi_0(B, u)]. \tag{3.23} \\
 & \cdot \int_{-1}^{+1} \frac{P_m(\mu)}{\left[1 - \frac{iB_1\mu}{\Sigma_t(u)}\right]} d\mu + \sum_{n=1}^{+\infty} \left(\frac{2n+1}{2} \right) \frac{\Sigma_s(u)\varphi_n(B, u)}{\Sigma_t(u)(1 - \alpha)} \\
 & \cdot \int_{-1}^{+1} \frac{P_n(\mu)P_m(\mu)}{\left[1 - \frac{iB_1\mu}{\Sigma_t(u)}\right]} d\mu \int_c^u du' P_n(\xi(A, u', u))e^{u'-u}.
 \end{aligned}$$

From [17] the following definitions and properties are taken:

$$A_{n,m}(B, u) = \frac{1}{2} \int_{-1}^{+1} \frac{P_n(\mu)P_m(\mu)}{\left[1 - \frac{iB_1\mu}{\Sigma_t(u)}\right]} d\mu \tag{3.24}$$

where $A_{n,m}(B, u)$ is the element in position (n, m) of the matrix A . The matrix A is evaluated with the following definitions:

$$y = \frac{iB_1}{\Sigma_t(u)}; \tag{3.25}$$

$$A_{0,0} = \frac{\tanh^{-1}(y)}{y}. \tag{3.26}$$

Some properties of the matrix are here presented. The first property is the symmetry of the matrix A :

$$A_{i,j} = A_{j,i}; \tag{3.27}$$

another property is the recursive relation between the elements of the matrix A :

$$\frac{1}{y}(2l+1)A_{j,l} - (l+1)A_{j,l+1} - lA_{j,l-1} = \frac{\delta_{j,l}}{y}. \tag{3.28}$$

After the isolation of the term $A_{j,l+1}$, it becomes:

$$A_{j,l+1} = \frac{1}{y} \frac{2l+1}{l+1} A_{j,l} - \frac{l}{l+1} A_{j,l-1} - \frac{\delta_{j,l}}{y(l+1)}. \tag{3.29}$$

Substituting formula (3.24) in formula (3.30) the following formula is obtained:

$$\begin{aligned}
 \varphi_m(B, u) = & \sum_{n=0}^{\infty} (2n+1) \frac{S_n(B, u)}{\Sigma_t(u)} A_{n,m}(B, u) + \\
 & + \frac{\Sigma_s(u) \varphi_0(B, u) (1 - e^{c-u})}{\Sigma_t(u) (1 - \alpha)} A_{0,m}(B, u) + \\
 & + \frac{[-1 - (c-u)e^{c-u} + e^{c-u}]}{\Sigma_t(u) (1 - \alpha)} \frac{\partial}{\partial u} [\Sigma_s(u) \varphi_0(B, u)] A_{0,m}(B, u) + \\
 & + \sum_{n=1}^{+\infty} (2n+1) \frac{\Sigma_s(u) \varphi_n(B, u)}{\Sigma_t(u) (1 - \alpha)} A_{n,m}(B, u) \int_c^u du' P_n(\xi(A, u', u)) e^{u'-u}.
 \end{aligned} \tag{3.30}$$

3.2 Greuling-Goertzel approach

In this section a similar approximation with respect to the previous section has been used. The collision density, also in this case, is considered as a slowly varying function over the lethargy range of the scattering integral, but instead of using a linear variation of the collision density, a second order variation is considered, only for the zero order moment:

$$\begin{aligned}
 \Sigma_s(u') \varphi_n(B, u') \approx & \Sigma_s(u) \varphi_n(B, u) + \\
 & + (u' - u) \frac{\partial}{\partial u} [\Sigma_s(u) \varphi_n(B, u)] \cdot \delta_{n,0} + \\
 & + \frac{1}{2} (u' - u)^2 \frac{\partial^2}{\partial u^2} [\Sigma_s(u) \varphi_n(B, u)] \cdot \delta_{n,0};
 \end{aligned} \tag{3.31}$$

substituting this approximation in formula(2.36), the following formula is obtained:

$$\begin{aligned}
 iB\mu\varphi(B, u, \mu) + \Sigma_t(u)\varphi(B, u, \mu) = & S(B, u, \mu) + \\
 & + \sum_{n=0}^{+\infty} \left(\frac{2n+1}{2} \right) P_n(\mu) \int_c^u \left[\Sigma_s(u) \varphi_n(B, u) + (u' - u) \cdot \right. \\
 & \cdot \frac{\partial}{\partial u} [\Sigma_s(u) \varphi_n(B, u)] \cdot \delta_{n,0} + \frac{1}{2} (u' - u)^2 \frac{\partial^2}{\partial u^2} [\Sigma_s(u) \varphi_n(B, u)] \cdot \delta_{n,0} \left. \right] \cdot \\
 & \cdot \frac{P_n(\xi(A, u', u)) e^{u'-u}}{1 - \alpha} du';
 \end{aligned} \tag{3.32}$$

then separating the terms of order zero from the other terms and separating the three terms of order zero themselves the equation becomes:

$$\begin{aligned}
 iB\mu\varphi(B, u, \mu) + \Sigma_t(u)\varphi(B, u, \mu) &= S(B, u, \mu) + \frac{1}{2(1-\alpha)} \cdot \\
 &\cdot P_0(\mu)\Sigma_s(u)\varphi_0(B, u) \int_c^u du' P_0(\xi(A, u', u))e^{u'-u} + \\
 &+ \frac{1}{2(1-\alpha)} P_0(\mu) \frac{\partial}{\partial u} [\Sigma_s(u)\varphi_0(B, u)] \cdot \\
 &\cdot \int_c^u du' (u' - u) P_0(\xi(A, u', u))e^{u'-u} + \\
 &+ \frac{1}{2} \cdot \frac{1}{2(1-\alpha)} P_0(\mu) \frac{\partial^2}{\partial u^2} [\Sigma_s(u)\varphi_0(B, u)] \cdot \\
 &\cdot \int_c^u du' (u' - u)^2 P_0(\xi(A, u', u))e^{u'-u} + \\
 &+ \sum_{n=1}^{+\infty} \left(\frac{2n+1}{2} \right) P_n(\mu) \cdot \\
 &\cdot \int_c^u du' [\Sigma_s(u)\varphi_n(B, u)] \frac{P_n(\xi(A, u', u))e^{u'-u}}{1-\alpha};
 \end{aligned} \tag{3.33}$$

considering that the Legendre polynomial of order zero is equal to one the formula becomes:

$$\begin{aligned}
 iB\mu\varphi(B, u, \mu) + \Sigma_t(u)\varphi(B, u, \mu) &= S(B, u, \mu) + \\
 &+ \frac{1}{2(1-\alpha)} \Sigma_s(u)\varphi_0(B, u) \int_c^u du' e^{u'-u} + \\
 &+ \frac{1}{2(1-\alpha)} \frac{\partial}{\partial u} [\Sigma_s(u)\varphi_0(B, u)] \int_c^u du' (u' - u) e^{u'-u} + \\
 &+ \frac{1}{2} \cdot \frac{1}{2(1-\alpha)} \frac{\partial^2}{\partial u^2} [\Sigma_s(u)\varphi_0(B, u)] \int_c^u du' (u' - u)^2 e^{u'-u} + \\
 &+ \sum_{n=1}^{+\infty} \left(\frac{2n+1}{2} \right) P_n(\mu) \Sigma_s(u)\varphi_n(B, u) \cdot \\
 &\cdot \int_c^u du' \frac{P_n(\xi(A, u', u))e^{u'-u}}{1-\alpha}.
 \end{aligned} \tag{3.34}$$

As it has been already done in section 3.1, the first two integrals are evaluated with formulas (3.5, 3.6) and the last integral is evaluated numerically for the same reason considered before. The third integral is also a trivial integral and it has been

evaluated as follow:

$$\int_c^u du' (u' - u)^2 e^{u'-u} = - (c - u)^2 e^{(c-u)} + 2(c - u)e^{(c-u)} + 2e^{(c-u)} + 2. \quad (3.35)$$

Using these integrals formula (3.34) becomes:

$$\begin{aligned} iB\mu\varphi(B, u, \mu) + \Sigma_t(u)\varphi(B, u, \mu) &= S(B, u, \mu) + \\ &+ \frac{1}{2(1 - \alpha)}\Sigma_s(u)\varphi_0(B, u)(1 - e^{c-u}) + \\ &+ \frac{1}{2(1 - \alpha)}\frac{\partial}{\partial u}[\Sigma_s(u)\varphi_0(B, u)] \left[-1 - (c - u)e^{c-u} + e^{c-u} \right] + \\ &+ \frac{1}{2} \cdot \frac{1}{2(1 - \alpha)}\frac{\partial^2}{\partial u^2}[\Sigma_s(u)\varphi_0(B, u)] \cdot \left[- (c - u)^2 e^{(c-u)} + \right. \\ &+ \left. 2(c - u)e^{(c-u)} - 2e^{(c-u)} + 2 \right] + \\ &+ \sum_{n=1}^{+\infty} \left(\frac{2n + 1}{2} \right) \frac{P_n(\mu)}{1 - \alpha} \Sigma_s(u)\varphi_n(B, u) \int_c^u du' P_n(\xi(A, u', u))e^{u'-u}. \end{aligned} \quad (3.36)$$

3.2.1 P_N approximation

In order to do the P_N approximation the expansions in formulas (3.8,3.9) are substituted in the previous formula to obtain:

$$\begin{aligned} iB\mu \sum_{n=0}^{\infty} \left(\frac{2n + 1}{2} \right) \varphi_n(B, u)P_n(\mu) + \\ + \Sigma_t(u) \sum_{n=0}^{\infty} \left(\frac{2n + 1}{2} \right) \varphi_n(B, u)P_n(\mu) = \\ = \sum_{n=0}^{\infty} \left(\frac{2n + 1}{2} \right) S_n(B, u)P_n(\mu) + \\ + \frac{1}{2(1 - \alpha)}\Sigma_s(u)\varphi_0(B, u)(1 - e^{c-u}) + \\ + \frac{1}{2(1 - \alpha)}\frac{\partial}{\partial u}[\Sigma_s(u)\varphi_0(B, u)] \left[-1 - (c - u)e^{c-u} + e^{c-u} \right] + \\ + \frac{1}{2} \cdot \frac{1}{2(1 - \alpha)}\frac{\partial^2}{\partial u^2}[\Sigma_s(u)\varphi_0(B, u)] \cdot \left[- (c - u)^2 e^{(c-u)} + \right. \\ + \left. 2(c - u)e^{(c-u)} - 2e^{(c-u)} + 2 \right] + \\ + \sum_{n=1}^{+\infty} \left(\frac{2n + 1}{2} \right) \frac{P_n(\mu)}{1 - \alpha} \Sigma_s(u)\varphi_n(B, u) \int_c^u du' P_n(\xi(A, u', u))e^{u'-u}. \end{aligned} \quad (3.37)$$

In order to find an equation for each flux moment the property in formula (3.10) is used; it means to multiply each term of the previous formula per $P_m(\mu)$ and integrate between minus one and plus one in $d\mu$ as it is illustrated in the following formula:

$$\begin{aligned}
 & iB \sum_{n=0}^{\infty} \left(\frac{2n+1}{2} \right) \varphi_n(B, u) \int_{-1}^{+1} \mu P_n(\mu) P_m(\mu) d\mu + \\
 & + \Sigma_t(u) \sum_{n=0}^{\infty} \left(\frac{2n+1}{2} \right) \varphi_n(B, u) \int_{-1}^{+1} P_n(\mu) P_m(\mu) d\mu = \\
 & = \sum_{n=0}^{\infty} \left(\frac{2n+1}{2} \right) S_n(B, u) \int_{-1}^{+1} P_n(\mu) P_m(\mu) d\mu + \\
 & + \frac{1}{2(1-\alpha)} \Sigma_s(u) \varphi_0(B, u) (1 - e^{c-u}) \int_{-1}^{+1} P_m(\mu) d\mu + \\
 & + \frac{1}{2(1-\alpha)} \frac{\partial}{\partial u} [\Sigma_s(u) \varphi_0(B, u)] [-1 - (c-u)e^{c-u} + e^{c-u}] \cdot \\
 & \cdot \int_{-1}^{+1} P_m(\mu) d\mu + \frac{1}{2} \cdot \frac{1}{2(1-\alpha)} \frac{\partial^2}{\partial u^2} [\Sigma_s(u) \varphi_0(B, u)] \cdot \\
 & \cdot [- (c-u)^2 e^{c-u} + 2(c-u)e^{c-u} - 2e^{c-u} + 2] \cdot \\
 & \cdot \int_{-1}^{+1} P_m(\mu) d\mu + \sum_{n=1}^{+\infty} \left(\frac{2n+1}{2(1-\alpha)} \right) \int_{-1}^{+1} P_n(\mu) P_m(\mu) d\mu \cdot \\
 & \cdot \Sigma_s(u) \varphi_n(B, u) \int_c^u du' P_n(\xi(A, u', u)) e^{u'-u}.
 \end{aligned} \tag{3.38}$$

Using the integral solutions that have been presented in formulas (3.14,3.15,3.16) this last equation becomes:

$$\begin{aligned}
 & iB \left[\frac{m+1}{2m+1} \varphi_{m+1}(B, u) + \frac{m}{2m+1} \varphi_{m-1}(B, u) \right] + \Sigma_t(u) \varphi_m(B, u) = \\
 & = S_m(B, u) + \frac{1}{1-\alpha} \Sigma_s(u) \varphi_0(B, u) (1 - e^{c-u}) \delta_{m,0} + \\
 & + \frac{1}{1-\alpha} \frac{\partial}{\partial u} [\Sigma_s(u) \varphi_0(B, u)] [-1 - (c-u)e^{c-u} + e^{c-u}] \delta_{m,0} + \\
 & + \frac{1}{2} \cdot \frac{1}{(1-\alpha)} \frac{\partial^2}{\partial u^2} [\Sigma_s(u) \varphi_0(B, u)] \cdot \\
 & \cdot [- (c-u)^2 e^{c-u} + 2(c-u)e^{c-u} - 2e^{c-u} + 2] \delta_{m,0} + \\
 & + \left(\frac{1}{1-\alpha} \right) \Sigma_s(u) \varphi_{m>0}(B, u) \int_c^u du' P_{m>0}(\xi(A, u', u)) e^{u'-u}
 \end{aligned} \tag{3.39}$$

Also in this case a truncation as well as a closure equation are needed, as in section 3.1.1, in order to have a finite number of equation and a closed system of equation. The closure equation, that is used, is the one in formula (3.18).

3.3 Discrete lethargy approach

In this section no approximations are introduced for the collision density. Instead, the scattering integral is approximated using the composite trapezoidal rule [18]. The general formula of the composite trapezoidal rule is given in the following formula:

$$\int_a^b f(x)dx \approx \frac{b-a}{n} \left(\frac{f(a)}{2} + \sum_{k=1}^{n-1} \left(f\left(a + k \frac{b-a}{n}\right) \right) + \frac{f(b)}{2} \right), \quad (3.40)$$

where n is the number of subintervals.
Calling:

$$h = \frac{b-a}{n}, \quad (3.41)$$

where h is the amplitude of each subinterval. The formula (3.40) becomes:

$$\int_a^b f(x)dx \approx \frac{h}{2} \left(f(a) + 2 \sum_{k=1}^{n-1} \left(f\left(a + k \frac{b-a}{n}\right) \right) + f(b) \right). \quad (3.42)$$

In order to apply this approximation a lethargy discretization is necessary; that discretization will be presented in the next chapter. For the time being the composite trapezoidal rule is used as follow. This approximation is applied to equation

(2.36). The scattering integral becomes:

$$\begin{aligned}
 & \int_c^u du' \Sigma_s(u') \varphi_n(B, u') \frac{P_n(\xi(A, u', u)) e^{u'-u}}{1-\alpha} \approx \\
 & \approx \frac{h}{2} \left(\Sigma_s(c) \varphi_n(B, c) \frac{P_n(\xi(A, c, u)) e^{c-u}}{1-\alpha} + \right. \\
 & \quad \left. + 2 \sum_{i=1}^{N-1} \left(\Sigma_s(u_i) \varphi_n(B, u_i) \frac{P_n(\xi(A, u_i, u)) e^{u_i-u}}{1-\alpha} \right) + \right. \\
 & \quad \left. + \Sigma_s(u) \varphi_n(B, u) \frac{P_n(\xi(A, u, u)) e^{u-u}}{1-\alpha} \right) = \\
 & = \frac{h}{2} \left(\Sigma_s(c) \varphi_n(B, c) \frac{P_n(\xi(A, c, u)) e^{c-u}}{1-\alpha} + \right. \\
 & \quad \left. + 2 \sum_{i=1}^{N-1} \left(\Sigma_s(u_i) \varphi_n(B, u_i) \frac{P_n(\xi(A, u_i, u)) e^{u_i-u}}{1-\alpha} \right) + \right. \\
 & \quad \left. + \frac{\Sigma_s(u) \varphi_n(B, u)}{1-\alpha} \right), \tag{3.43}
 \end{aligned}$$

where:

$$u_i = c + hi. \tag{3.44}$$

Substituting this approximation in equation (2.36) the following formula is obtained:

$$\begin{aligned}
 iB\mu\varphi(B, u, \mu) + \Sigma_t(u)\varphi(B, u, \mu) &= S(B, u, \mu) + \sum_{n=0}^{+\infty} \left(\frac{2n+1}{2} \right) \cdot \\
 & \cdot P_n(\mu) \frac{h}{2} \left(\Sigma_s(c) \varphi_n(B, c) \frac{P_n(\xi(A, c, u)) e^{c-u}}{1-\alpha} + \right. \\
 & \quad \left. + 2 \sum_{i=1}^{N-1} \left(\Sigma_s(u_i) \varphi_n(B, u_i) \frac{P_n(\xi(A, u_i, u)) e^{u_i-u}}{1-\alpha} \right) + \right. \\
 & \quad \left. + \frac{\Sigma_s(u) \varphi_n(B, u)}{1-\alpha} \right). \tag{3.45}
 \end{aligned}$$

3.3.1 P_N approximation

Also in this case the problem is solved through the use of the P_N approximation. The same procedure of the previous cases is applied. First of all the expansions

for the source and for the flux (formulas (3.8,3.9) are substituted in the previous formula:

$$\begin{aligned}
 & iB\mu \sum_{n=0}^{\infty} \left(\frac{2n+1}{2} \right) \varphi_n(B, u) P_n(\mu) + \\
 & + \Sigma_t(u) \sum_{n=0}^{\infty} \left(\frac{2n+1}{2} \right) \varphi_n(B, u) P_n(\mu) = \\
 & = \sum_{n=0}^{\infty} \left(\frac{2n+1}{2} \right) S_n(B, u) P_n(\mu) + \sum_{n=0}^{+\infty} \left(\frac{2n+1}{2} \right) \cdot \\
 & \cdot P_n(\mu) \frac{h}{2} \left(\Sigma_s(c) \varphi_n(B, c) \frac{P_n(\xi(A, c, u)) e^{c-u}}{1-\alpha} + \right. \\
 & + 2 \sum_{i=1}^{N-1} \left(\Sigma_s(u_i) \varphi_n(B, u_i) \frac{P_n(\xi(A, u_i, u)) e^{u_i-u}}{1-\alpha} \right) + \\
 & \left. + \frac{\Sigma_s(u) \varphi_n(B, u)}{1-\alpha} \right); \tag{3.46}
 \end{aligned}$$

then each term that has been obtained is multiplied per $P_m(\mu)$ and integrate between minus one and plus one in $d\mu$. Having done these procedures, the following formula is obtained:

$$\begin{aligned}
 & iB \sum_{n=0}^{\infty} \left(\frac{2n+1}{2} \right) \varphi_n(B, u) \int_{-1}^{+1} \mu P_n(\mu) P_m(\mu) d\mu + \\
 & + \Sigma_t(u) \sum_{n=0}^{\infty} \left(\frac{2n+1}{2} \right) \varphi_n(B, u) \int_{-1}^{+1} P_n(\mu) P_m(\mu) d\mu = \\
 & = \sum_{n=0}^{\infty} \left(\frac{2n+1}{2} \right) S_n(B, u) \int_{-1}^{+1} P_n(\mu) P_m(\mu) d\mu + \\
 & + \sum_{n=0}^{+\infty} \left(\frac{2n+1}{2} \right) \int_{-1}^{+1} P_n(\mu) P_m(\mu) d\mu \cdot \\
 & \cdot \frac{h}{2} \left(\Sigma_s(c) \varphi_n(B, c) \frac{P_n(\xi(A, c, u)) e^{c-u}}{1-\alpha} + \right. \\
 & + 2 \sum_{i=1}^{N-1} \left(\Sigma_s(u_i) \varphi_n(B, u_i) \frac{P_n(\xi(A, u_i, u)) e^{u_i-u}}{1-\alpha} \right) + \\
 & \left. + \frac{\Sigma_s(u) \varphi_n(B, u)}{1-\alpha} \right). \tag{3.47}
 \end{aligned}$$

Using the integral solutions that have been presented in formulas (3.14,3.15,3.16) the following equation is obtained:

$$\begin{aligned}
 & iB \left[\frac{m+1}{2m+1} \varphi_{m+1}(B, u) + \frac{m}{2m+1} \varphi_{m-1}(B, u) \right] + \Sigma_t(u) \varphi_m(B, u) = \\
 & = S_m(B, u) + \frac{h}{2} \left(\Sigma_s(c) \varphi_m(B, c) \frac{P_m(\xi(A, c, u)) e^{c-u}}{1-\alpha} + \right. \\
 & + 2 \sum_{i=1}^{N-1} \left(\Sigma_s(u_i) \varphi_m(B, u_i) \frac{P_m(\xi(A, u_i, u)) e^{u_i-u}}{1-\alpha} \right) + \\
 & \left. + \frac{\Sigma_s(u) \varphi_m(B, u)}{1-\alpha} \right). \tag{3.48}
 \end{aligned}$$

Also in this case a truncation as well as a closure equation are needed, as in section 3.1.1, in order to have a finite number of equation and a closed system of equation. The closure equation that has been used is the one in formula (3.18).

3.4 Selengut-Goertzel approach

In this section the case of the water as moderator is treated. In order to use the continuous Fermi slowing down the hypothesis of small loss of energy per interaction has been done. In the case in which hydrogen is part of the moderator molecule's, this hypothesis is not verified, because the hydrogen mass is comparable with the neutron mass and so the loss of energy per interaction becomes relevant; for this reason for the hydrogen the hypothesis of linear collision density is not verified. In order to deal with this problem, the scattering integral is divided in two terms: one for the hydrogen part of the molecule; one for non-hydrogen part of the molecule. For water the scattering integral becomes:

$$\begin{aligned}
 & \int_c^u du' \Sigma_s(u') \varphi_n(B, u') \frac{P_n(\xi(A, u', u)) e^{u'-u}}{1-\alpha} = \\
 & = \int_{c_O}^u du' \Sigma_{s,O}(u') \varphi_n(B, u') \frac{P_n(\xi_O(A_O, u', u)) e^{u'-u}}{1-\alpha_O} + \\
 & + \int_{c_H}^u du' \Sigma_{s,H}(u') \varphi_n(B, u') \frac{P_n(\xi_H(A_H, u', u)) e^{u'-u}}{1-\alpha_H}, \tag{3.49}
 \end{aligned}$$

where:

$$c_O = \max[u + \ln(\alpha_O), 0]; \tag{3.50}$$

$$c_H = \max[u + \ln(\alpha_H), 0]. \tag{3.51}$$

In the case of the zero order moment for the oxygen part the Fermi continuous slowing down is used for the collision density(formula (3.1)); instead for the hydrogen part the composite trapezoidal rule is used (formula (3.43)). In the cases of successive order moments, the collision density is considered approximately constant (like the Fermi continuous slowing down case). Substituting these approximations in equation (2.36) the following formula is obtained:

$$\begin{aligned}
 iB\mu\varphi(B, u, \mu) + \Sigma_t(u)\varphi(B, u, \mu) = & S(B, u, \mu) + \\
 & + \frac{1}{2(1 - \alpha_O)}\Sigma_{s,O}(u)\varphi_0(B, u)(1 - e^{c_O - u}) + \\
 & + \frac{1}{2(1 - \alpha_O)}\frac{\partial}{\partial u}[\Sigma_{s,O}(u)\varphi_0(B, u)] \cdot \\
 & \cdot [-1 - (c_O - u)e^{c_O - u} + e^{c_O - u}] + \\
 & + \sum_{n=1}^{+\infty} \left(\frac{2n+1}{2} \right) \frac{P_n(\mu)}{1 - \alpha_O} \Sigma_{s,O}(u)\varphi_n(B, u) \cdot \\
 & \cdot \int_{c_O}^u du' P_n(\xi_O(A_O, u', u))e^{u' - u} + \\
 & + \frac{1}{2} \cdot \frac{h}{2} \left[\Sigma_{s,H}(c_H)\varphi_0(B, c_H) \frac{e^{c_H - u}}{1 - \alpha_H} + \right. \\
 & + 2 \sum_{i=1}^{N-1} \left(\Sigma_{s,H}(u_i)\varphi_0(B, u_i) \frac{e^{u_i - u}}{1 - \alpha_H} \right) + \\
 & \left. + \frac{\Sigma_{s,H}(u)\varphi_0(B, u)}{1 - \alpha_H} \right] + \sum_{n=1}^{+\infty} \left(\frac{2n+1}{2} \right) \frac{P_n(\mu)}{1 - \alpha_H} \cdot \\
 & \cdot \Sigma_{s,H}(u)\varphi_n(B, u) \int_{c_H}^u du' P_n(\xi_H(A_H, u', u))e^{u' - u}
 \end{aligned} \tag{3.52}$$

3.4.1 P_N approximation

Also in this case the problem is solved through the use of the P_N approximation. The same procedure of the other cases is applied. First of all the expansions for the source and for the flux (formulas (3.8,3.9)) are substituted in the previous formula; then each term that has been obtained is multiplied per $P_m(\mu)$ and integrate between minus one and plus one in $d\mu$. Since the formulas used for this method

are of the same type of previous cases, the final formula is presented:

$$\begin{aligned}
 & iB \left[\frac{m+1}{2m+1} \varphi_{m+1}(B, u) + \frac{m}{2m+1} \varphi_{m-1}(B, u) \right] + \Sigma_t(u) \varphi_m(B, u) = \\
 & = S_m(B, u) + \frac{1}{1 - \alpha_O} \Sigma_{s,O}(u) \varphi_0(B, u) (1 - e^{c_O - u}) \delta_{m,0} + \\
 & + \frac{1}{1 - \alpha_O} \frac{\partial}{\partial u} [\Sigma_{s,O}(u) \varphi_0(B, u)] \cdot \\
 & \cdot [-1 - (c_O - u) e^{c_O - u} + e^{c_O - u}] \delta_{m,0} + \\
 & + \left(\frac{1}{1 - \alpha_O} \right) \Sigma_{s,O}(u) \varphi_{m>0}(B, u) \cdot \\
 & \cdot \int_{c_O}^u du' P_{m>0}(\xi_O(A_O, u', u)) e^{u' - u} + \\
 & + \frac{h}{2} \left[\Sigma_{s,H}(c_H) \varphi_0(B, c_H) \frac{e^{c_H - u}}{1 - \alpha_H} + \right. \\
 & + 2 \sum_{i=1}^{N-1} \left(\Sigma_{s,H}(u_i) \varphi_0(B, u_i) \frac{e^{u_i - u}}{1 - \alpha_H} \right) + \\
 & \left. + \frac{\Sigma_{s,H}(u) \varphi_0(B, u)}{1 - \alpha_H} \right] \delta_{m,0} + \left(\frac{1}{1 - \alpha_H} \right) \Sigma_{s,H}(u) \varphi_{m>0}(B, u) \cdot \\
 & \cdot \int_{c_H}^u du' P_{m>0}(\xi_H(A_H, u', u)) e^{u' - u}.
 \end{aligned} \tag{3.53}$$

Also in this case a truncation as well as a closure equation are needed, as in section 3.1.1, in order to have a finite number of equation and a closed system of equation. The closure equation that has been used is the one in formula (3.18).

Chapter 4

The numerical procedure to solve the neutron spectra in a homogeneous slab

In this chapter the numerical procedure to solve the problem, with the different approximation methods, that are presented in the previous chapters, is explained. In order to do that, the lethargy discretization in general is firstly presented; then the numerical discretization for each approximation method is reported.

4.1 Discretization

In order to solve the neutron transport with the methods explained in the previous chapter, a lethargy discretization is necessary. Then, the introduction of discretization formulas for first and second order derivative are used in order to solve almost all the approximations. For simplicity an uniform lethargy grid is used; with this assumption the derivative approximations in an internal point are given in the following formulas; these formulas have been found through the use of the central difference scheme [18]; the following formula is used for the first derivative:

$$f'(x_j) = \frac{f(x_{j+1}) - f(x_{j-1}))}{2\Delta x}; \quad (4.1)$$

the following formula is used for the second derivative:

$$f''(x_j) = \frac{f(x_{j+1}) - 2f(x_j) + f(x_{j-1}))}{(\Delta x)^2}. \quad (4.2)$$

The approximation of the derivatives in the first lethargy point (zero lethargy) are not necessary, because the derivatives are inside the scattering integral that in the

first lethargy point is zero (integral in a point). In the last lethargy point, there is no possibility to consider the point $j + 1$ because it is outside the domain. The formulas used are no more based on a central difference scheme but on an upwind scheme. The formulas used in this case are reported below:

$$f'(x_j) = \frac{f(x_j) - f(x_{j-1})}{\Delta x}; \quad (4.3)$$

$$f''(x_j) = \frac{(f(x_j) - f(x_{j-1}))(x_{j-1} - x_{j-2}) - (f(x_{j-1}) - f(x_{j-2}))(x_j - x_{j-1}))}{(x_j - x_{j-1})^2(x_{j-1} - x_{j-2})}. \quad (4.4)$$

For the discrete method the approximation used is the one presented in formula (3.42).

Using these approximations, the problem is reduced into a linear system of the type:

$$\mathbf{A} \cdot \varphi = \mathbf{b}; \quad (4.5)$$

where:

- φ is the vector containing all the flux moment for each lethargy value considered, with M number of point in the lethargy grid; the vector φ has the following form:

$$\varphi = \begin{bmatrix} \varphi_0(u_0) \\ \varphi_1(u_0) \\ \vdots \\ \varphi_N(u_0) \\ \varphi_0(u_1) \\ \varphi_1(u_1) \\ \vdots \\ \varphi_N(u_1) \\ \vdots \\ \varphi_0(u_j) \\ \varphi_1(u_j) \\ \vdots \\ \varphi_N(u_j) \\ \vdots \\ \varphi_0(u_M) \\ \vdots \\ \varphi_N(u_M) \end{bmatrix}; \quad (4.6)$$

- \mathbf{A} is a $[(N + 2) \times M, (N + 2) \times M]$ matrix for the P_N method and a $[(N + 1) \times M, (N + 1) \times M]$ matrix for the B_N method with the coefficient of each flux

moment for each lethargy, with M number of lethargy point and N the order of the approximation; the matrix has the following form:

$$\mathbf{A} = \begin{bmatrix} a_{11} & a_{12} & \dots \\ a_{21} & a_{22} & \dots \\ \vdots & \vdots & \ddots \end{bmatrix}; \quad (4.7)$$

- \mathbf{b} is the vector containing the source term.

4.1.1 Fermi continuous slowing down model, \mathbf{P}_N approximation

For the continuous Fermi slowing down, formulas (4.1, 4.3) are needed; substituting in equation (3.17), the following results are obtained. First of all, the formula for the first lethargy point (the zero lethargy point) is reported:

$$iB \frac{m+1}{2m+1} \varphi_{m+1}(B,0) + iB \frac{m}{2m+1} \varphi_{m-1}(B,0) + \Sigma_t(0) \varphi_m(B,0) = S_m(B,0). \quad (4.8)$$

Then the following formulas report the discretized equation for the other lethargy points. For a lethargy point inside the interval the following formula is obtained:

$$\begin{aligned} & iB \left[\frac{m+1}{2m+1} \varphi_{m+1}(B, u_j) + \frac{m}{2m+1} \varphi_{m-1}(B, u_j) \right] + \\ & + \Sigma_t(u_j) \varphi_m(B, u_j) = S_m(B, u_j) + \\ & + \frac{1}{1-\alpha} \Sigma_s(u_j) \varphi_0(B, u_j) (1 - e^{c-u_j}) \delta_{m,0} + \\ & + \frac{1}{1-\alpha} \frac{\Sigma_s(u_{j+1}) \varphi_0(B, u_{j+1}) - \Sigma_s(u_{j-1}) \varphi_0(B, u_{j-1})}{u_{j+1} - u_{j-1}} \cdot \\ & \cdot [-1 - (c - u_j) e^{c-u_j} + e^{c-u_j}] \delta_{m,0} + \\ & + \left(\frac{1}{1-\alpha} \right) \Sigma_s(u_j) \varphi_{m>0}(B, u_j) \cdot \\ & \cdot \int_c^{u_j} du' P_{m>0}(\xi(A, u', u_j)) e^{u'-u_j}; \end{aligned} \quad (4.9)$$

for the last lethargy point the following formula is obtained:

$$\begin{aligned}
 & iB \left[\frac{m+1}{2m+1} \varphi_{m+1}(B, u_j) + \frac{m}{2m+1} \varphi_{m-1}(B, u_j) \right] + \\
 & + \Sigma_t(u_j) \varphi_m(B, u_j) = S_m(B, u_j) + \\
 & + \frac{1}{1-\alpha} \Sigma_s(u_j) \varphi_0(B, u_j) (1 - e^{c-u}) \delta_{m,0} + \\
 & + \frac{1}{1-\alpha} \frac{\Sigma_s(u_j) \varphi_0(B, u_j) - \Sigma_s(u_{j-1}) \varphi_0(B, u_{j-1})}{u_j - u_{j-1}}. \tag{4.10} \\
 & \cdot [-1 - (c - u_j) e^{c-u_j} + e^{c-u_j}] \delta_{m,0} + \\
 & + \left(\frac{1}{1-\alpha} \right) \Sigma_s(u_j) \varphi_{m>0}(B, u_j) \cdot \\
 & \cdot \int_c^{u_j} du' P_{m>0}(\xi(A, u', u_j)) e^{u'-u_j}.
 \end{aligned}$$

Putting together the same order moment at same energy the following formula is obtained for a point inside the lethargy interval:

$$\begin{aligned}
 & iB \frac{m+1}{2m+1} \varphi_{m+1}(B, u_j) + iB \frac{m}{2m+1} \varphi_{m-1}(B, u_j) + \\
 & + \varphi_m(B, u_j) \left[\Sigma_t(u_j) - \frac{1}{1-\alpha} \Sigma_s(u_j) (1 - e^{c-u_j}) \delta_{m,0} + \right. \\
 & - \left. \left(\frac{1}{1-\alpha} \right) \Sigma_s(u_j) \int_c^{u_j} du' P_{m>0}(\xi(A, u', u_j)) e^{u'-u_j} \cdot \right. \\
 & \cdot (m > 0) \left. \right] + \varphi_0(B, u_{j+1}) \frac{-1}{1-\alpha} \frac{\Sigma_s(u_{j+1})}{u_{j+1} - u_{j-1}}. \tag{4.11} \\
 & \cdot [-1 - (c - u_j) e^{c-u_j} + e^{c-u_j}] \delta_{m,0} + \\
 & + \varphi_0(B, u_{j-1}) \frac{1}{1-\alpha} \frac{\Sigma_s(u_{j-1})}{u_{j+1} - u_{j-1}} \cdot \\
 & \cdot [-1 - (c - u_j) e^{c-u_j} + e^{c-u_j}] \delta_{m,0} = S_m(B, u_j),
 \end{aligned}$$

instead the following one is obtained for the last lethargy point:

$$\begin{aligned}
 & iB \frac{m+1}{2m+1} \varphi_{m+1}(B, u_j) + iB \frac{m}{2m+1} \varphi_{m-1}(B, u_j) + \\
 & + \varphi_m(B, u_j) \left[\Sigma_t(u_j) - \frac{1}{1-\alpha} \Sigma_s(u_j) (1 - e^{c-u_j}) \delta_{m,0} + \right. \\
 & - \left. \left(\frac{1}{1-\alpha} \right) \Sigma_s(u_j) \int_c^{u_j} du' P_{m>0}(\xi(A, u', u_j)) e^{u'-u_j} \right. \\
 & \cdot (m > 0) - \frac{1}{1-\alpha} \frac{\Sigma_s(u_j)}{u_j - u_{j-1}} \\
 & \cdot \left. \left[-1 - (c - u_j) e^{c-u_j} + e^{c-u_j} \right] \delta_{m,0} \right] + \\
 & + \varphi_0(B, u_{j-1}) \frac{1}{1-\alpha} \frac{\Sigma_s(u_{j-1})}{u_j - u_{j-1}} \\
 & \cdot \left[-1 - (c - u_j) e^{c-u_j} + e^{c-u_j} \right] \delta_{m,0} = S_m(B, u_j).
 \end{aligned} \tag{4.12}$$

The terms that multiply the flux momenta are the coefficient of the matrix \mathbf{A} ; instead the part on the right hand side of the equal are the terms of the vector \mathbf{b} . For this approximation method, the matrix \mathbf{A} of formula (4.5) is a five diagonal matrix, with non zero elements in the principal diagonal, in the first diagonal above and below the principal diagonal and in the $N + 2$ diagonal above and below the principal one; the only exception are the rows multiple of $N + 2$ where the closure equation is imposed.

4.1.2 Fermi continuous slowing down model, \mathbf{B}_N approximation

Since the approach is again the continuous Fermi slowing down, formulas (4.1, 4.3) are needed; substituting in equation (3.30), the following results are obtained. First of all, the formula for the first lethargy point (the zero lethargy point) is reported:

$$\varphi_m(B, 0) = \sum_{n=0}^{\infty} (2n+1) \frac{S_n(B, 0)}{\Sigma_t(0)} A_{n,m}(B, 0). \tag{4.13}$$

Then the following formulas report the discretized equation for the other lethargy points. For a lethargy point inside the interval the following formula is obtained:

$$\begin{aligned}
 \varphi_m(B, u_j) = & \sum_{n=0}^{\infty} (2n+1) \frac{S_n(B, u_j)}{\Sigma_t(u_j)} A_{n,m}(B, u_j) + \\
 & + \frac{\Sigma_s(u_j)\varphi_0(B, u_j)(1 - e^{c-u_j})}{\Sigma_t(u_j)(1 - \alpha)} A_{0,m}(B, u_j) + \\
 & + \frac{[-1 - (c - u_j)e^{c-u_j} + e^{c-u_j}]}{\Sigma_t(u_j)(1 - \alpha)} A_{0,m}(B, u_j). \tag{4.14} \\
 & \cdot \frac{\Sigma_s(u_{j+1})\varphi_0(B, u_{j+1}) - \Sigma_s(u_{j-1})\varphi_0(B, u_{j-1})}{u_{j+1} - u_{j-1}} + \\
 & + \sum_{n=1}^{+\infty} (2n+1) \frac{\Sigma_s(u_j)\varphi_n(B, u_j)}{\Sigma_t(u_j)(1 - \alpha)} A_{n,m}(B, u_j) \int_c^{u_j} du' P_n(\xi(A, u', u_j)) e^{u'-u_j};
 \end{aligned}$$

for the last lethargy point the following formula is obtained:

$$\begin{aligned}
 \varphi_m(B, u_j) = & \sum_{n=0}^{\infty} (2n+1) \frac{S_n(B, u_j)}{\Sigma_t(u_j)} A_{n,m}(B, u_j) + \\
 & + \frac{\Sigma_s(u_j)\varphi_0(B, u_j)(1 - e^{c-u_j})}{\Sigma_t(u_j)(1 - \alpha)} A_{0,m}(B, u_j) + \\
 & + \frac{[-1 - (c - u_j)e^{c-u_j} + e^{c-u_j}]}{\Sigma_t(u_j)(1 - \alpha)} A_{0,m}(B, u_j). \tag{4.15} \\
 & \cdot \frac{\Sigma_s(u_j)\varphi_0(B, u_j) - \Sigma_s(u_{j-1})\varphi_0(B, u_{j-1})}{u_j - u_{j-1}} + \\
 & + \sum_{n=1}^{+\infty} (2n+1) \frac{\Sigma_s(u_j)\varphi_n(B, u_j)}{\Sigma_t(u_j)(1 - \alpha)} A_{n,m}(B, u_j) \int_c^{u_j} du' P_n(\xi(A, u', u_j)) e^{u'-u_j}.
 \end{aligned}$$

Putting together the same order moment at same energy the following formula is obtained for a point inside the lethargy interval:

$$\begin{aligned}
 & \varphi_0(B, u_j) \frac{\Sigma_s(u_j)(1 - e^{c-u_j})}{\Sigma_t(u_j)(1 - \alpha)} A_{0,m}(B, u_j) + \\
 & + \varphi_0(B, u_{j+1}) \frac{[-1 - (c - u_j)e^{c-u_j} + e^{c-u_j}]}{\Sigma_t(u_j)(1 - \alpha)} A_{0,m}(B, u_j) \frac{\Sigma_s(u_{j+1})}{u_{j+1} - u_{j-1}} + \\
 & + \varphi_0(B, u_{j-1}) \frac{[-1 - (c - u_j)e^{c-u_j} + e^{c-u_j}]}{\Sigma_t(u_j)(1 - \alpha)} A_{0,m}(B, u_j) \frac{-\Sigma_s(u_{j-1})}{u_{j+1} - u_{j-1}} + \\
 & + \sum_{n=1}^{+\infty} (2n + 1) \frac{\Sigma_s(u_j)\varphi_n(B, u_j)}{\Sigma_t(u_j)(1 - \alpha)} A_{n,m}(B, u_j) \cdot \\
 & \cdot \int_c^{u_j} du' P_n(\xi(A, u', u_j)) e^{u'-u_j} - \varphi_m(B, u_j) = \\
 & = - \sum_{n=0}^{\infty} (2n + 1) \frac{S_n(B, u_j)}{\Sigma_t(u_j)} A_{n,m}(B, u_j);
 \end{aligned} \tag{4.16}$$

instead the following one is obtained for the last lethargy point:

$$\begin{aligned}
 & \varphi_0(B, u_j) \frac{\Sigma_s(u_j)A_{0,m}(B, u_j)}{\Sigma_t(u_j)(1 - \alpha)} \left[(1 - e^{c-u_j}) + \frac{[-1 - (c - u_j)e^{c-u_j} + e^{c-u_j}]}{u_j - u_{j-1}} \right] + \\
 & + \varphi_0(B, u_{j-1}) \frac{[-1 - (c - u_j)e^{c-u_j} + e^{c-u_j}]}{\Sigma_t(u_j)(1 - \alpha)} A_{0,m}(B, u_j) \frac{-\Sigma_s(u_{j-1})}{u_j - u_{j-1}} + \\
 & + \sum_{n=1}^{+\infty} (2n + 1) \varphi_n(B, u_j) \frac{\Sigma_s(u_j)}{\Sigma_t(u_j)(1 - \alpha)} A_{n,m}(B, u_j) \cdot \\
 & \cdot \int_c^{u_j} du' P_n(\xi(A, u', u_j)) e^{u'-u_j} - \varphi_m(B, u_j) = \\
 & = - \sum_{n=0}^{\infty} (2n + 1) \frac{S_n(B, u_j)}{\Sigma_t(u_j)} A_{n,m}(B, u_j).
 \end{aligned} \tag{4.17}$$

The terms that multiply the flux momenta are the coefficient of the matrix \mathbf{A} ; instead the part on the right hand side of the equal are the terms of the vector \mathbf{b} . For this approximation method, the matrix \mathbf{A} of formula (4.5) is a full matrix, since all flux momenta appear in the equation for the generic momentum of order m .

4.1.3 Greuling-Goertzel approach, \mathbf{P}_N approximation

For the Greuling-Goertzel approach, formulas (4.1, 4.2, 4.3, 4.4) are needed; substituting in equation (3.39), the following results are obtained. First of all, the

formula for the first lethargy point (the zero lethargy point) is reported:

$$iB \frac{m+1}{2m+1} \varphi_{m+1}(B,0) + iB \frac{m}{2m+1} \varphi_{m-1}(B,0) + \Sigma_t(0) \varphi_m(B,0) = S_m(B,0). \quad (4.18)$$

Then the following formulas report the discretized equation for the other lethargy points. For a lethargy point inside the interval the following formula is obtained:

$$\begin{aligned} & iB \left[\frac{m+1}{2m+1} \varphi_{m+1}(B, u_j) + \frac{m}{2m+1} \varphi_{m-1}(B, u_j) \right] + \Sigma_t(u_j) \varphi_m(B, u_j) = \\ & = S_m(B, u_j) + \frac{1}{1-\alpha} \Sigma_s(u_j) \varphi_0(B, u_j) (1 - e^{c-u_j}) \delta_{m,0} + \\ & + \frac{1}{1-\alpha} \frac{\Sigma_s(u_{j+1}) \varphi_0(B, u_{j+1}) - \Sigma_s(u_{j-1}) \varphi_0(B, u_{j-1})}{u_{j+1} - u_{j-1}} \cdot \\ & \cdot \left[-1 - (c - u_j) e^{c-u_j} + e^{c-u_j} \right] \delta_{m,0} + \frac{1}{2} \cdot \frac{1}{(1-\alpha)} \cdot \\ & \cdot \frac{\Sigma_s(u_{j+1}) \varphi_0(B, u_{j+1}) - 2\Sigma_s(u_j) \varphi_0(B, u_j) + \Sigma_s(u_{j-1}) \varphi_0(B, u_{j-1})}{(u_j - u_{j-1})^2} \cdot \\ & \cdot \left[-(c - u_j)^2 e^{(c-u_j)} + 2(c - u_j) e^{(c-u_j)} - 2e^{(c-u_j)} + 2 \right] \delta_{m,0} + \\ & + \left(\frac{1}{1-\alpha} \right) \Sigma_s(u_j) \varphi_{m>0}(B, u_j) \int_c^{u_j} du' P_{m>0}(\xi(A, u', u_j)) e^{u'-u_j}; \end{aligned} \quad (4.19)$$

for the last lethargy point the following formula is obtained:

$$\begin{aligned} & iB \left[\frac{m+1}{2m+1} \varphi_{m+1}(B, u_j) + \frac{m}{2m+1} \varphi_{m-1}(B, u_j) \right] + \Sigma_t(u_j) \varphi_m(B, u_j) = \\ & = S_m(B, u_j) + \frac{1}{1-\alpha} \Sigma_s(u_j) \varphi_0(B, u_j) (1 - e^{c-u_j}) \delta_{m,0} + \\ & + \frac{1}{1-\alpha} \frac{\Sigma_s(u_j) \varphi_0(B, u_j) - \Sigma_s(u_{j-1}) \varphi_0(B, u_{j-1})}{u_j - u_{j-1}} \cdot \\ & \cdot \left[-1 - (c - u_j) e^{c-u_j} + e^{c-u_j} \right] \delta_{m,0} + \frac{1}{2} \cdot \frac{1}{(1-\alpha)} \cdot \\ & \cdot \left[\Sigma_s(u_j) \varphi_0(B, u_j) (u_{j-1} - u_{j-2}) - \Sigma_s(u_{j-1}) \varphi_0(B, u_{j-1}) (u_j - u_{j-2}) + \right. \\ & \left. + \Sigma_s(u_{j-2}) \varphi_0(B, u_{j-2}) (u_j - u_{j-1}) \right] \div \left[(u_j - u_{j-1})^2 (u_{j-1} - u_{j-2}) \right] \cdot \\ & \cdot \left[-(c - u_j)^2 e^{(c-u_j)} + 2(c - u_j) e^{(c-u_j)} - 2e^{(c-u_j)} + 2 \right] \delta_{m,0} + \\ & + \left(\frac{1}{1-\alpha} \right) \Sigma_s(u_j) \varphi_{m>0}(B, u_j) \int_c^{u_j} du' P_{m>0}(\xi(A, u', u_j)) e^{u'-u_j}. \end{aligned} \quad (4.20)$$

Putting together the same order moment at same energy the following formula is obtained for a point inside the lethargy interval:

$$\begin{aligned}
 & iB \frac{m+1}{2m+1} \varphi_{m+1}(B, u_j) + iB \frac{m}{2m+1} \varphi_{m-1}(B, u_j) + \\
 & + \varphi_m(B, u_j) \left\{ \Sigma_t(u_j) - \frac{1}{1-\alpha} \Sigma_s(u_j) \left[(1 - e^{c-u_j}) \delta_{m,0} + \right. \right. \\
 & \left. \left. - \frac{[-(c-u_j)^2 e^{(c-u_j)} + 2(c-u_j)e^{(c-u_j)} - 2e^{(c-u_j)} + 2]}{(u_j - u_{j-1})^2} \right] \delta_{m,0} + \right. \\
 & \left. + \int_c^{u_j} du' P_{m>0}(\xi(A, u', u_j)) e^{u'-u_j} (m > 0) \right\} + \\
 & + \varphi_0(B, u_{j+1}) \frac{-\Sigma_s(u_{j+1})}{1-\alpha} \left\{ \frac{[-1 - (c-u_j)e^{c-u_j} + e^{c-u_j}]}{u_{j+1} - u_{j-1}} + \right. \\
 & \left. + \frac{1}{2} \cdot \frac{[-(c-u_j)^2 e^{(c-u_j)} + 2(c-u_j)e^{(c-u_j)} - 2e^{(c-u_j)} + 2]}{(u_j - u_{j-1})^2} \right\} \delta_{m,0} + \\
 & + \varphi_0(B, u_{j-1}) \frac{\Sigma_s(u_{j-1})}{1-\alpha} \left\{ \frac{[-1 - (c-u_j)e^{c-u_j} + e^{c-u_j}]}{u_{j+1} - u_{j-1}} + \right. \\
 & \left. - \frac{1}{2} \cdot \frac{[-(c-u_j)^2 e^{(c-u_j)} + 2(c-u_j)e^{(c-u_j)} - 2e^{(c-u_j)} + 2]}{(u_j - u_{j-1})^2} \right\} \delta_{m,0} = \\
 & = S_m(B, u_j),
 \end{aligned} \tag{4.21}$$

instead the following one is obtained for the last lethargy point:

$$\begin{aligned}
 & iB \frac{m+1}{2m+1} \varphi_{m+1}(B, u_j) + iB \frac{m}{2m+1} \varphi_{m-1}(B, u_j) + \\
 & + \varphi_m(B, u_j) \left\{ \Sigma_t(u_j) - \frac{1}{1-\alpha} \Sigma_s(u_j) \left[(1 - e^{c-u_j}) \delta_{m,0} + \right. \right. \\
 & + \left. \frac{[-1 - (c - u_j)e^{c-u_j} + e^{c-u_j}]}{u_j - u_{j-1}} \delta_{m,0} + \right. \\
 & + \left. \frac{1}{2} \frac{[-(c - u_j)^2 e^{c-u_j} + 2(c - u_j)e^{c-u_j} - 2e^{c-u_j} + 2]}{(u_j - u_{j-1})^2} \right] \delta_{m,0} + \\
 & + \left. \int_c^{u_j} du' P_{m>0}(\xi(A, u', u_j)) e^{u'-u_j} (m > 0) \right\} + \\
 & + \varphi_0(B, u_{j-1}) \frac{\Sigma_s(u_{j-1})}{1-\alpha} \left\{ \frac{[-1 - (c - u_j)e^{c-u_j} + e^{c-u_j}]}{u_j - u_{j-1}} + \right. \\
 & + \frac{1}{2} \cdot \frac{[-(c - u_j)^2 e^{c-u_j} + 2(c - u_j)e^{c-u_j} - 2e^{c-u_j} + 2]}{(u_j - u_{j-1})^2 (u_{j-1} - u_{j-2})} \\
 & \cdot (u_j - u_{j-2}) \left. \right\} \delta_{m,0} + \varphi_0(B, u_{j-2}) \frac{-\Sigma_s(u_{j-2})}{1-\alpha} \left\{ \frac{1}{2} \cdot \right. \\
 & \cdot \left. \frac{[-(c - u_j)^2 e^{c-u_j} + 2(c - u_j)e^{c-u_j} - 2e^{c-u_j} + 2]}{(u_j - u_{j-1})^2 (u_{j-1} - u_{j-2})} (u_j - u_{j-1}) \right\} \delta_{m,0} = \\
 & = S_m(B, u_j).
 \end{aligned} \tag{4.22}$$

The terms that multiply the flux momenta are the coefficient of the matrix \mathbf{A} ; instead the part on the right hand side of the equal are the terms of the vector \mathbf{b} . For this approximation method, the matrix \mathbf{A} of formula (4.5) is a five diagonal matrix, with non zero elements in the principal diagonal, in the first diagonal above and below the principal diagonal and in the $N + 2$ diagonal above and below the principal one; the only exception are the rows multiple of $N + 2$ where the closure equation is imposed.

4.1.4 Discrete lethargy approach, \mathbf{P}_N approximation

The discretization for this approach has been already presented in formula (3.48). In this case the lethargy point position in the interval is not important; the only difference is on the first lethargy point, where the integral is zero. For the first

lethargy point the formula is the following one:

$$iB \frac{m+1}{2m+1} \varphi_{m+1}(B,0) + iB \frac{m}{2m+1} \varphi_{m-1}(B,0) + \Sigma_t(0) \varphi_m(B,0) = S_m(B,0). \quad (4.23)$$

Then the following formulas report the discretized equation for the other lethargy points. For the general lethargy point, starting from formula (3.48), putting together the same order moment at same energy the following formula is obtained:

$$\begin{aligned} & iB \frac{m+1}{2m+1} \varphi_{m+1}(B, u) + iB \frac{m}{2m+1} \varphi_{m-1}(B, u) + \\ & + \varphi_m(B, u) \left[\Sigma_t(u) - \frac{h}{2} \cdot \frac{\Sigma_s(u) \varphi_m(B, u)}{1-\alpha} \right] + \\ & - \frac{h}{2} \left[\Sigma_s(c) \varphi_m(B, c) \frac{P_m(\xi(A, c, u)) e^{c-u}}{1-\alpha} + \right. \\ & \left. + 2 \sum_{i=1}^{N-1} \left(\Sigma_s(u_i) \varphi_m(B, u_i) \frac{P_m(\xi(A, u_i, u)) e^{u_i-u}}{1-\alpha} \right) \right] = \\ & = S_m(B, u). \end{aligned} \quad (4.24)$$

The terms that multiply the flux momenta are the coefficient of the matrix \mathbf{A} ; instead the part on the right hand side of the equal are the terms of the vector \mathbf{b} . For this approximation method, the matrix \mathbf{A} of formula (4.5) has the elements in the diagonals above and below the principal one, up to the number of point between $u + \log(\alpha)$ and u .

4.1.5 Selengut-Goertzel approach , P_N approximation

For the Selengut-Goertzel approach, formulas (4.1, 4.3) are needed for the oxygen part; instead the discretization for the hydrogen part has been already presented in formula (3.53). Substituting in equation (3.53) the discretization for the first derivative, the following results are obtained. First of all, the formula for the first lethargy point (the zero lethargy point) is reported:

$$iB \frac{m+1}{2m+1} \varphi_{m+1}(B,0) + iB \frac{m}{2m+1} \varphi_{m-1}(B,0) + \Sigma_t(0) \varphi_m(B,0) = S_m(B,0). \quad (4.25)$$

Then the following formulas report the discretized equation for the other lethargy points. For a lethargy point inside the interval the following formula is obtained:

$$\begin{aligned} & iB \left[\frac{m+1}{2m+1} \varphi_{m+1}(B, u_j) + \frac{m}{2m+1} \varphi_{m-1}(B, u_j) \right] + \Sigma_t(u_j) \varphi_m(B, u_j) = \\ & = S_m(B, u_j) + \frac{1}{1-\alpha_O} \Sigma_{s,O}(u_j) \varphi_0(B, u_j) (1 - e^{c_O - u_j}) \delta_{m,0} + \\ & + \frac{1}{1-\alpha_O} \frac{\Sigma_{s,O}(u_{j+1}) \varphi_0(B, u_{j+1}) - \Sigma_{s,O}(u_{j-1}) \varphi_0(B, u_{j-1})}{u_{j+1} - u_{j-1}} \cdot \\ & \cdot [-1 - (c_O - u_j) e^{c_O - u_j} + e^{c_O - u_j}] \delta_{m,0} + \\ & + \left(\frac{1}{1-\alpha_O} \right) \Sigma_{s,O}(u_j) \varphi_{m>0}(B, u_j) \cdot \\ & \cdot \int_{c_O}^{u_j} du' P_{m>0}(\xi_O(A_O, u', u_j)) e^{u' - u_j} + \\ & + \frac{h}{2} \left[\Sigma_{s,H}(c_H) \varphi_0(B, c_H) \frac{e^{c_H - u_j}}{1-\alpha_H} + \right. \\ & + 2 \sum_{i=1}^{N-1} \left(\Sigma_{s,H}(u_i) \varphi_0(B, u_i) \frac{e^{u_i - u_j}}{1-\alpha_H} \right) + \\ & + \left. \frac{\Sigma_{s,H}(u_j) \varphi_0(B, u_j)}{1-\alpha_H} \right] \delta_{m,0} + \left(\frac{1}{1-\alpha_H} \right) \Sigma_{s,H}(u_j) \varphi_{m>0}(B, u_j) \cdot \\ & \cdot \int_{c_H}^{u_j} du' P_{m>0}(\xi_H(A_H, u', u_j)) e^{u' - u_j}; \end{aligned} \quad (4.26)$$

for the last lethargy point the following formula is obtained:

$$\begin{aligned}
 & iB \left[\frac{m+1}{2m+1} \varphi_{m+1}(B, u_j) + \frac{m}{2m+1} \varphi_{m-1}(B, u_j) \right] + \Sigma_t(u_j) \varphi_m(B, u_j) = \\
 & = S_m(B, u_j) + \frac{1}{1-\alpha_O} \Sigma_{s,O}(u_j) \varphi_0(B, u_j) (1 - e^{c_O - u_j}) \delta_{m,0} + \\
 & + \frac{1}{1-\alpha_O} \frac{\Sigma_{s,O}(u_j) \varphi_0(B, u_{j+1}) - \Sigma_{s,O}(u_{j-1}) \varphi_0(B, u_{j-1})}{u_j - u_{j-1}} \cdot \\
 & \cdot [-1 - (c_O - u_j) e^{c_O - u_j} + e^{c_O - u_j}] \delta_{m,0} + \\
 & + \left(\frac{1}{1-\alpha_O} \right) \Sigma_{s,O}(u_j) \varphi_{m>0}(B, u_j) \cdot \\
 & \cdot \int_{c_O}^{u_j} du' P_{m>0}(\xi_O(A_O, u', u_j)) e^{u' - u_j} + \\
 & + \frac{h}{2} \left[\Sigma_{s,H}(c_H) \varphi_0(B, c_H) \frac{e^{c_H - u_j}}{1-\alpha_H} + \right. \\
 & + 2 \sum_{i=1}^{N-1} \left(\Sigma_{s,H}(u_i) \varphi_0(B, u_i) \frac{e^{u_i - u_j}}{1-\alpha_H} \right) + \\
 & + \left. \frac{\Sigma_{s,H}(u_j) \varphi_0(B, u_j)}{1-\alpha_H} \right] \delta_{m,0} + \left(\frac{1}{1-\alpha_H} \right) \Sigma_{s,H}(u_j) \varphi_{m>0}(B, u_j) \cdot \\
 & \cdot \int_{c_H}^{u_j} du' P_{m>0}(\xi_H(A_H, u', u_j)) e^{u' - u_j}.
 \end{aligned} \tag{4.27}$$

Putting together the same order moment at same energy the following formula is obtained for a point inside the lethargy interval:

$$\begin{aligned}
& iB \frac{m+1}{2m+1} \varphi_{m+1}(B, u_j) + iB \frac{m}{2m+1} \varphi_{m-1}(B, u_j) + \\
& + \varphi_m(B, u_j) \left\{ \Sigma_t(u_j) - \frac{\Sigma_{s,O}(u_j)}{1-\alpha_O} \left[(1 - e^{c_O - u_j}) \delta_{m,0+} + \right. \right. \\
& + \left. \int_{c_O}^{u_j} du' P_{m>0}(\xi_O(A_O, u', u_j)) e^{u' - u_j} (m > 0) \right] - \frac{h \Sigma_{s,H}(u_j)}{2(1-\alpha_H)} \delta_{m,0+} \\
& - \left. \frac{\Sigma_{s,H}(u_j)}{1-\alpha_H} \int_{c_H}^{u_j} du' P_{m>0}(\xi_H(A_H, u', u_j)) e^{u' - u_j} (m > 0) \right\} + \\
& + \varphi_0(B, u_{j+1}) \frac{-\Sigma_{s,O}(u_{j+1}) [-1 - (c_O - u_j) e^{c_O - u_j} + e^{c_O - u_j}]}{1-\alpha_O} \frac{u_{j+1} - u_{j-1}}{u_{j+1} - u_{j-1}} \delta_{m,0+} \\
& + \varphi_0(B, u_{j-1}) \frac{\Sigma_{s,O}(u_{j-1}) [-1 - (c_O - u_j) e^{c_O - u_j} + e^{c_O - u_j}]}{1-\alpha_O} \frac{u_{j+1} - u_{j-1}}{u_{j+1} - u_{j-1}} \delta_{m,0+} \\
& - \frac{h}{2} \left[\Sigma_{s,H}(c_H) \varphi_0(B, c_H) \frac{e^{c_H - u_j}}{1-\alpha_H} + 2 \sum_{i=1}^{N-1} \left(\Sigma_{s,H}(u_i) \varphi_0(B, u_i) \frac{e^{u_i - u_j}}{1-\alpha_H} \right) \right] = \\
& = S_m(B, u_j);
\end{aligned} \tag{4.28}$$

instead the following one is obtained for the last lethargy point:

$$\begin{aligned}
& iB \frac{m+1}{2m+1} \varphi_{m+1}(B, u_j) + iB \frac{m}{2m+1} \varphi_{m-1}(B, u_j) + \\
& + \varphi_m(B, u_j) \left\{ \Sigma_t(u_j) - \frac{\Sigma_{s,O}(u_j)}{1-\alpha_O} \left[(1 - e^{c_O - u_j}) \delta_{m,0+} + \right. \right. \\
& + \left. \frac{[-1 - (c_O - u_j) e^{c_O - u_j} + e^{c_O - u_j}]}{u_j - u_{j-1}} \delta_{m,0+} \right. \\
& + \left. \int_{c_O}^{u_j} du' P_{m>0}(\xi_O(A_O, u', u_j)) e^{u' - u_j} (m > 0) \right] - \frac{h \Sigma_{s,H}(u_j)}{2(1-\alpha_H)} \delta_{m,0+} \\
& - \left. \frac{\Sigma_{s,H}(u_j)}{1-\alpha_H} \int_{c_H}^{u_j} du' P_{m>0}(\xi_H(A_H, u', u_j)) e^{u' - u_j} (m > 0) \right\} + \\
& + \varphi_0(B, u_{j-1}) \frac{\Sigma_{s,O}(u_{j-1}) [-1 - (c_O - u_j) e^{c_O - u_j} + e^{c_O - u_j}]}{1-\alpha_O} \frac{u_j - u_{j-1}}{u_j - u_{j-1}} \delta_{m,0+} \\
& - \frac{h}{2} \left[\Sigma_{s,H}(c_H) \varphi_0(B, c_H) \frac{e^{c_H - u_j}}{1-\alpha_H} + 2 \sum_{i=1}^{N-1} \left(\Sigma_{s,H}(u_i) \varphi_0(B, u_i) \frac{e^{u_i - u_j}}{1-\alpha_H} \right) \right] = \\
& = S_m(B, u_j).
\end{aligned} \tag{4.29}$$

The terms that multiply the flux momenta are the coefficient of the matrix \mathbf{A} ; instead the part on the right hand side of the equal are the terms of the vector \mathbf{b} . Since this method is a combination between the Fermi continuous slowing down method and the discrete lethargy approach the matrix A of formula (4.5) is of the same type of the discrete lethargy method.

Chapter 5

Test cases, results and discussion

In this chapter the solution of the neutron spectra in a homogeneous moderator media, in slab configuration, using the methods presented in the previous chapter, is carried out. In order to evaluate the solution of the transport equation the software MATLAB is used [19]. For this reason, a discretization in lethargy is required. Then, in order to reduce the error due to the scheme used for the simulation, a grid independence for each methods and for the lowest order of approximation is carried out; the lowest order of approximation is used because it is expected that increasing the order of approximation (it means increase the order of the last momentum used for the flux) the error, with respect to the real result, decrease.

5.1 Simulation setup

In order to solve the problem, the nuclear data are required; so the nuclear cross sections are taken from the library JEFF-3.3 [20], through the use of the java-based nuclear information software JANIS [21]. Then a source definition is required, since it is the known term on the equation. For the solution of this simple problem it has been decided to use an isotropic source, with constant value equal to one in the energy interval between $2MeV$ and $0.2MeV$; considering the lethargy variable it corresponds to the lethargy interval between 0 and $\log(10)$. Since the source is assumed isotropic, only the zero order moment exist; so the expatiation (3.9) becomes:

$$S(B, u, \mu) = \frac{1}{2}S_0(B, u); \quad (5.1)$$

the momenta of larger order than zero are imposed equal to zero:

$$S_m(B, u) = 0 \text{ if } m > 0. \quad (5.2)$$

Then in order to do some comparison three different buckling are used. As already said the material used is a homogeneous media, composed of moderator material.

The moderators used for the calculations are graphite, light water and heavy water.

5.2 Grid independence

In order to reduce the error for each method a grid independence is carried out. Except for the discrete method the lethargy interval is divided into an increasing number of point using the command `linspace` in MATLAB; for the discrete method, since the flux moments remain inside the integral, the value of the flux moment in each lethargy step is required and mostly the value in $u + \ln(\alpha)$ is required, the interval is divided using a decreasing fraction of $\ln(\alpha)$. In order to evaluate the error, the integral of the flux is taken in all the lethargy interval; for each grid the value is compared with the integral obtained with the most refined grid. So, the error used is defined as follow:

$$err_{rel} = \frac{|I - I_{\infty}|}{|I_{\infty}|} \quad (5.3)$$

where:

- I is the integral of the flux in the lethargy interval:

$$I = \int_0^{u_{max}} \varphi(B, u, \mu) du; \quad (5.4)$$

- I_{∞} is the integral of the flux in the lethargy interval with the most refined grid

Doing that procedure, the assumption that the grid independence converge has been done.

5.2.1 Fermi continuous slowing down model, P_N approximation

For this approximation the calculation is done for graphite, light water and heavy water. The results of the grid independence are presented in the following figures:

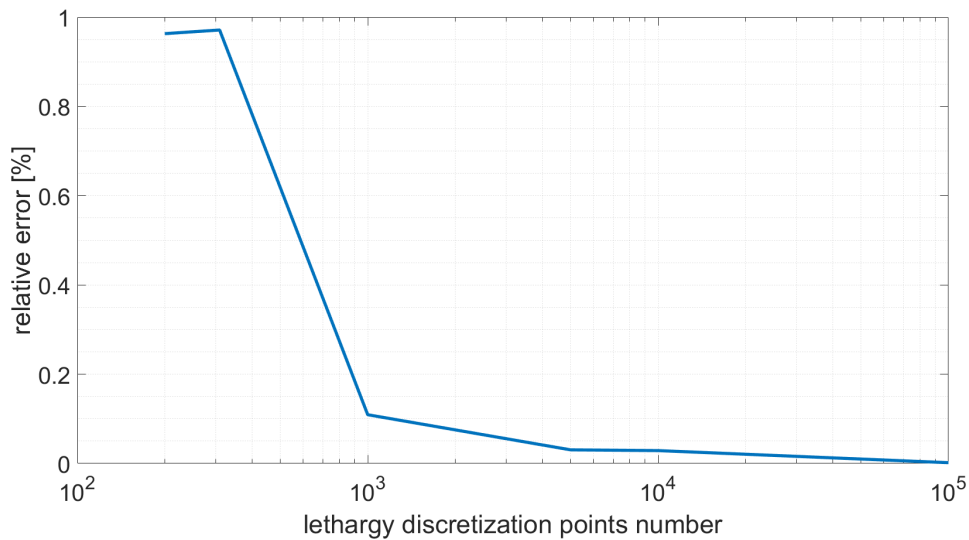


Figure 5.1: Grid independence for Fermi continuous slowing down method with P_1 approximation, $B = 0.01$, using graphite as moderator material.

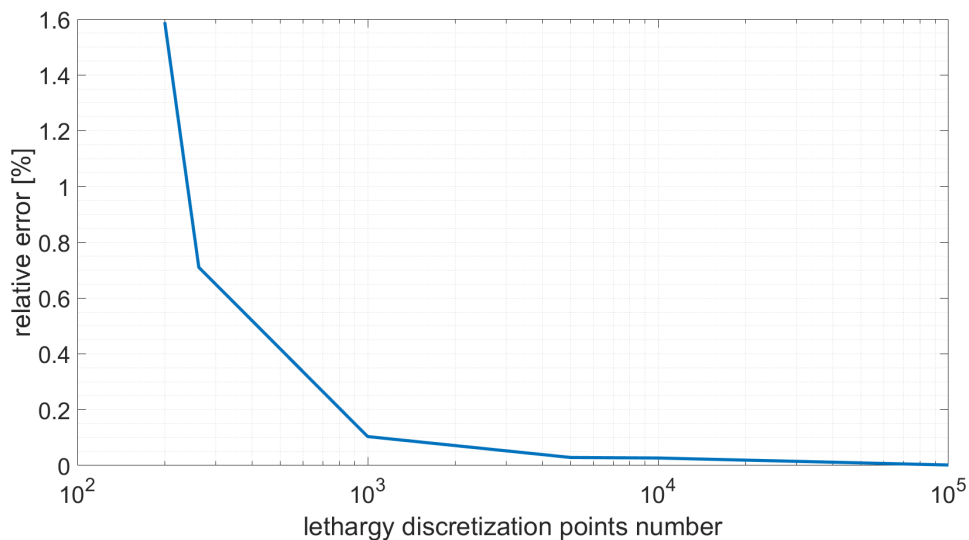


Figure 5.2: Grid independence for Fermi continuous slowing down method with P_1 approximation, $B = 0.01$, using light water as moderator material.

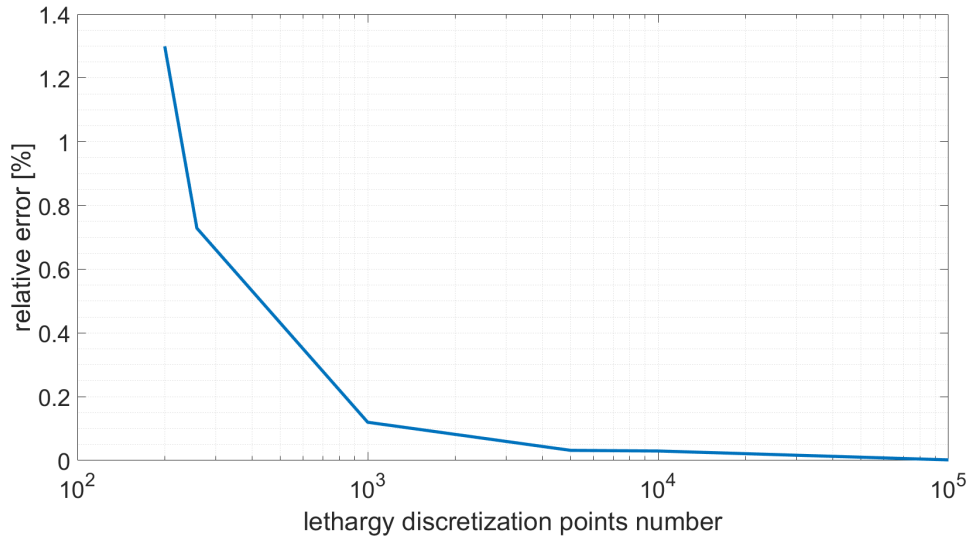


Figure 5.3: Grid independence for Fermi continuous slowing down method with P_1 approximation, $B = 0.01$, using heavy water as moderator material.

Since the relative error has a small reduction starting from 10^3 lethargy points, this value is considered for the simulations that are carried out.

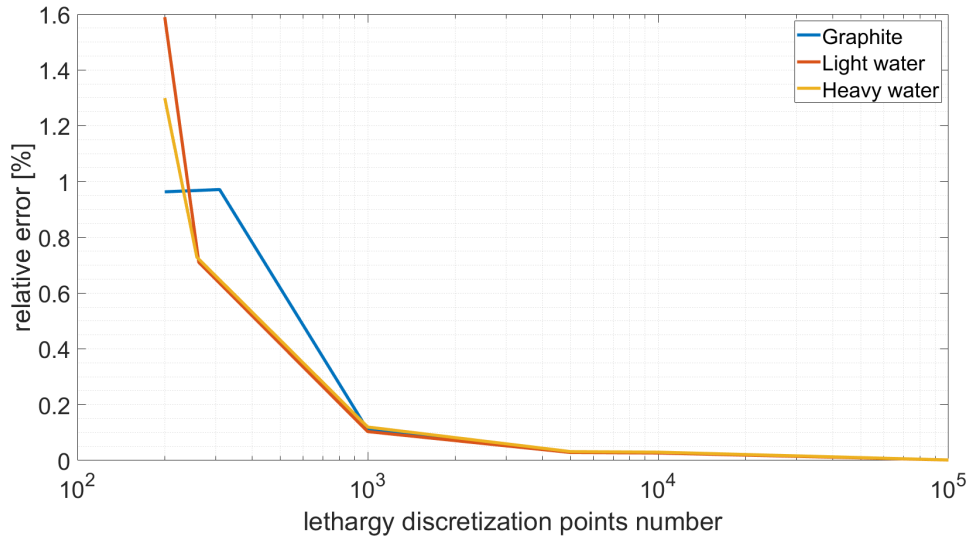


Figure 5.4: Grid independence for Fermi continuous slowing down method with P_1 approximation, $B = 0.01$; comparison between graphite, light water and heavy water as moderator material.

A comparison is also done for the three materials in order to compare the convergence speed. The previous plot is the result of the superposition of the three previous plots; considering this last figure, it is possible to say that, in the first part, simulations with light water and heavy water converge faster than simulation with graphite; instead close to the convergence all the three grid independence converge with the same speed.

5.2.2 Fermi continuous slowing down model, B_N approximation

For this approximation the calculation has been done for graphite. The result of the grid independence is presented in the following figure:

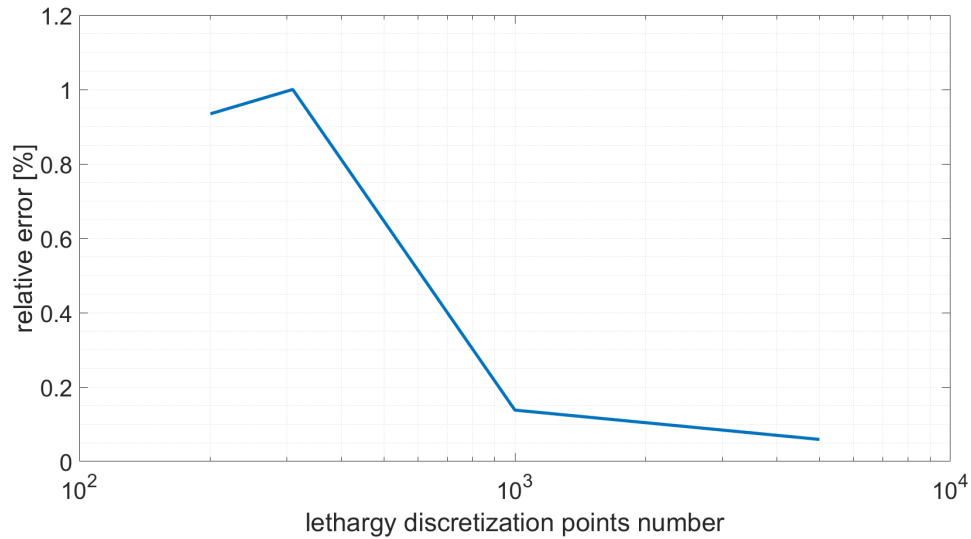


Figure 5.5: Grid independence for Fermi continuous slowing down method with B_1 approximation, $B = 0.01$, using graphite as moderator material .

Since the relative error has a small reduction starting from 10^3 lethargy points, this value is considered for the simulations that are carried out.

5.2.3 Greuling-Goertzel approach, P_N approximation

For this approximation the calculation has been done for graphite, light water and heavy water. The results of the grid independence are presented in the following figures:

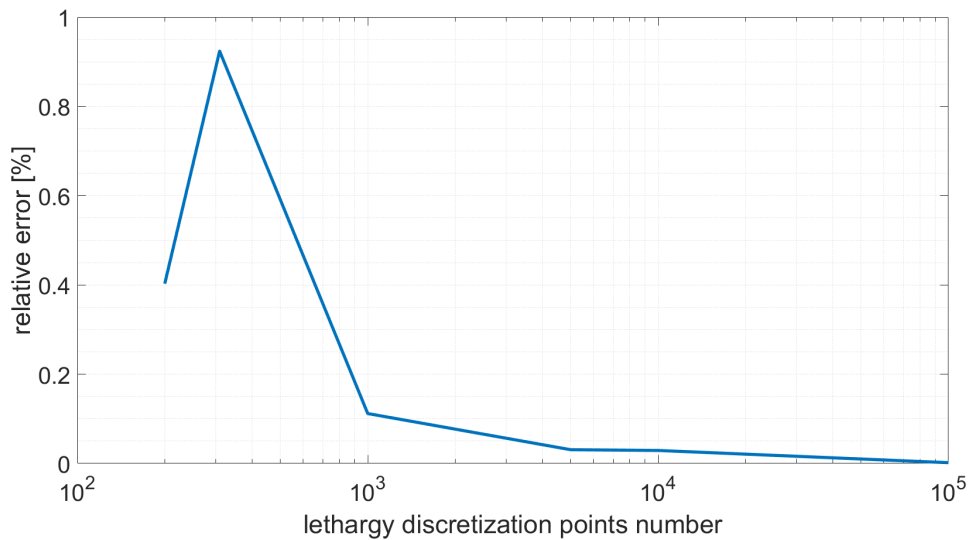


Figure 5.6: Grid independence for Greuling-Goertzel approach with P_1 approximation, $B = 0.01$, using graphite as moderator material.

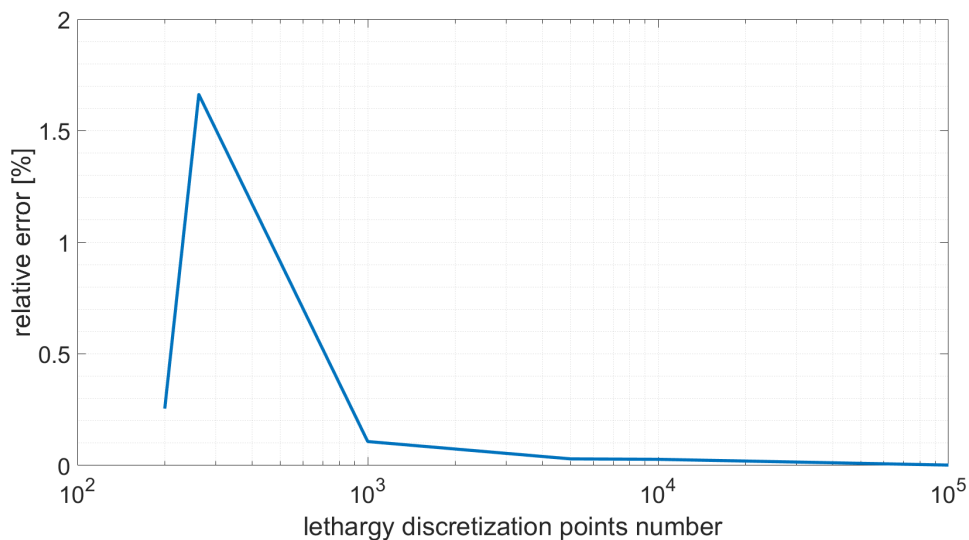


Figure 5.7: Grid independence for Greuling-Goertzel approach with P_1 approximation, $B = 0.01$, using light water as moderator material.

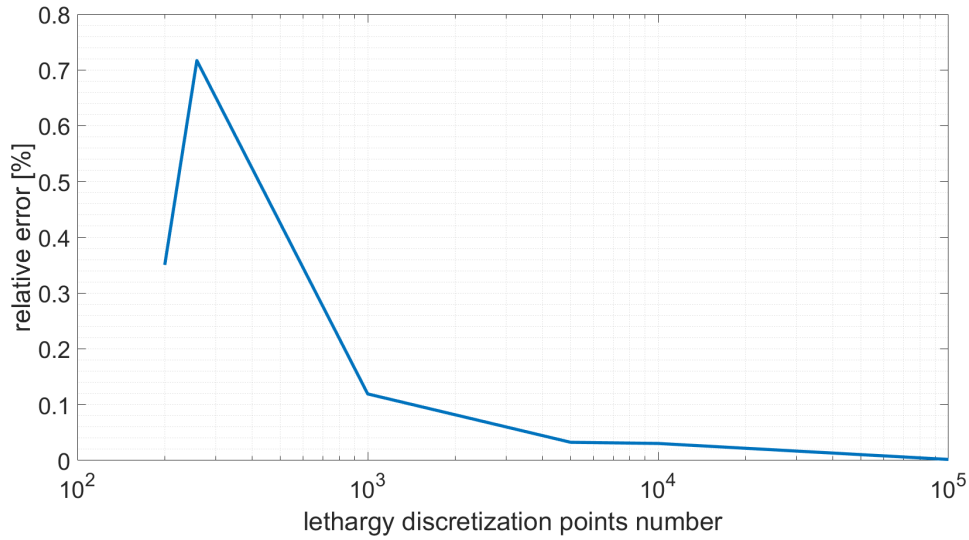


Figure 5.8: Grid independence for Greuling-Goertzel approach with P_1 approximation, $B = 0.01$, using heavy water as moderator material.

Since the relative error has a small reduction starting from 10^3 lethargy points, this value is considered for the simulations that are carried out.

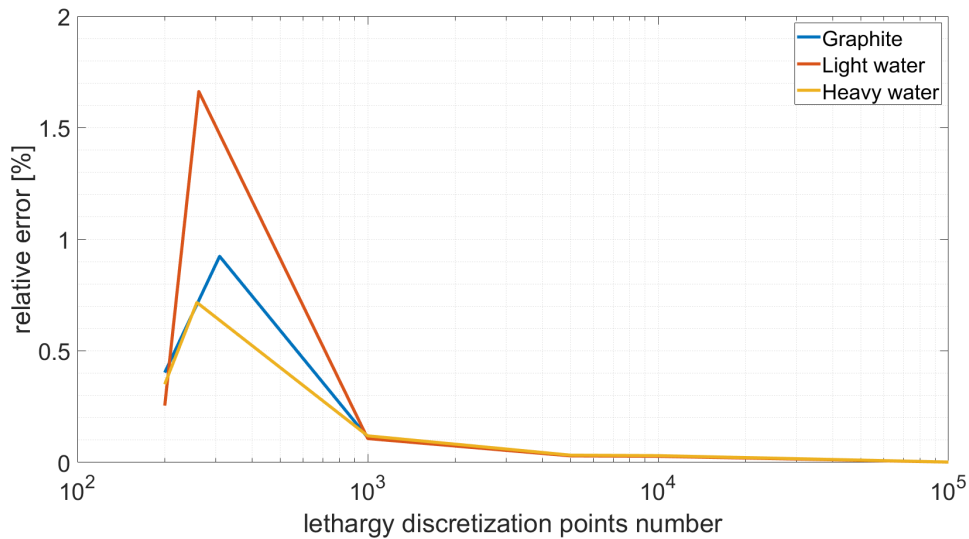


Figure 5.9: Grid independence for Greuling-Goertzel approach with P_1 approximation, $B = 0.01$; comparison between graphite, light water and heavy water as moderator material.

A comparison is also done for the three materials in order to compare the convergence speed. The previous plot is the result of the superposition of the three previous plots; considering this last plot, it is possible to say that, in the first part, simulation with heavy water converge faster than simulation with graphite, that converge faster than simulation with light water; instead close to the convergence all the three grid independence converge with the same speed.

5.2.4 Discrete lethargy approach, P_N approximation

For this approximation the calculation has been done for graphite, light water and heavy water. The results of the grid independence are presented in the following figures:

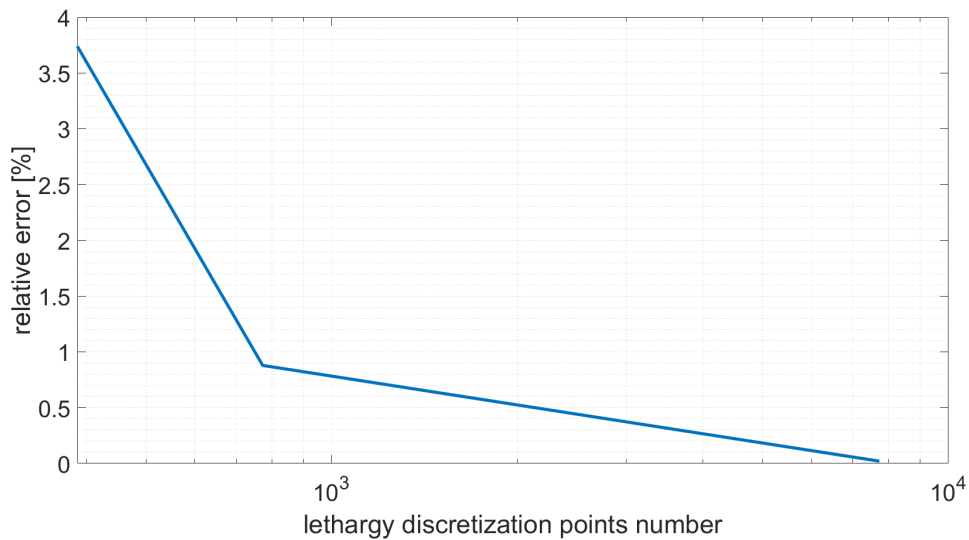


Figure 5.10: Grid independence for discrete lethargy approach with P_1 approximation, $B = 0.01$, using graphite as moderator material.

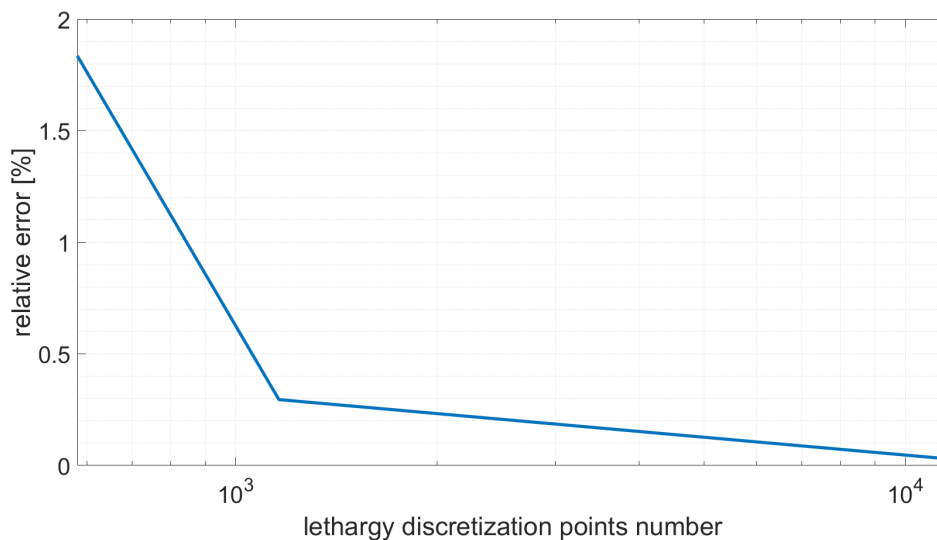


Figure 5.11: Grid independence for discrete lethargy approach with P_1 approximation, $B = 0.01$, using light water as moderator material.

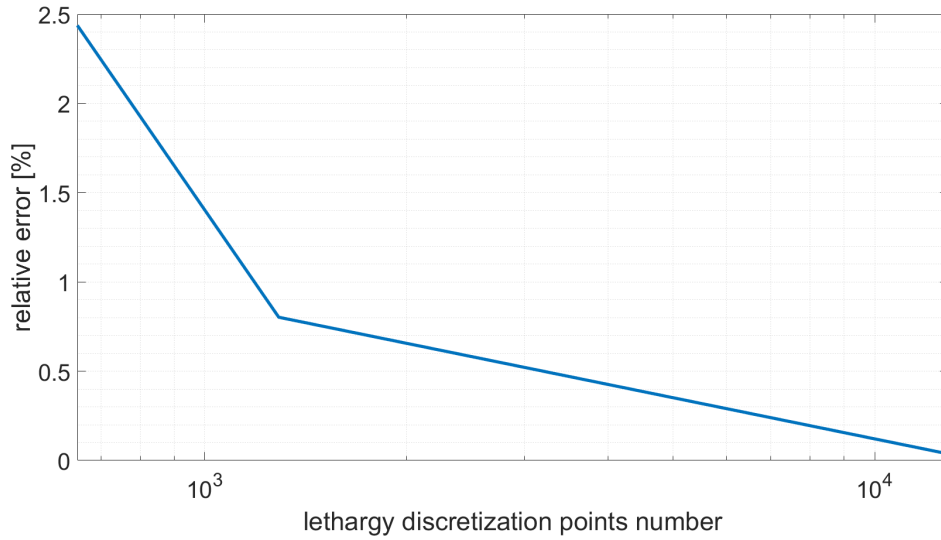


Figure 5.12: Grid independence for discrete lethargy approach with P_1 approximation, $B = 0.01$, using heavy water as moderator material.

In this case for the simulation the lethargy step is taken as $\ln(\alpha)/10$; so respectively for graphite, light water and heavy water 773,1160 and 1289 lethargy points have been considered.

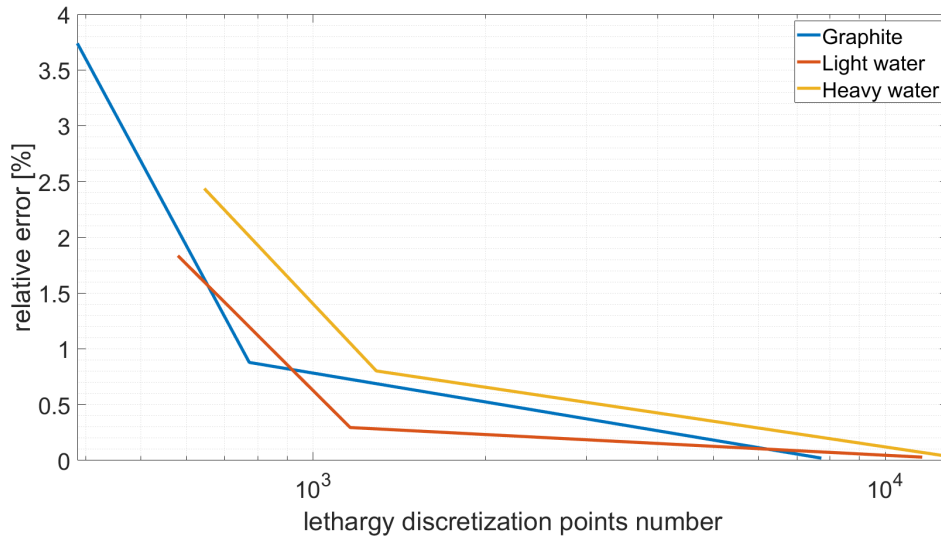


Figure 5.13: Grid independence for discrete lethargy approach with P_1 approximation, $B = 0.01$; comparison between graphite, light water and heavy water as moderator material.

A comparison is also done for the three materials in order to compare the convergence speed. The previous plot is the result of the superposition of the three previous plots; considering this last plot, it is possible to say that simulation with light water converge faster than simulation with graphite, that converge faster than simulation with heavy water.

5.2.5 Selengut-Goertzel approach , P_N approximation

For this approximation the calculation has been done for light water and heavy water. The results of the grid independence are presented in the following figures:

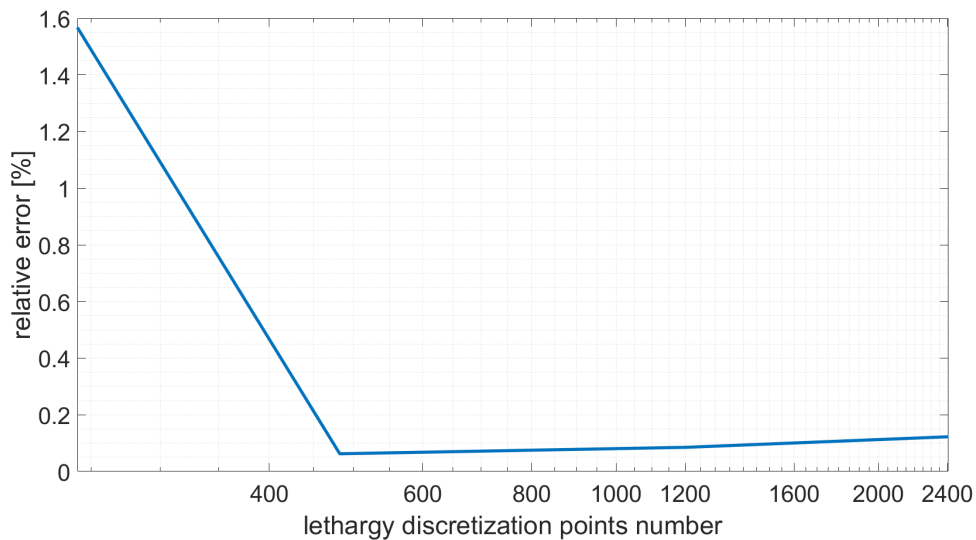


Figure 5.14: Grid independence for Selengut-Goertzel approach with P_1 approximation, $B = 0.01$, using light water as moderator material.

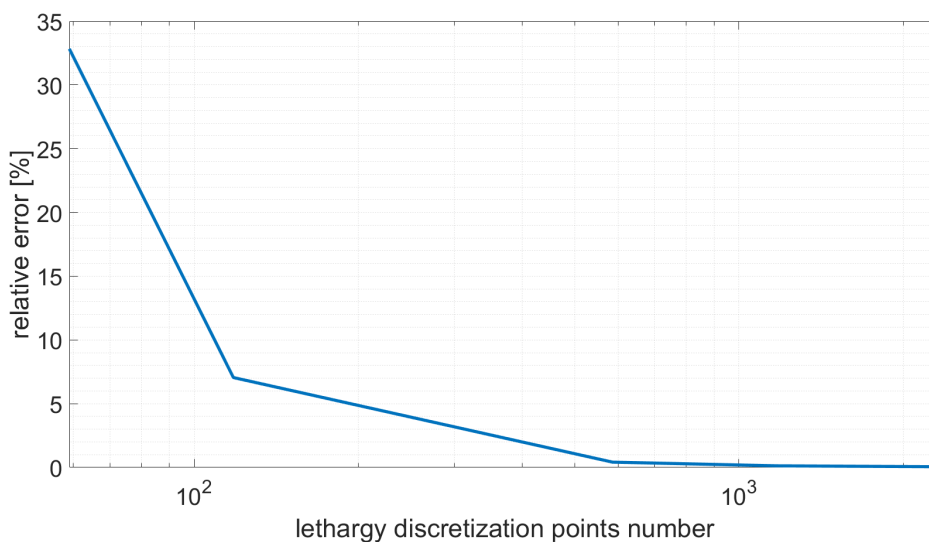


Figure 5.15: Grid independence for Selengut-Goertzel approach with P_1 approximation, $B = 0.01$, using heavy water as moderator material.

In this case for the simulation the interval has been taken as $\ln(\alpha_H)/200$ for light water and $\ln(\alpha_D)/100$ for heavy water; so respectively for light water and heavy water 482 and 1172 lethargy points have been considered. A comparison is also done for the two materials in order to compare the convergence speed. The previous plot is the result of the superposition of the two previous plots:

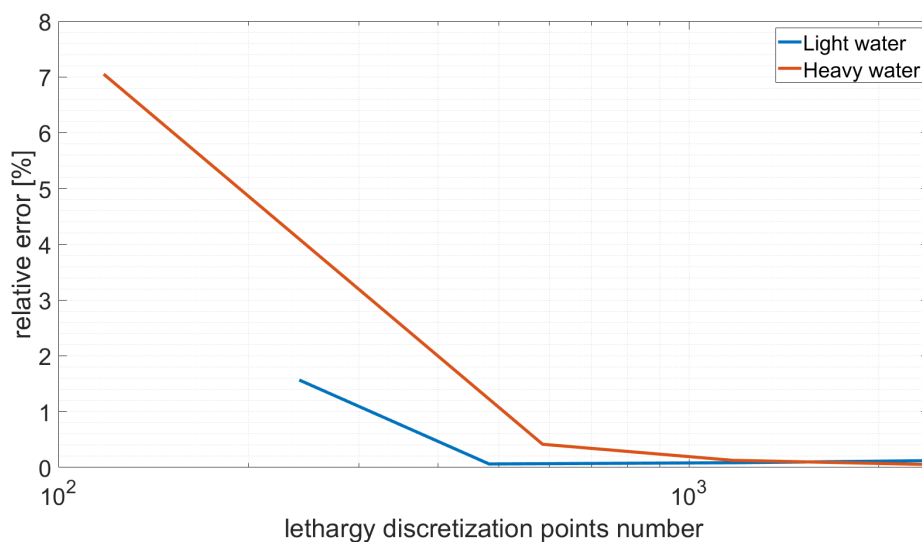


Figure 5.16: Grid independence for Selengut-Goertzel approach with P_1 approximation, $B = 0.01$; comparison between light water and heavy water as moderator material.

Considering this last plot, it is possible to say that simulation with light water converge faster than simulation with heavy water.

5.3 Results

In this section some results are presented. First of all, the dependence on the geometry is presented; then for each moderator a comparison between the various methods and the different order of approximation. To conclude a comparison between light water and heavy water is reported.

5.3.1 Geometry dependence

The geometry dependence is here analysed. In this way the problem is solved using:

- the Fermi continuous slowing down method in P_{19} approximation;
- different values of buckling.

To analyse the results the flux zero order moments are plotted. The following results are obtained:

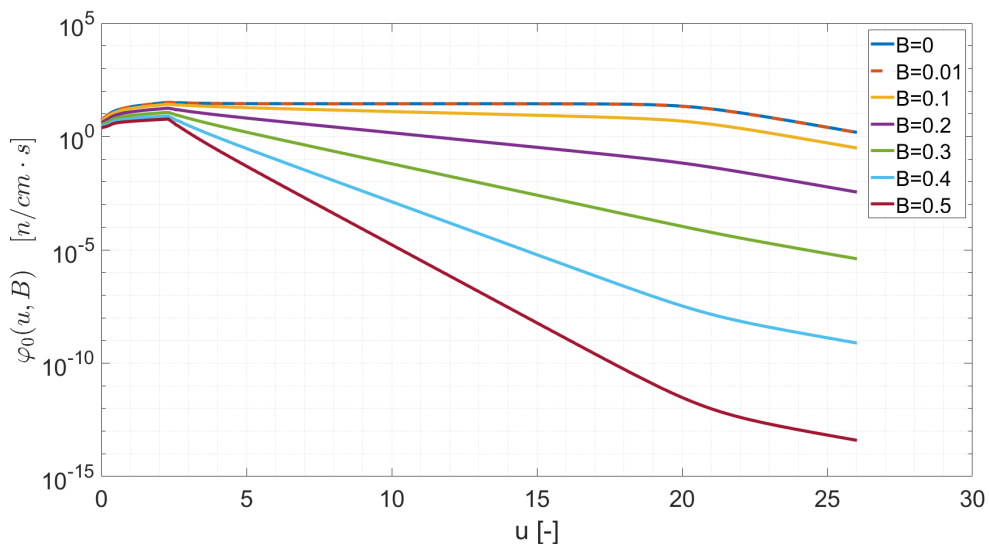


Figure 5.17: Neutron spectra, evaluated with Fermi continuous slowing down method in P_{19} approximation, in a homogeneous slab of graphite.

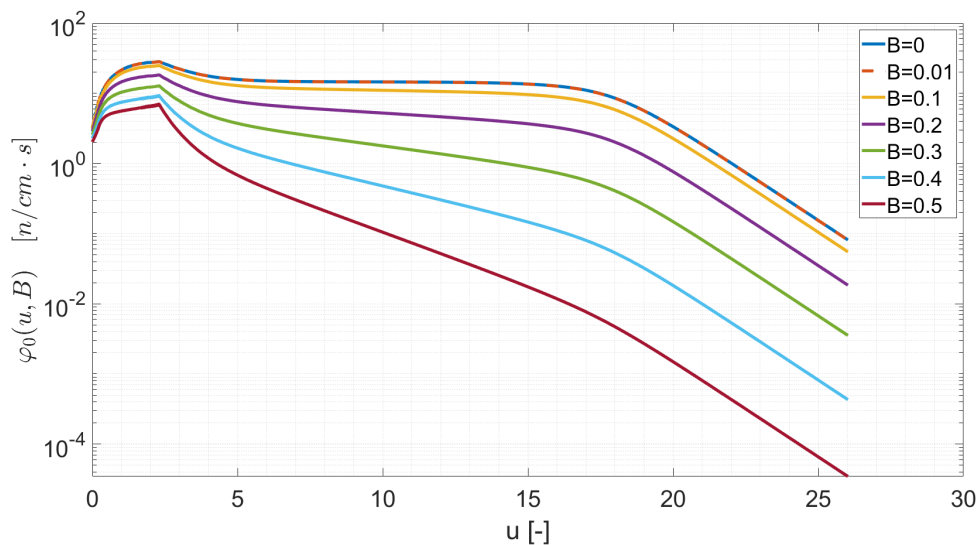


Figure 5.18: Neutron spectra, evaluated with Fermi continuous slowing down method in P_{19} approximation, in a homogeneous slab of light water.

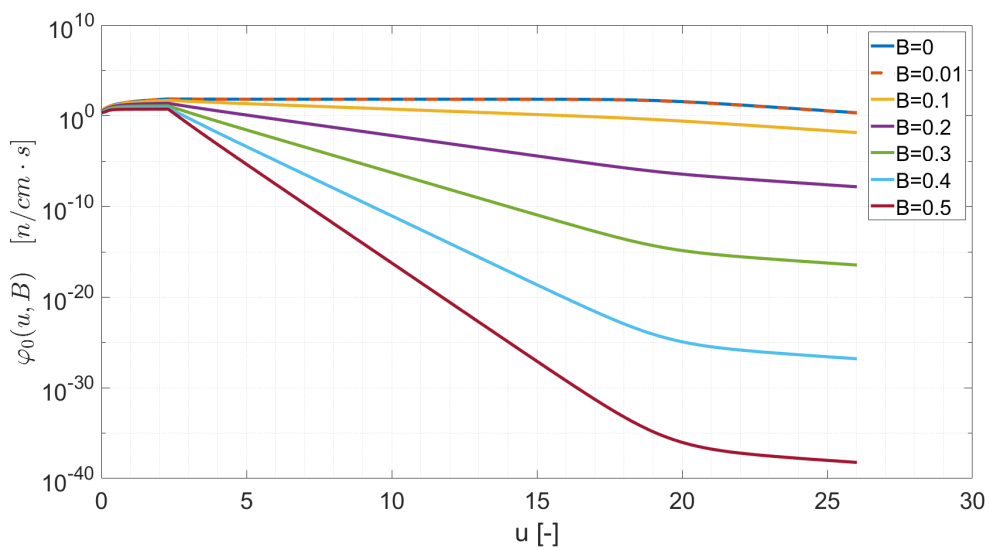


Figure 5.19: Neutron spectra, evaluated with Fermi continuous slowing down method in P_{19} approximation, in a homogeneous slab of heavy water.

It is noticeable that there is a strong dependence on the buckling value. The neutron spectra, as expected, decrease while the buckling increase; in fact, to increase of the buckling means to decrease the geometry dimension, so more leakages are expected and less neutrons are able to slowing down. It is also visible the increase

of the neutron spectra in the interval where there is the source.

5.3.2 Results for a graphite system

Here the results for the graphite as moderator materials are reported. First of all a comparison between the Fermi continuous slowing down, discrete lethargy approach and the Greuling-Goertzel approach is presented; the results are reported below; in the following plot the flux zero order moment, evaluated with the P_{19} approximation, is presented:

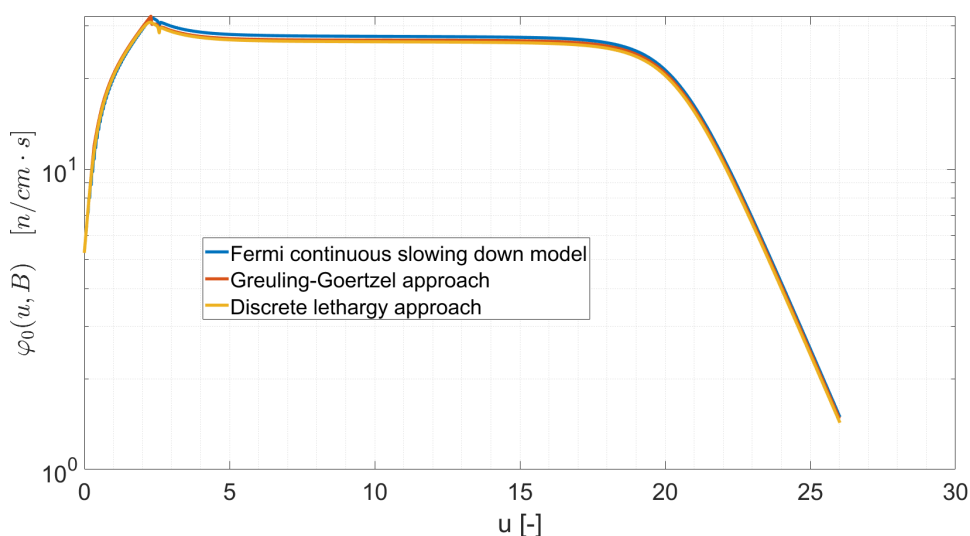


Figure 5.20: Neutron spectra, evaluated with Fermi continuous slowing down method, discrete lethargy approach and the Greuling-Goertzel approach in P_{19} approximation, in a homogeneous slab of graphite, with $B = 0.01$.

From the plot the three methods give a similar result; in order to compare the three methods a new error definition is introduced:

$$err_x = \frac{|I_d - I_x|}{|I_d|}, \quad (5.5)$$

where:

- I_d is the integral of the flux, evaluated with the discrete approach, in the lethargy interval;
- I_x is the integral of the flux, evaluated with the x approach (one between the other methods), in the lethargy integral.

The errors are referred to the discrete lethargy approach, because in that case there is no approximation in the collision density, so this method is expected to be the more accurate. With this definition the errors obtained are:

$$err_F = \frac{|I_d - I_F|}{|I_d|} = 2.44\%, \quad (5.6)$$

where F corresponds to the Fermi continuous slowing down method;

$$err_G = \frac{|I_d - I_G|}{|I_d|} = 1.34\%, \quad (5.7)$$

where G corresponds to the Greuling-Goertzel approach.

From these results it is possible to say that the Greuling-Goertzel approach is, as expected, more accurate than the Fermi continuous slowing down method; since the discretization matrices are of the same type for the two methods, the computational cost is the same, so the use of the Greuling-Goertzel approach is recommended. The discrete lethargy approach is recommended if a large accuracy is required, but since the use of the Greuling-Goertzel approach generate an error of the 1.34% with respect to the discrete lethargy approach, it is not a big mistake the use of the Greuling-Goertzel approach in order to reduce the computational cost.

In the remaining part of this section, for each method, that has been used, the comparison between different orders of approximation are analysed; in order to compare the different orders of approximation the following absolute error definition is introduced:

$$err = |\varphi_{19,0} - \varphi_{x,0}|, \quad (5.8)$$

where:

- $\varphi_{19,0}$ is the zero order moment of the neutron flux evaluated in P_{19} approximation;
- $\varphi_{x,0}$ is the zero order moment of the neutron flux evaluated in P_x approximation.

Using this definition, first of all, the solutions for the Fermi continuous slowing down method are analysed:

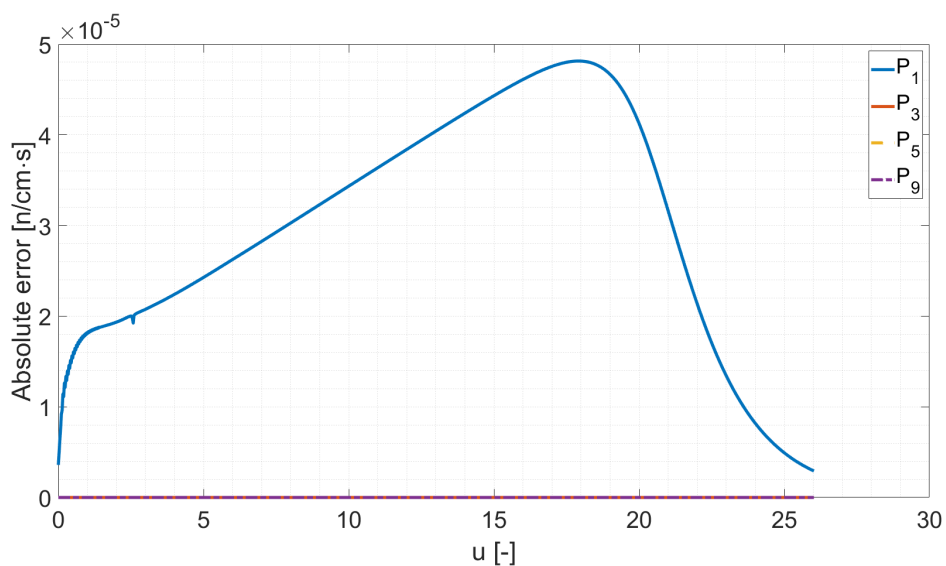


Figure 5.21: Absolute error with respect to the solution with the P_{19} approximation, using the Fermi continuous slowing down method, in a homogeneous slab of graphite, with $B = 0.01$ in linear scale.

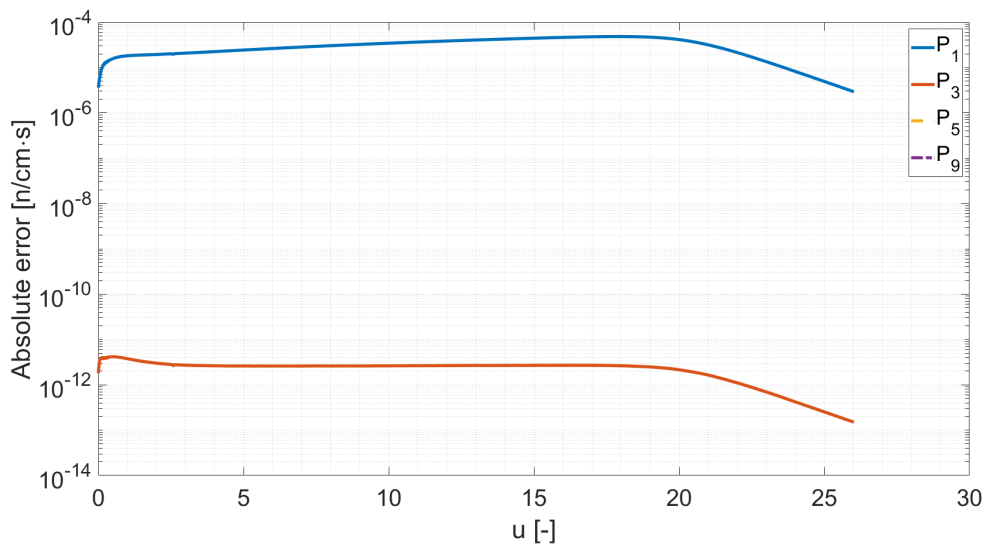


Figure 5.22: Absolute error with respect to the solution with the P_{19} approximation, using the Fermi continuous slowing down method, in a homogeneous slab of graphite, with $B = 0.01$ in logarithmic scale.

The first plot is done in linear scale; except for the P_1 approximation, it seems

that the error is zero for the higher order approximation. In order to better understand the order of the error for the higher order approximation, a plot in logarithmic scale is presented in the second plot; from this picture it is appreciable that the third order moment is of the order of $10^{-12} \frac{n}{cm \cdot s}$, instead fifth and ninth order moments are non represented; it means that the value of the error with respect to P_{19} approximation is exactly zero. With these results it is possible to say that the use of the fifth order is a good choice, because no improvements are expected increasing the approximation order.

As second case the solutions for the Greuling-Goertzel approach are analysed; the following two plot represents the errors for different order of approximation, also in this case, in linear and logarithmic scale. From the comparison of these two plot it is possible to understand that in this case the approximation of third order has as order of magnitude an error of $10^{-12} \frac{n}{cm \cdot s}$; instead for the first order moment and for the order higher or equal than the fifth, the error is exactly zero. It means that the use of the fifth order is a good choice, because no improvements are expected increasing the approximation order.

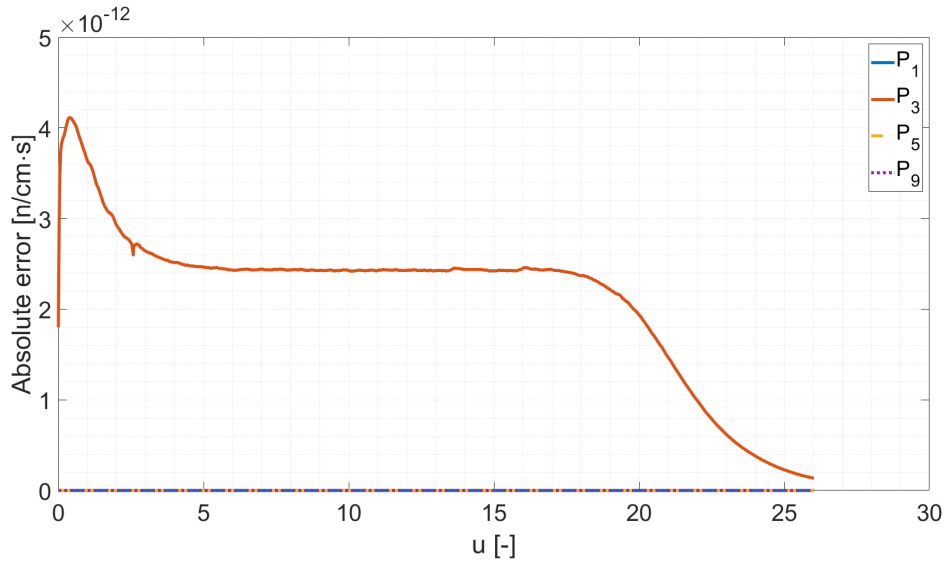


Figure 5.23: Absolute error with respect to the solution with the P_{19} approximation, using the Greuling-Goertzel approach, in a homogeneous slab of graphite, with $B = 0.01$ in linear scale.

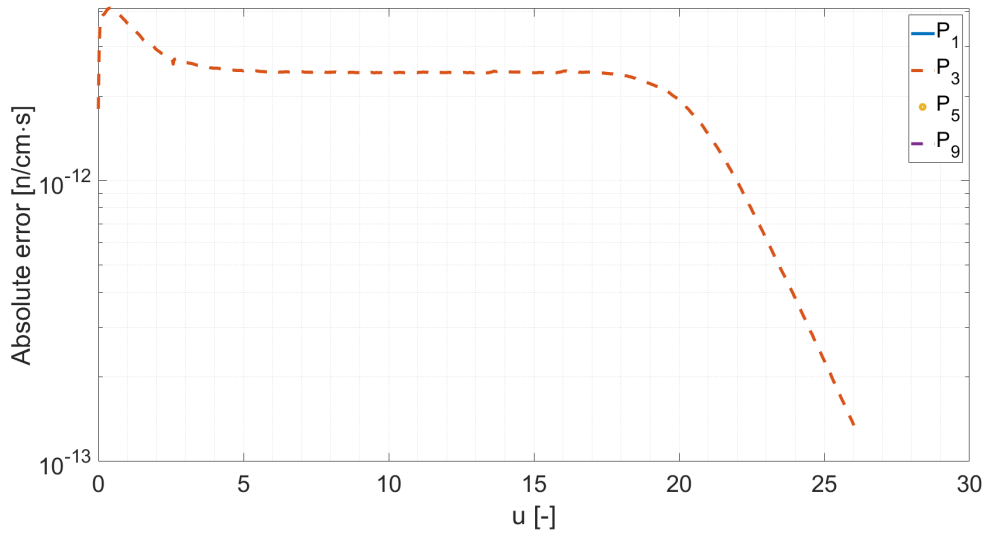


Figure 5.24: Absolute error with respect to the solution with the P_{19} approximation, using the Greuling-Goertzel approach, in a homogeneous slab of graphite, with $B = 0.01$ in logarithmic scale.

As third case the solutions for the discrete lethargy approach are here presented:

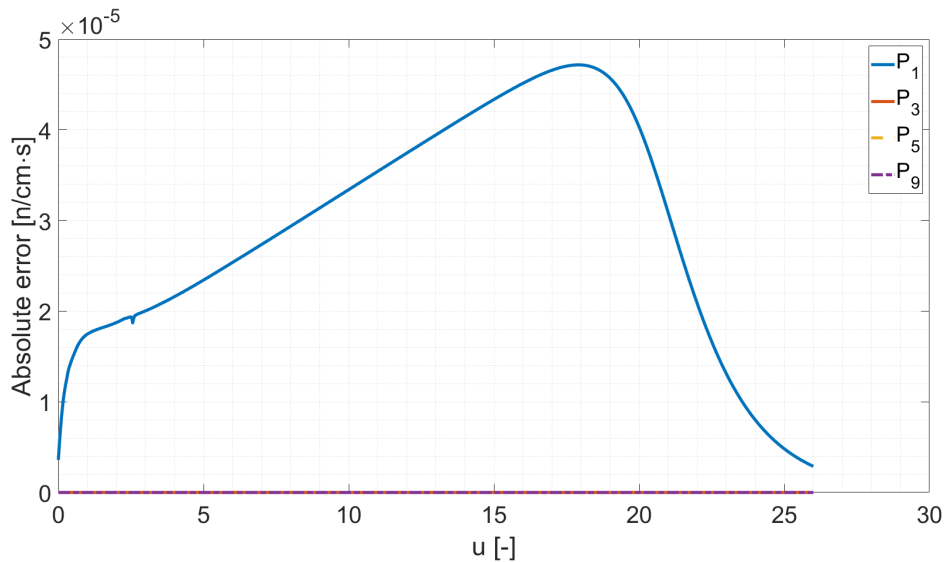


Figure 5.25: Absolute error with respect to the solution with the P_{19} approximation, using the discrete lethargy approach, in a homogeneous slab of graphite, with $B = 0.01$ in linear scale.

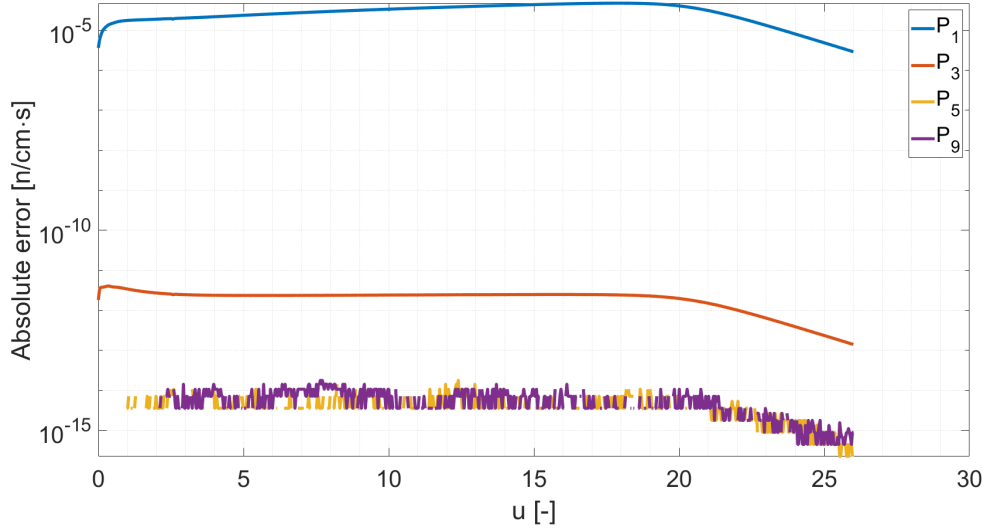


Figure 5.26: Absolute error with respect to the solution with the P_{19} approximation, using the discrete lethargy approach, in a homogeneous slab of graphite, with $B = 0.01$ in logarithmic scale.

In this case the error for the third order approximation has an order of magnitude of $10^{-12} \frac{n}{cm \cdot s}$; instead fifth and ninth order approximation have as error the order of magnitude of the machine precision, so, the error is practically zero. In this way, also for the discrete lethargy approach it seems that using the fifth order approximation is a good choice.

For the graphite moderator the same plot is done using the B_n approximation with the Fermi continuous slowing down method; defining the error as:

$$err = |\varphi_{5,0} - \varphi_{x,0}|, \quad (5.9)$$

where:

- $\varphi_{5,0}$ is the zero order of the neutron flux evaluated in B_5 approximation;
- $\varphi_{x,0}$ is the zero order of the neutron flux evaluated in B_x approximation;

the following plot is obtained:

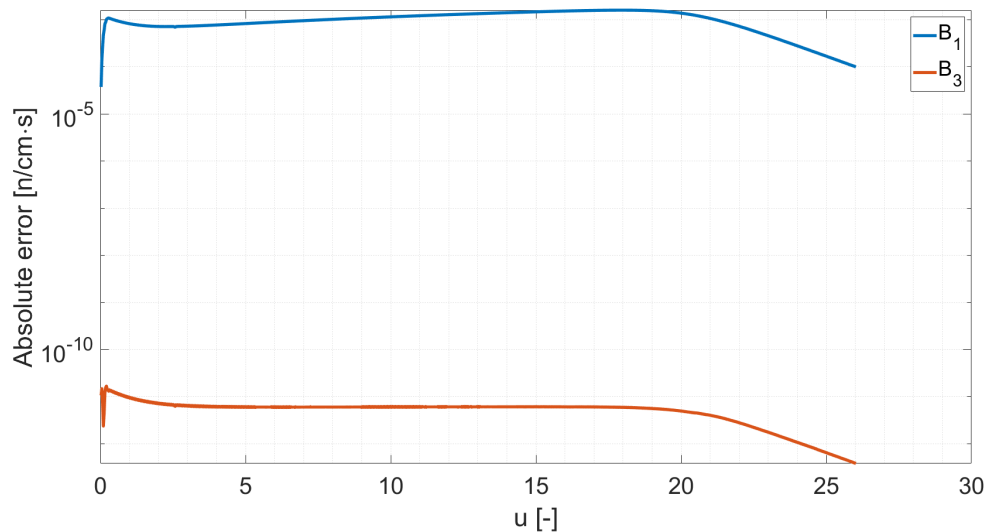


Figure 5.27: Absolute error with respect to the solution with the B_5 approximation, using the Fermi continuous slowing down method, in a homogeneous slab of graphite, with $B = 0.01$ in logarithmic scale.

In this case the fifth order is used as reference because instabilities occur for higher order of approximation; as in the previous case the error for the third order approximation has as order of magnitude a value of $10^{-12} \frac{n}{cm.s}$; so, it is a good choice the use of the third order approximation, though the use of the fifth order give better results.

5.3.3 Results for a light water system

Here the results for the water as moderator materials are reported. First of all a comparison between the Fermi continuous slowing down, discrete lethargy approach, Greuling-Goertzel approach and Selengut-Goertzel approach is presented; the results are reported below; in the following plot the flux zero order moment, evaluated with the P_{19} approximation, is presented:

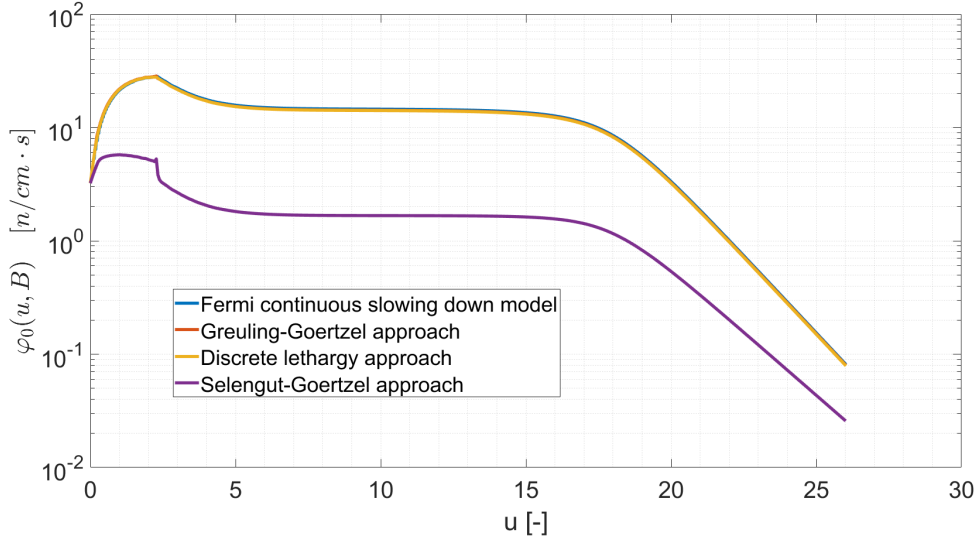


Figure 5.28: Neutron spectra, evaluated with Fermi continuous slowing down method, discrete lethargy approach, Greuling-Goertzel approach and Selengut-Goertzel approach in P_{19} approximation, in a homogeneous slab of light water, with $B = 0.01$.

For water moderated system the Fermi continuous slowing down method, the Greuling-Goertzel approach and the discrete lethargy approach give very similar results; instead the Selengut-Goertzel approach give a completely different result. Even if the three methods give similar results, the last one should be the more accurate because the different way of treating the water molecule; in fact in the first three methods the water is treated as a whole, instead in the Selengut-Goertzel approach the water components are treated separately. In this last case the scattering integral is divided in two integrals: the first integral for the oxygen part, where the Fermi continuous slowing down is applicable, due to the big mass of the atom; the second integral for the hydrogen part, where the discrete lethargy approach is applied. Doing this differentiation in the integral, the term A considered in the elastic scattering (formula (2.35)) is different for the two atoms, so different loss of energy is considered for the two atoms; instead in the first three methods the properties have been considered as an average. Consequently, the results for the Selengut-Goertzel approach are expected more accurate than the other methods. In the remaining part of this section, for each method, that has been used, the comparison between different order of approximation is analysed; in order to compare the different orders of approximation the error definition in formula (5.8) is used; first of all the solutions for the Fermi continuous slowing down method are analysed:

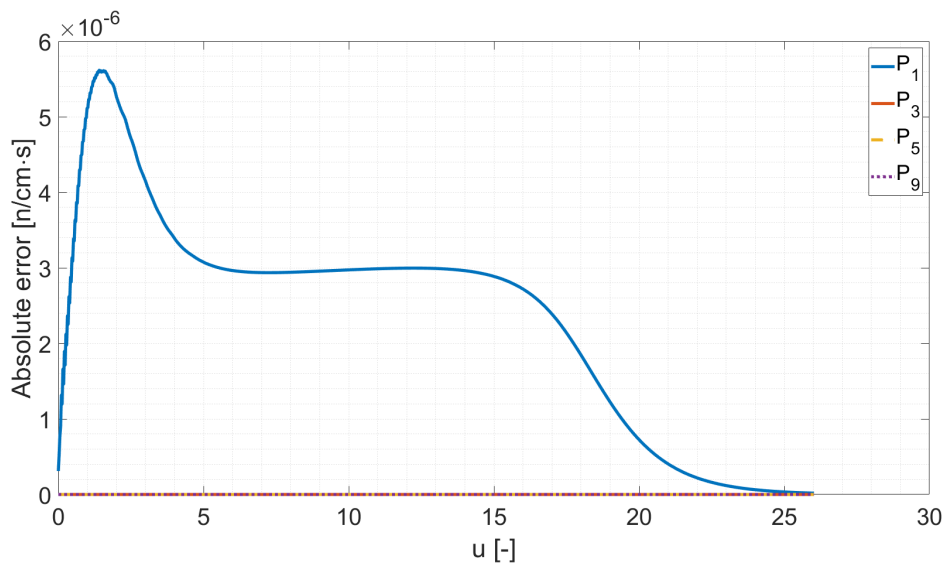


Figure 5.29: Absolute error with respect to the solution with the P_{19} approximation, using the Fermi continuous slowing down method, in a homogeneous slab of light water, with $B = 0.01$ in linear scale.

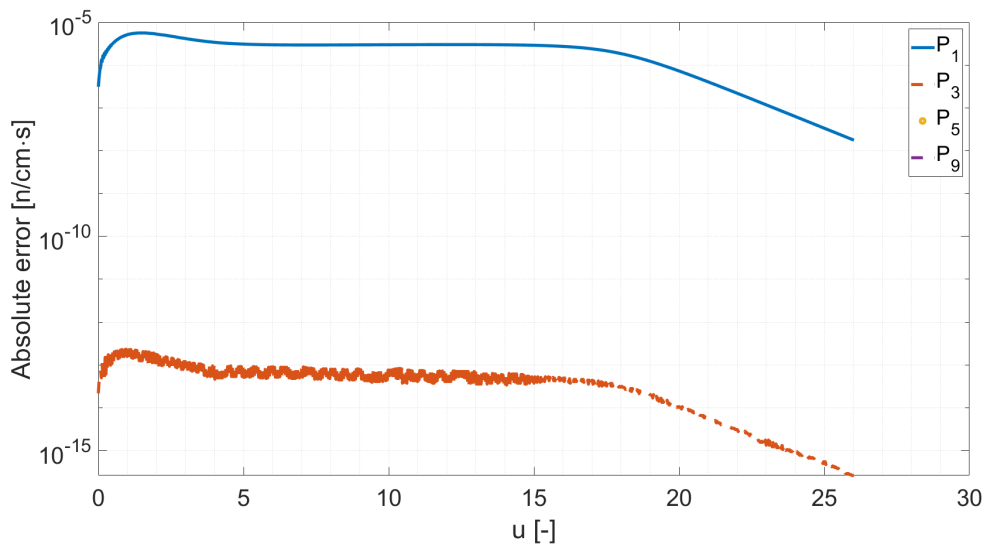


Figure 5.30: Absolute error with respect to the solution with the P_{19} approximation, using the Fermi continuous slowing down method, in a homogeneous slab of light water, with $B = 0.01$ in logarithmic scale.

The first plot is done in linear scale; except for the P_1 approximation, it seems

that the error is zero for the higher order approximation. In order to better understand the order of the error for the higher order approximation, a plot in logarithmic scale is presented in the second plot; from this picture it is appreciable that the third order moment is of the order of $10^{-13} \frac{n}{cm \cdot s}$, instead fifth and ninth order moments are non represented; it means that the value of the error with respect to P_{19} approximation is exactly zero. With these results it is possible to say that the use of the fifth order is a good choice, because no improvements are expected increasing the approximation order.

As second case the solutions for the Greuling-Goertzel approach are analysed; the following two plots represents the errors for different order of approximation, also in this case, in linear and logarithmic scale. As the previous case, looking at the linear scale plot, it seems that the error is zero for higher order of approximation than one. Instead looking at the logarithmic scale plot the third order approximation has as order of magnitude an error in between $10^{-13} \frac{n}{cm \cdot s}$ and $10^{-15} \frac{n}{cm \cdot s}$; instead for the order higher or equal than the fifth, the error is exactly zero. It means that the use of the fifth order is a good choice, because no improvements are expected increasing the approximation order.

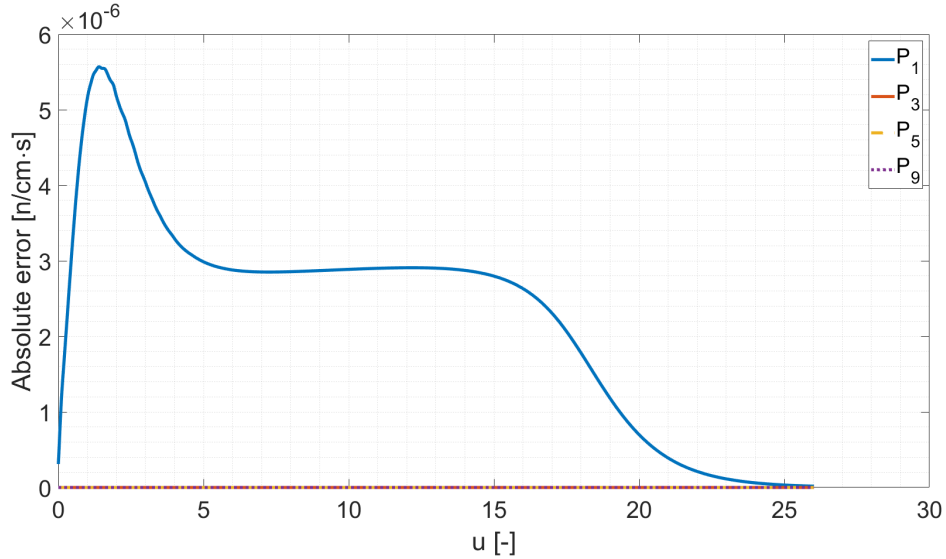


Figure 5.31: Absolute error with respect to the solution with the P_{19} approximation, using the Greuling-Goertzel approach, in a homogeneous slab of light water, with $B = 0.01$ in linear scale.

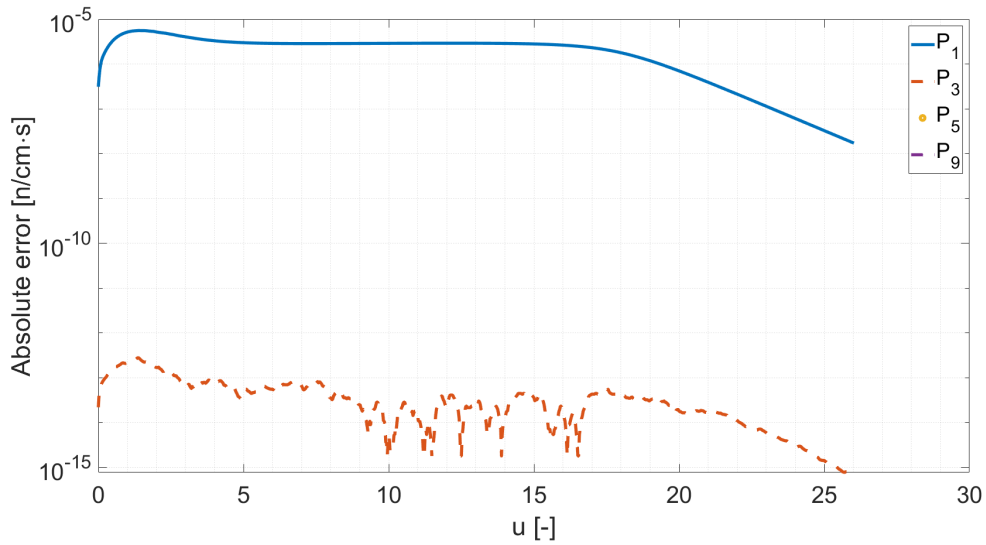


Figure 5.32: Absolute error with respect to the solution with the P_{19} approximation, using the Greuling-Goertzel approach, in a homogeneous slab of light water, with $B = 0.01$ in logarithmic scale.

As third case the solutions for the discrete lethargy approach are here presented:

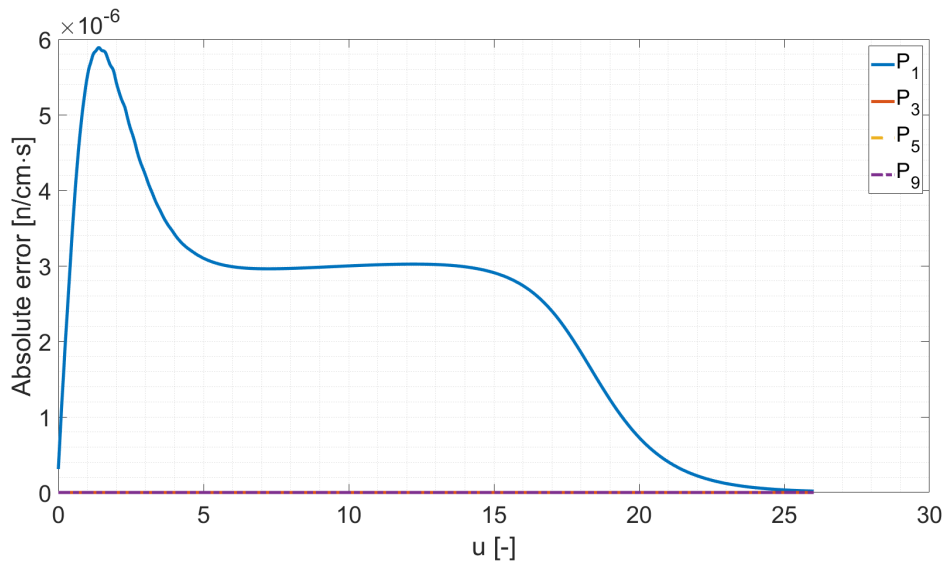


Figure 5.33: Absolute error with respect to the solution with the P_{19} approximation, using the discrete lethargy approach, in a homogeneous slab of light water, with $B = 0.01$ in linear scale.

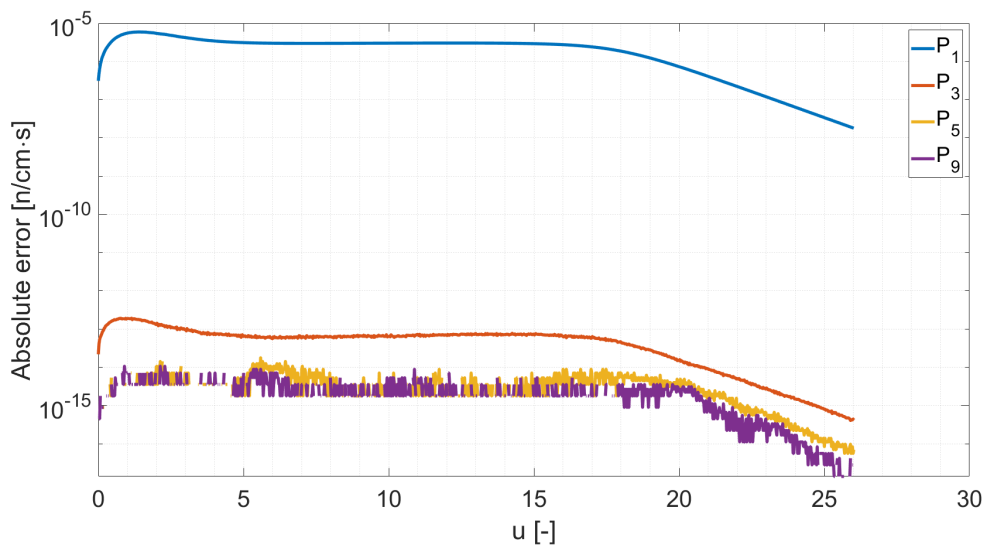


Figure 5.34: Absolute error with respect to the solution with the P_{19} approximation, using the discrete lethargy approach, in a homogeneous slab of light water, with $B = 0.01$ in logarithmic scale.

In this case the error for the third order approximation has an order of magnitude of $10^{-13} \frac{n}{cm \cdot s}$; instead fifth and ninth order approximation have as error the order of magnitude of the machine precision, so, the error is practically zero. In this way, also for the discrete lethargy approach it seems that using the fifth order approximation is a good choice.

As last case the solutions for the Selengut-Goertzel approach are analysed; in the following two plots the errors, for different order of approximation, in linear and logarithmic scale, are represented. In this case the third order approximation has an error in between $10^{-13} \frac{n}{cm \cdot s}$ and $10^{-15} \frac{n}{cm \cdot s}$; instead for the fifth order the error is comparable with the machine precision, and, moreover, the ninth order approximation has exactly zero error; so, also in this case it seems that using the fifth order approximation is a good choice.

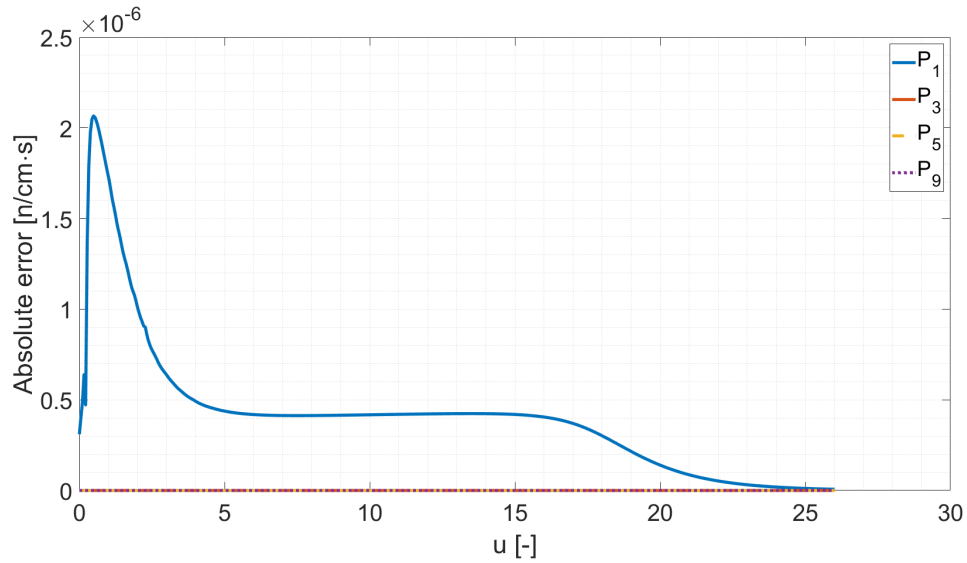


Figure 5.35: Absolute error with respect to the solution with the P_{19} approximation, using the Selengut-Goertzel approach, in a homogeneous slab of light water, with $B = 0.01$ in linear scale.

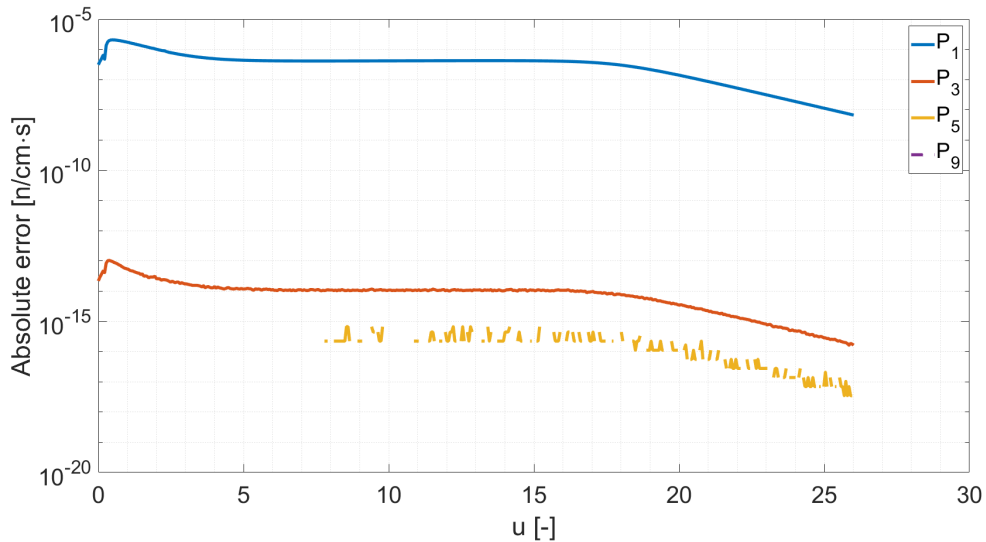


Figure 5.36: Absolute error with respect to the solution with the P_{19} approximation, using the Selengut-Goertzel approach, in a homogeneous slab of light water, with $B = 0.01$ in logarithmic scale.

5.3.4 Results for a heavy water system

Here the results for the heavy water as moderator materials are reported. First of all a comparison between the Fermi continuous slowing down, discrete lethargy approach, Greuling-Goertzel approach and Selengut-Goertzel approach is presented; the results are reported below; in the following plot the flux zero order moment, evaluated with the P_{19} approximation, is presented:

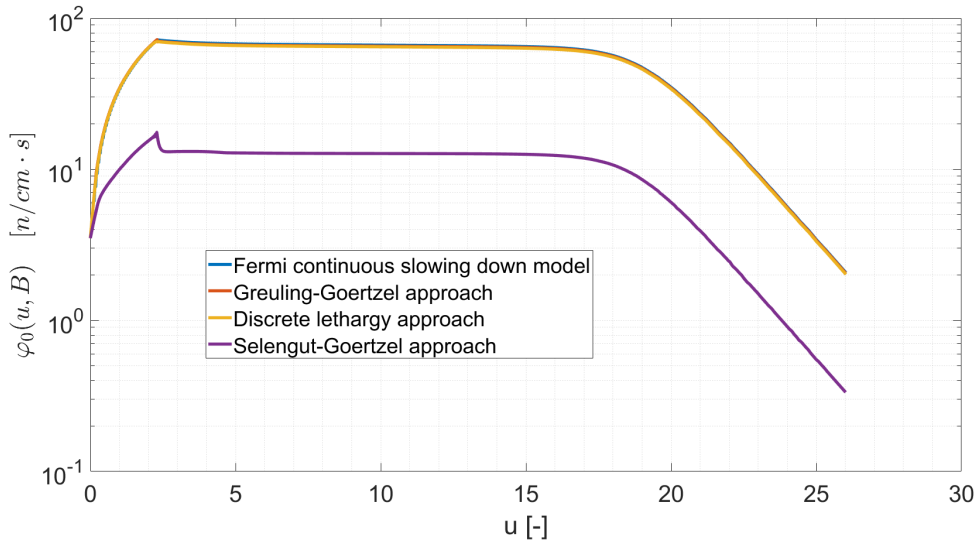


Figure 5.37: Neutron spectra, evaluated with Fermi continuous slowing down method, discrete lethargy approach, Greuling-Goertzel approach and Selengut-Goertzel approach in P_{19} approximation, in a homogeneous slab of heavy water with $B = 0.01$.

In order to analyse this plot the same consideration of the case with light water as moderating material can be done; therefore, also for the heavy water, the Selengut-Goertzel approach is expected to give better results with respect to the other three methods.

In the remaining part of this section, for each method, that has been used, the comparison between different order of approximation is analysed; in order to compare the different orders of approximation the error definition in formula (5.8) is used; first of all the solutions for the Fermi continuous slowing down method are analysed:

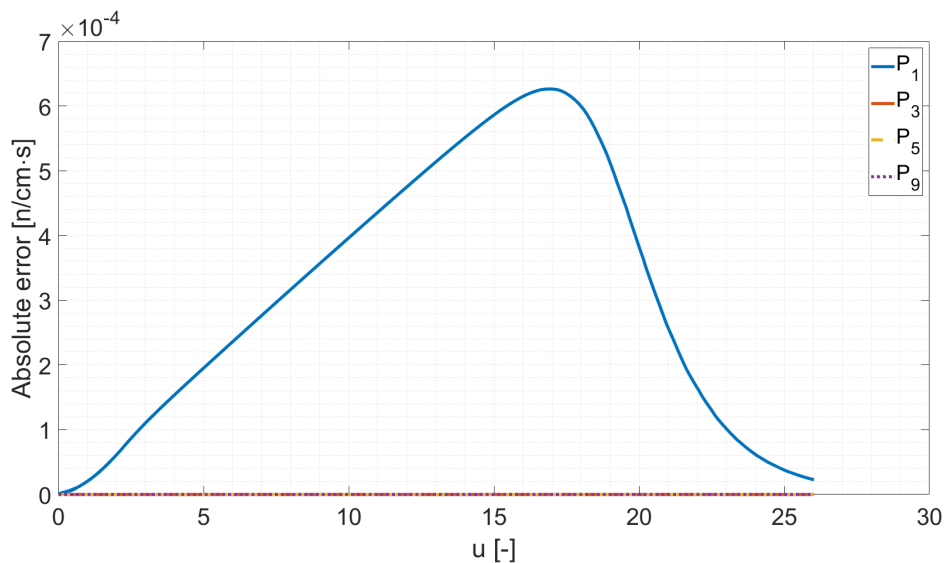


Figure 5.38: Absolute error with respect to the solution with the P_{19} approximation, using the Fermi continuous slowing down method, in a homogeneous slab of heavy water, with $B = 0.01$ in linear scale.

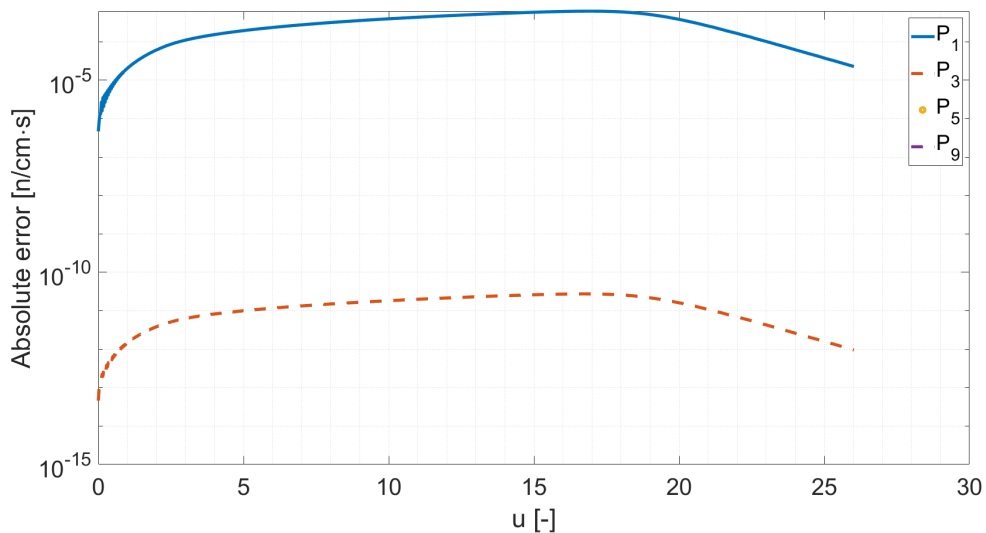


Figure 5.39: Absolute error with respect to the solution with the P_{19} approximation, using the Fermi continuous slowing down method, in a homogeneous slab of heavy water, with $B = 0.01$ in logarithmic scale.

The first plot is done in linear scale; except for the P_1 approximation, it seems

that the error is zero for the higher order approximation. In order to better understand the order of the error for the higher order approximation, a plot in logarithmic scale is presented in the second plot; from this picture it is appreciable that the third order moment is of the order of $10^{-1} \frac{n}{cm \cdot s}$, instead fifth and ninth order moments are non represented; it means that the value of the error with respect to P_{19} approximation is exactly zero. With these results it is possible to say that the use of the fifth order is a good choice, because no improvements are expected increasing the approximation order.

As second case the solutions for the Greuling-Goertzel approach are analysed; the following two plot represents the errors for different order of approximation, also in this case, in linear and logarithmic scale. As the previous case, looking at the linear scale plot, it seems that the error is zero for higher order of approximation than one. Instead looking at the logarithmic scale plot the third order approximation has as order of magnitude an error of $10^{-12} \frac{n}{cm \cdot s}$; instead for the order higher or equal than the fifth, the error is exactly zero. It means that the use of the fifth order is a good choice, because no improvements are expected increasing the approximation order.

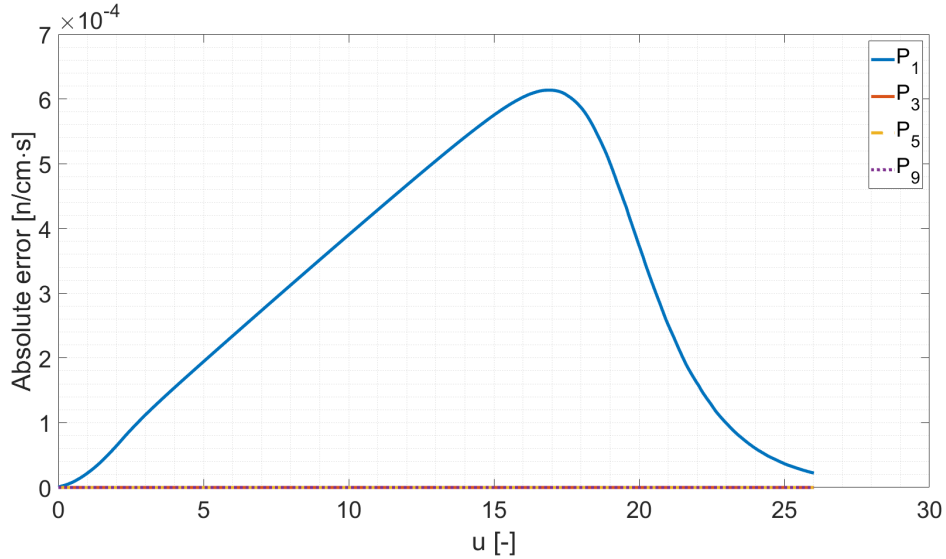


Figure 5.40: Absolute error with respect to the solution with the P_{19} approximation, using the Greuling-Goertzel approach, in a homogeneous slab of heavy water, with $B = 0.01$ in linear scale.

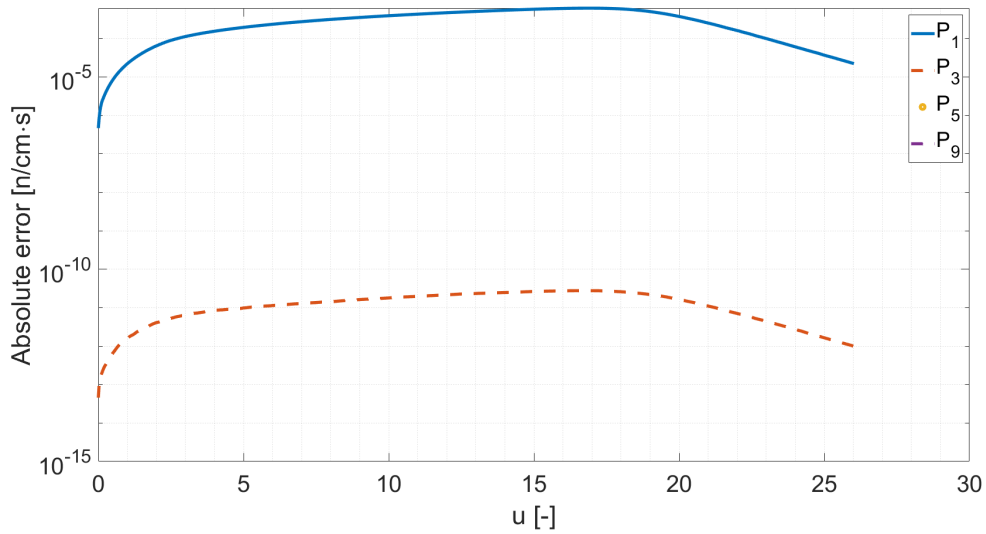


Figure 5.41: Absolute error with respect to the solution with the P_{19} approximation, using the Greuling-Goertzel approach, in a homogeneous slab of heavy water, with $B = 0.01$ in logarithmic scale.

As third case the solutions for the discrete lethargy approach are presented in the following two plots:

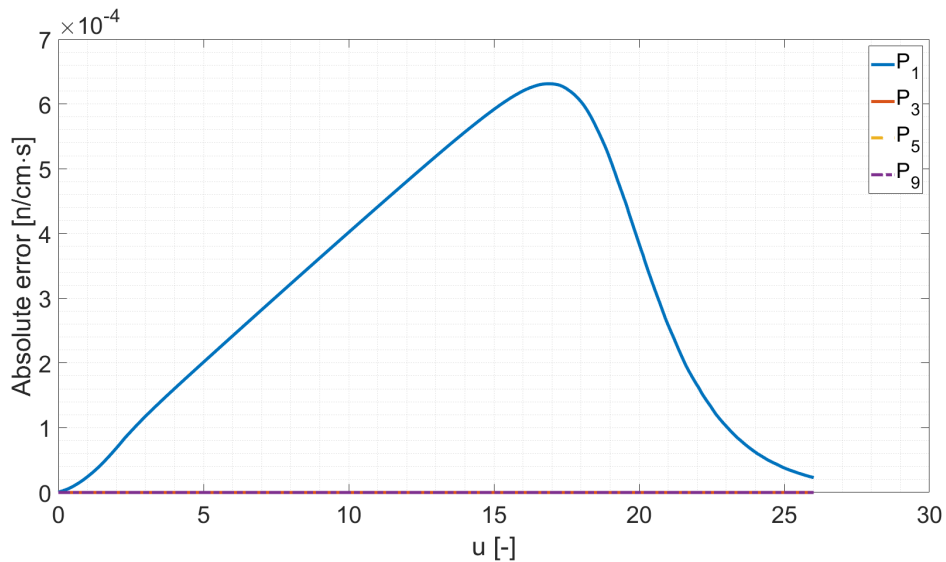


Figure 5.42: Absolute error with respect to the solution with the P_{19} approximation, using the discrete lethargy approach, in a homogeneous slab of heavy water, with $B = 0.01$ in linear scale.

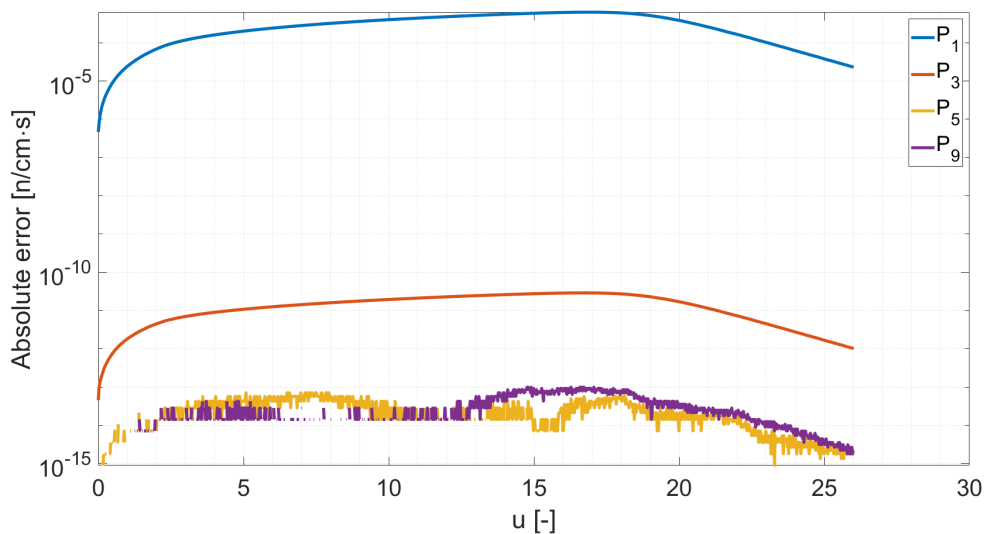


Figure 5.43: Absolute error with respect to the solution with the P_{19} approximation, using the discrete lethargy approach, in a homogeneous slab of heavy water, with $B = 0.01$ in logarithmic scale.

In this case the error for the third order approximation has an order of magnitude of $10^{-12} \frac{n}{cm \cdot s}$; instead fifth and ninth order approximation have as error the order of magnitude of the machine precision, so, the error is practically zero. In this way, also for the discrete lethargy approach it seems that using the fifth order approximation is a good choice.

As last case the solutions for the Selengut-Goertzel approach are analysed; in the following two plots the errors, for different order of approximation, in linear and logarithmic scale, are represented. In this case the third order approximation has an error of $10^{-13} \frac{n}{cm \cdot s}$; instead for the fifth order and the ninth order approximation have exactly zero error; so, also in this case it seems that using the fifth order approximation is a good choice.

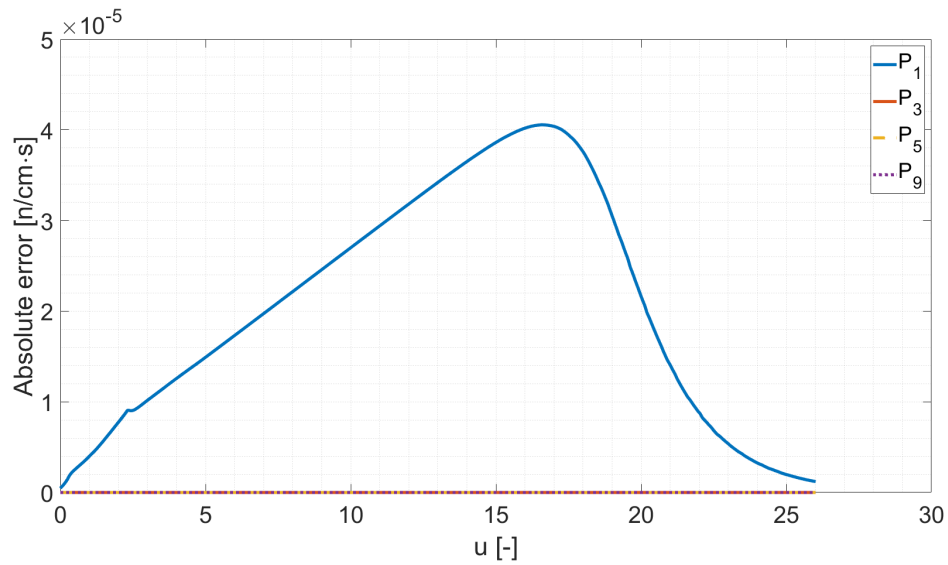


Figure 5.44: Absolute error with respect to the solution with the P_{19} approximation, using the Selengut-Goertzel approach, in a homogeneous slab of heavy water, with $B = 0.01$ in linear scale.

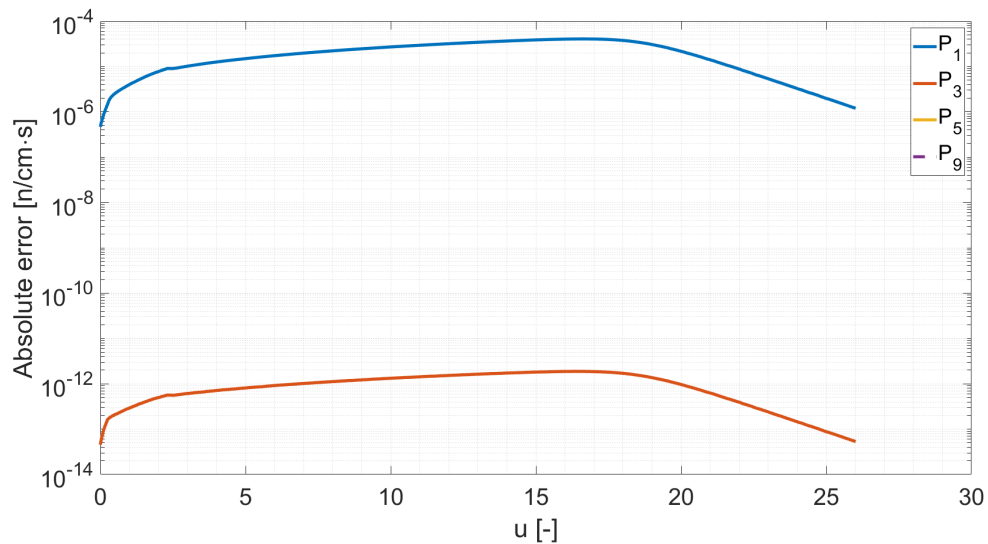


Figure 5.45: Absolute error with respect to the solution with the P_{19} approximation, using the Selengut-Goertzel approach, in a homogeneous slab of heavy water, with $B = 0.01$ in logarithmic scale.

5.3.5 Light and heavy water comparison

In this section a comparison between light water and heavy water as moderating material is carried out. In order to do a comparison the neutron spectra, evaluated through the use of the Selengut-Goertzel approach, with $B = 0.01$ and P_{19} approximation, is used; in the following plot the two neutron spectra are reported.

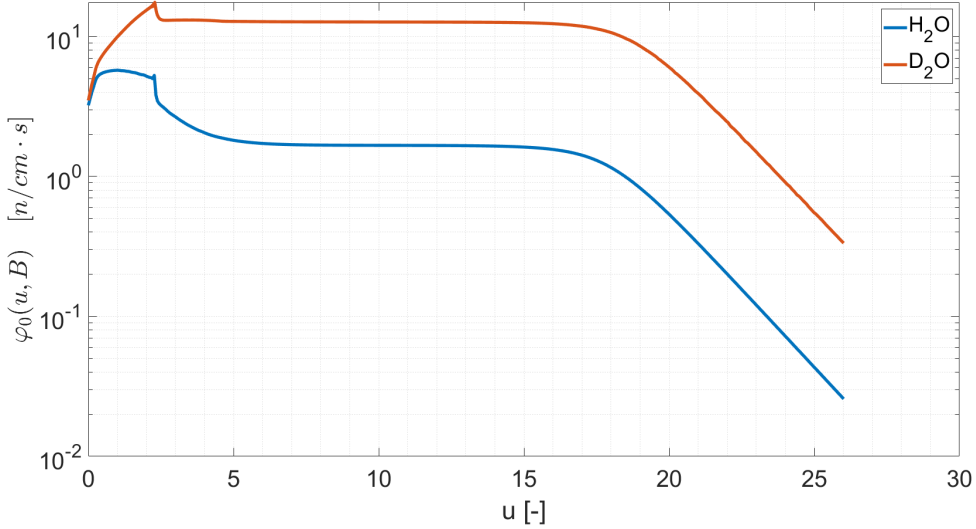


Figure 5.46: Neutron spectra, evaluated with Selengut-Goertzel approach in P_{19} approximation, in a homogeneous slab of light water and of heavy water with $B = 0.01$.

Comparing the two curves, it is clear that the spectrum for heavy water moderator is higher than the spectrum for light water moderator. It is due to the fact that the light water has hydrogen in the molecule, instead heavy water has deuterium; the mass of the deuterium is about the double of the hydrogen mass, so, it generate a lower loss of energy for each collision; in this way neutron that collide with hydrogen has a large lethargy increase, so less neutron reach the first part of the lethargy range. This is the reason why in the first part of the lethargy range the spectrum for the deuterium reach an higher value. Moreover, the effect of the absorption cross section is relevant. The absorption cross section is defined as:

$$\Sigma_a(u) = \Sigma_t(u) - \Sigma_s(u), \quad (5.10)$$

where $\Sigma_a(u)$ is the absorption cross section.

In the following plot the absorption cross section for hydrogen and for deuterium is represented.

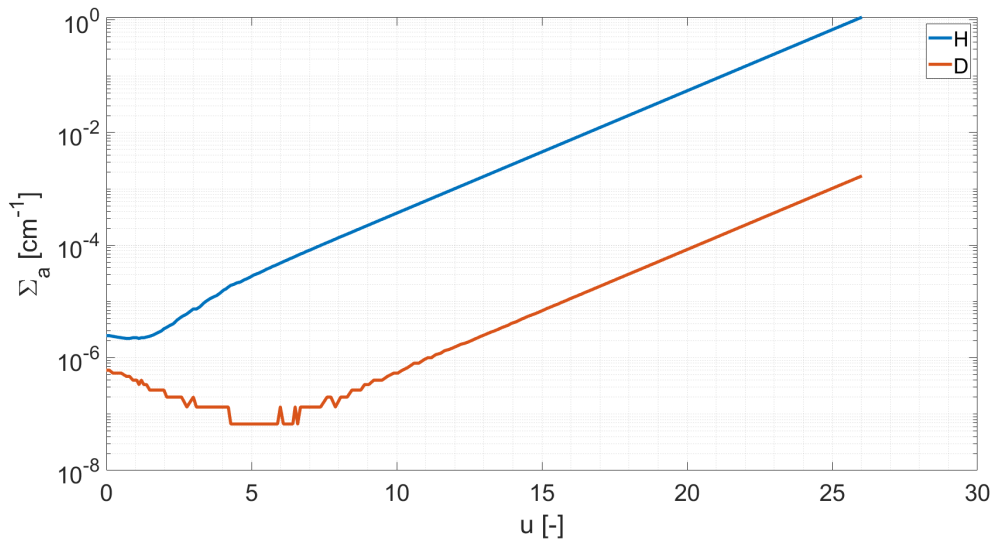


Figure 5.47: Absorption cross section for hydrogen and deuterium

Analysing this plot the reason why the light water energy spectrum is lower than the heavy water energy spectrum is more clear; in fact the absorption cross section for hydrogen is larger than the absorption cross section for deuterium, so more neutrons are able to slow down for heavy water with respect to light water. Only on the basis of the energy spectrum in a homogeneous moderating system, between light water and heavy water, it is possible to say that heavy water is a better moderator material than light water. Actually the selection of a moderating material in a nuclear reactor is more complex, because it requires the analysis of more complex phenomena; just to give an example the energy loss for collision in heavy water is lower, so in a water reactor more neutrons pass through the resonance of the absorption cross section of the Uranium-238, so more neutrons are absorbed in the Uranium-238 and so a higher enrichment is required.

Chapter 6

Concluding remarks

In this work the neutron energy spectrum for a homogeneous slab has been evaluated. Different materials have been considered, in particular graphite, light water and heavy water.

The solution is obtained assuming different slowing down models, based on a continuous energy approach, i.e. the Fermi continuous slowing down method, the Greuling-Goertzel, the discrete lethargy and the Selengut-Goertzel approaches. The solutions have been evaluated using the P_N and the B_N angular approximations.

Some comparisons between the solutions with different methods have been carried out. Such comparison allow to draw some conclusions on the better choice of the method to be used for a specific material.

Future developments will include the analysis of heterogeneous systems and the optimization of the procedure for the determination of multigroup data for deterministic transport codes.

Bibliography

- [1] F. Rahnema and M. S. McKinley, “High-order cross-section homogenization method,” *Annals of Nuclear Energy*, vol. 29, no. 7, pp. 875–899, 2001.
- [2] S. Yasserli and F. Rahnema, “Consistent spatial homogenization in transport theory,” *Nuclear Science and Engineering*, vol. 176, pp. 292–311, 2014.
- [3] G. Kooreman and F. Rahnema, “Enhanced hybrid diffusion-transport spatial homogenization method,” *Nuclear Technology*, vol. 192, pp. 264–277, 2015.
- [4] G. Kooreman and F. Rahnema, “Hybrid diffusion–transport spatial homogenization method,” *Annals of Nuclear Energy*, vol. 72, pp. 95–103, 2014.
- [5] S. Yasserli and F. Rahnema, “On the consistent spatial homogenization method in neutron transport theory,” *Journal of Computational and Theoretical Transport*, vol. 43, pp. 240–261, 2014.
- [6] F. Rahnema and E. M. Nichita, “Leakage corrected spatial (assembly) homogenization technique,” *Annals of Nuclear Energy*, vol. 24, no. 6, pp. 477–488, 1997.
- [7] M. Gamarino, *Modal methods for rehomogenization of nodal cross sections in nuclear reactor core analysis*. PhD thesis, 11 2018.
- [8] A. Marvin and M. Jim, “The finite element with discontinuous support multi-group method: Theory,” 2015.
- [9] W. L. Filippone, “The generalized spencer-lewis equation,” *Transport Theory and Statistical Physics*, vol. 15, no. 5, pp. 629–649, 1986.
- [10] K. M. Case, J. H. Ferziger, and P. F. Zweifel, “Asymptotic reactor theory,” *Nuclear Science and Engineering*, vol. 10, no. 4, pp. 352–356, 1961.
- [11] H. Hurwitz and P. F. Zweifel, “Slowing down of neutrons by hydrogenous moderators,” *Journal of Applied Physics*, vol. 26, no. 8, 1955.
- [12] S. Dulla, S. Canepa, and P. Ravetto, “From transport to diffusion through a space asymptotic approach,” *Mathematics and Computers in Simulation*, vol. 80, pp. 2134–2141, jul 2010.
- [13] S. Dulla, B. D. Ganapol, and P. Ravetto, “Space asymptotic method for the study of neutron propagation,” *Annals of nuclear energy*, vol. 33, no. 10, pp. 932–940, 2006.
- [14] B. Davison, *Neutron transport theory*. Clarendon press, 1958.

- [15] R. V. Meghreblian and D. K. Holmes, *Reactor Analysis*. New York: McGraw-Hill, 1960.
- [16] G. B. Arfken and H. J. Weber, *Mathematical methods for physicists*. Elsevier Academic Press, sixth ed., 2005.
- [17] G. I. Bell and S. Glasstone, *Nuclear Reactor Theory*. Van Nostrand Reinhold, 1970.
- [18] K. E. Atkinson, *An introduction to numerical analysis*. John Wiley & Sons, second ed., 1989.
- [19] MATLAB, *version 9.6.0.1072779 (R2019a)*. Natick, Massachusetts: The MathWorks Inc., 2019.
- [20] O. D. Bank, “The JEFF-3.3 nuclear data library,” nov 2017.
- [21] N. Soppera, M. Bossant, and E. Dupont, *JANIS 4: An Improved Version of the NEA Java-based Nuclear Data Information System*, vol. 120. Nuclear Data Sheets, jun 2014.